# ATOM TRAPPING VAPOR GENERATION ATOMIC ABSORPTION SPECTROMETRY FOR INORGANICARSENIC SPECIATION ANALYSIS

A THESIS SUBMITTED TO
THE GRADUATE SCHOOL OF NATURAL AND APPLIED SCIENCES
OF
MIDDLE EAST TECHNICAL UNIVERSITY

BY
NJAW NJIE

IN PARTIAL FULFILLMENT OF THE REQUIREMENTS
FOR
THE DEGREE OF DOCTOR OF PHILOSOPHY
IN
CHEMISTRY

AUGUST 2014

Approval of the thesis:

**ATOM TRAPPING VAPOR GENERATION ATOMIC ABSORPTION SPECTROMETRY FOR INORGANIC ARSENIC SPECIATION ANALYSIS**

Submitted by **NJAW NJIE** in partial fulfillment of the requirements for the degree of **Doctor of** Philosophy **in Chemistry Department, Middle East Technical University** by,

Prof. Dr. Canan Özgen _____
Dean, Graduate School of **Natural and Applied Sciences**

Prof. Dr. İlker Özkan _____
Head of Department, **Chemistry**

Prof. Dr. O. Yavuz Ataman _____
Supervisor, **Chemistry Dept., METU**

**Examining Committee Members:**

Assoc. Prof. G. Inci Gokmen _____
Chemistry Dept., METU

Prof. Dr. O. Yavuz Ataman _____
Supervisor, Chemistry Dept., METU

Prof. Dr. Mürvet Volkan _____
Chemistry Dept., METU

Prof. Dr. Orhan Acar _____
Analitik Kimya Anabilim Dali Eczacilik Fak., Gazi Uni.

Prof. Dr. Nusret Ertaş _____
Analitik Kimya Anabilim Dali Eczacilik Fak., Gazi Uni.

**Date:** _____

**I hereby declare that all information in this document has been obtained and presented in accordance with academic rules and ethical conduct. I also declare that, as required by these rules and conduct, I have fully cited and referenced all material and results that are not original to this work.**

Name, Last name: Njaw Njie

Signature:

## ABSTRACT

ATOM TRAPPING VAPOR GENERATION ATOMIC ABSORPTION SPECTROMETRY FOR INORGANICARSENIC SPECIATION ANALYSIS

Njie, Njaw

Ph.D., Department of Chemistry

Supervisor: Prof. Dr. Osman Yavuz ATAMAN

August 2014, 187pages

Speciation analysis is important for arsenic. Novel methods to improve the sensitivity for determination of total arsenic and arsenic speciation have been developed. The techniques basically rely on generation of volatile arsenic species by reaction with sodium borohydride followed by trapping on a W-coil atomizer and finally releasing analyte atoms by heating the atomizer; the system is named as W-coil atom trapping electrothermal atomic absorption spectrometry (WC-ETAAS). Sample solution may be introduced both by continuous flow hydride generation (CF-HG-WC-ETAAS) or flow injection hydride generation (FI-HG-WC-ETAAS). Speciation analysis was performed by using high pressure liquid chromatography (HPLC) for separation followed by W-coil trapping; this method is named as HPLC-HG-WC-ETAAS. For optimization and comparison, an electrically heated quartz tube atomizer was also used for the systems named CF-HG-EHQTA-AAS and FI-HG-EHQTA-AAS. Both for FI and HPLC systems, rapid on-line reduction of As(V) to As(III) was realized by using 1.0% (v/v) thioglycollic acid in 0.002 mol/L HCl. In HPLC analyses, the collection of analyte was done only for As(III) and As(V), these species were then

collected and then atomized consecutively. The results are used to determine total inorganic arsenic content. The optimized temperatures for collection and atomization temperatures for W-coil were 720 ºC and 1920 ºC, respectively. Using CF-HG-WC-ETAAS and 180 s collection of 19.5 mL sample, limits of detection limits for As(III) and As(V) were 1.9 ng/L and 1.8 ng/L, respectively. For speciation analysis by HPLC-HG-WC-ETAAS, limits of detection were 0.25 ng/mL and 0.30 ng/mL for As(III) and As(V), respectively; a sample loop of 0.16 mL was used. For testing accuracy, Waste Water EU-L-2, Trace Elements in Water 1643e, Trace Elements in Spinach Leaves1570aand Tuna Fish Tissue BCR627 were used as certified reference materials. Applications on real samples were carried out on irrigation water, dill, lettuce, garden rocket and parsley. The methods developed offer novel alternatives in arsenic determination and speciation using only a simple atomic absorption spectrometer.

Keywords: Arsenic, arsenite, arsenate, speciation, tungsten coil, electrothermal atomization, thioglycolic acid, atom trapping

# ÖZ

İNORGANİK ARSENİK TÜRLENDİRME ANALİZİ İÇİN ATOM TUZAKLI BUHAR OLUŞTURMALI ATOMİK ABSORPSİYON SPEKTROMETRİ

Njie, Njaw
Doktora, Kimya Bölümü
Tez Yöneticisi: Prof. Dr. Osman Yavuz ATAMAN
Ağustos 2014, 187 sayfa

Arsenik tayininde türlendirme önemlidir. Toplam arsenik tayini ve arsenik türlendirmesinde duyarlılığın artırılması için yeni yöntemler geliştirildi. Tekniklerin dayandığı temel işlem, sodyum borohidrür ile uçucu arsenik türlerinin oluşturulması, bu türlerin bir W-sarmal üzerinde toplanması ve sonunda atomlaştırıcıyı ısıtarak atomların salınmasıdır; bu düzenek, W-sarmal atom tuzaklı elektrotermal atomik absorpsiyon spektrometri olarak adlandırıldı (WC-ETAAS). Örnek çözelti, hem sürekli akış (CF-HG-WC-ETAAS), hem de akışa enjeksiyon (FI-HG-WC-ETAAS) şeklinde sunulabilir. Türlendirme analizinde ise yüksek basınçlı sıvı kromatografi (HPLC) ile ayırmadan sonra W-sarmal ile tuzaklama kullanıldı; bu yöntem ise HPLC-HG-WC-ETAAS olarak adlandırıldı. En uygun parametrelerin bulunması ve kıyaslama amacıyla elektriksel ısıtılan bir kuvars boru atomlaştırıcı da CF-HG-EHQTA-AAS ve FI-HG-EHQTA-AAS olarak adlandırılan aygıtlarla kullanıldı. FI ve HPLC kullanılan yöntemlerde, As(V)'in hat üstünde As(III)'e indirgenmesi, 0.002 mol/L HCl içerisinde hazırlanmış %1.0 (v/v) tiyoglikolik asit ile gerçekleştirildi.

HPLC analizlerinde, yalnız As(III) ve As(V) türlerinin toplanması yapıldı, anılan türler ard arda W-coil üzerinde toplandı ve atomlaştırıldı. Sonuçlar, toplam inorganic arsenik tayini için kullanıldı. W-sarmal için optimize edilmiş toplama ve atomlaştırma sıcaklıkları, sırasıyla 720 ºC ve 1920 ºC olarak kullanıldı. CF-HG-WC-ETAAS yöntemi ile, 19.5 mL örnek çözeltinin 180 s içinde toplanmasıyla gözlenebilme sınırları, As(III) için 1.9 ng/mL, As(V) için 1.8 ng/mL olarak bulundu. HPLC-HG-WC-ETAAS kullanarak yapılan türlendirme analizinde ise gözlenebilme sınırları, As(III) için 0.25 ng/mL, As(V) için ise 0.30 ng/mL olarak saptandı; deneylerde 0.16 mL örnekleme halkası kullanıldı. Doğruluğun irdelenmesi için, Waste Water EU-L-2, Trace Elements in Water 1643e, Trace Elements in Spinach Leaves1570a and Tuna Fish Tissue BCR627 adlı sertifikalı referans maddeler kullanıldı. Gerçek örnek uygulamaları ise, tarımsal sulama suyu, dereotu, kıvırcık salatalık, roka ve maydanoz örnekler üzerinde yapıldı. Geliştirilen yöntemler, yalnızca basit bir atomik absorpsiyon spektrometre kullanarak arsenik tayini ve türlendirmesinde yeni seçenekler oluşturmaktadır.

Anahtar Kelimeler:Arsenik, arsenit, arsenat, türlendirme, tungsten sarmal, elektrotermal atomlaştırma, tiyoglikolik asit, atom tuzaklama

**To my family**

## ACKNOWLEDGMENTS

I would like express my sincere gratitude and my special appreciation to my advisor Prof. Dr. O Yavuz Ataman for his invaluable and professional guidance. He has been a tremendous mentor for me and always supported me by giving valuable suggestions throughout all stages of this thesis. Without our inspiring discussions, this thesis would not have been what it is today. I appreciate all his contributions of time, ideas, and funding to make my Ph.D. degree come through. His experience and productive achievement are stimulating. The joy and enthusiasm he has for his research was contagious and motivational for me, even during tough times in the Ph.D. I am also thankful for the excellent example he has provided as a successful analytical chemist. He meticulouslyadvised and guided his students to operate in the excellent principles of analytical chemistry, thus whenever you have to present your results to him, you have to show their reproducibility. Without you this thesis would not have been possible.

I would like to thank and express my sincere gratitude to thesis committee members, Prof. Dr. Mürvet Volkan, and Prof. Dr. Nusret Ertaş for their valuable guideline and contributions during the hard times of this thesis. Their suggestions and comments during the presentation of my work will never be forgotten and these also contributed to the success of this thesis.

I cannot find words to express my gratitude to my wife, Ndey Gaye Njie, and my two beloved children Muhammed Njie and Abie Njie for their affectionate and unwavering support during the many long days which we endeavored. My special thanks and sincere appreciation go to my wife, for her continuous understanding, patience, love, prayers and her infinite moral support during the hard days of this work.

I am indebted to my many colleagues who supported me and would like to give a sincere thanks to, Sezgin Bakırdere, Yasin Arslan, Emrah Yıldırım, Selin Bora, Pnar Akay Mercan, ErhanÖzdemir, Başak Dügencilifor sharing the joys and worries in the laboratories; I consider it a honor to work with all of you. They always encouraged and helped in various ways. I would like to express my special thanks to them.

I would like to express my special thanks to Assoc. Prof. Dr. Gülay Ertas for her unforgettable moral support, help and guidance.

I would like to express heartfelt thanks to my parents, my father-in-law, my sisters-in-law, my brothers and sisters for their infinite moral supports and prayers during my study. Their prayers and good wishes will never be forgotten.

This thesis would have remained a dream had it not been for the financial support provided to me by The Scientific and Technological Research Council of Turkey. Their financial support and motivating pressure were a lot to make this work come to a positive ending. I also want to thank the financial support of Middle East Technical University Research Fund through BAP project grants.

**TABLE OF CONTENTS**

## LIST OF TABLES

TABLES

## LIST OF FIGURES

FIGURES

## ABBREVIATIONS

AAS……..…Atomic Absorption Spectrometry

AES…….….Atomic Emission Spectrometry

AEX……..…Anion Exchange

AFS…….……..Atomic Fluorescent Spectrometry

As(III)…….…..Arsenite

As(V)……..…...Arsenate

$As_t$……..……Total Arsenic

ATP……..….. Adenosine Triphosphate

CE……..…..…..Capillary Electrophoresis

CEX…….……..….Cation Exchanger

CF-HG-EHQTA…….....Continuous Flow Hydride Generation Electrically Heated Quartz Tube Atomizer

CF-HG-WC-ETA…..….Continuous Flow Hydride Generation W-coil Electrothermal Atomization

CVG……..….Cold Vapor Generation

DL…….…….Detection Limit

DMA……..Dimethyl arsenic acid

DNA…….…..… Deoxyribonucleic Acid

EDL…….……...…Electrodeless Discharge Lamp

Eh…….……...…Redox Potential

EHQTA……..…..... Electrically Heated Quartz Tube Atomizer

ETA……..……..….Electrothermal Atomization

ETV…….....Electrothermal Vaporization

FAAS……. .....Flame Atomic Absorption Spectrometry

FI-HG-EHQTA……...…Flow Injection Hydride Generation Electrically Heater Tube Atomizer

FI-HG-WC-ETA…….…Flow Injection Hydride Generation W-coil Electrothermal Atomization

FIT…….…..Flame In-tube

GC…….…...…Gas Chromatography

GC-MS……..…..Gas Chromatography Mass Spectrometry

GF…….……...…Graphite Furnace

GF-AAS……..…..Graphite Furnace Atomic Absorption Spectrometry

GLS…….….Gas Liquid Separator

HG……..…..Hydride Generation

HG-AAS…….....Hydride Generation Atomic Absorption Spectrometry

HPLC……...…High Performance Liquid Chromatography

HPLC-HG-EHQTA……..High Performance Liquid Chromatography Hydride Generation Electrically Heated Quartz Atomizer

HPLC-HG-WC-ETA…..…High Performance Liquid Chromatography Hydride Generation W-coil Electrothermal Atomization

iAs……..…Inorganic Arsenic

IBMK……..…Isobutyl Methyl Ketone

ICP-AES……..Inductive Coupled Plasma Atomic Emission Spectrometry

ICP-MS…….Inductive Coupled Plasma Mass Spectrometry

ID……..…Internal Diameter

IEC…….....Ion Exchange Chromatography

IPC……Ion Pair Chromatography

LC…….……Liquid Chromatography

LLE……..…..Liquid-Liquid Extraction

LOD……..… Limit of Detection

MMA……..Monomethyl arsenic acid

MPC…….. Maximum Permissible Concentration

NADPH…… Nicotinamide Adenine Dinucleotide

oAs……Organic Arsenic Compound

PRC……...Pre-reduction Coil

QTA……..Quartz Tube Atomizer

RC…….....Reaction Coil

SC…….……Stripping Coil

SEC……..……..Size Exclusion Chromatography

SPE……...Solid Phase Extraction

SQTA…….……...Slotted Quartz Tube Atomization

SQTA-AT…….Slotted Quartz Tube Atomization Atom Trap

SRM……..…..Standard Reference Material

STPF…….....Stabilized Temperature Platform Furnace

TGA……. ……Thioglycolic Acid

THB…….….Tetrahydroborate

VCG…….....Volatile Compound Generation

VG…….Vapor Generation

WC……...W-coil or Tungsten Coil

WC-ETA……..W-coil Electrothermal Atomization

WC-ETV……..W-coil Electrothermal Vaporization

# CHAPTER 1

# INTRODUCTION

## 1.1- The nature of analytical chemistry

Analytical chemistry is a measurement science consisting of a set of powerful ideas and methods that are useful in all fields of science, engineering, and medicine. It involves the separation, identification, and quantification of chemical components of natural and artificial materials [1]. The separation of chemical components is often performed prior to qualitative and quantification analysis. Qualitative analysis gives an indication of the identity of the chemical species in the sample, and quantitative analysis determines the concentration of certain components in the substance.

Analytical methods can be separated into classical wet chemistry and instrumental techniques. Classical methods use separations such as precipitation, extraction, or distillation and classical qualitative analysis is by color, odor, or melting point. Classical quantitative analysis is achieved by measurement of weight or volume. Instrumental methods use apparatus to measure physical quantities of the analyte such as light absorption, fluorescence, conductivity or mass to charge ratio, and separation is accomplished by using chromatography, electrophoresis or field flow fractionation methods [2].

Analytical chemistry has long played a major role in the field of scientific investigation. In addition to providing new tools and techniques to facilitate experimental studies, it has also opened up new areas of research in modern sciences in the areas of forensics, bioanalysis, clinical analysis, environmental analysis, and materials analysis.

Most recently it has been focused on improvements in experimental design, chemometrics, and the creation of new measurement tools to provide better chemical information.

### 1.2- The history of atomic absorption spectrometry

The underlying principles of atomic absorption spectrometry were established in the second half of the 19th century by Robert Wilhelm Bunsen and Gustav Robert Kirchhoff. Both professors at the University of Heidelberg in Germany, systematically examined the line reversal in the spectra of alkali and alkaline-earth elements and conclusively demonstrated that the typical yellow line emitted by sodium salts in a flame identical to the black D line of the sun's spectrum that was discovered in 1802 by Wollaston and was later investigated in detail by Fraunhofer, who assigned letters to the strongest lines, starting at the red end of the spectrum with the letter A to the sodium D line [3].

Kirchhoff had already recognized the principle of atomic absorption in 1860 and formulated the relationship between emission and absorption in his law, which is generally valid and states that any material that can emit radiation at a given wavelength will also absorb radiation of that wavelength. But the connection between atomic structure and the interaction of atoms with radiation was established by Planck (1900) in the quantum law of absorption and emission of radiation, according to which an atom can only absorb radiation of well-defined wavelength $\boldsymbol{\lambda}$ or frequency $\boldsymbol{v}$, so the energy that an atom can absorb and release is a definite amount and is given $\boldsymbol{\mathcal{E}}$:

$$\boldsymbol{\mathcal{E} = hv} \qquad \text{Where } \boldsymbol{h} \text{ is Planck's constant}$$

Since Kirchhoff recognized the principle of atomic absorption in I860, the theoretical basis was steadily extending during the following decades; however, the practical significance of this technique was not recognized for a long time.

At that time, the principle of atomic absorption was mainly used by astronomers to determine the composition and concentration of metals in the atmospheres of stars. Chemical analyses were only carried out very sporadically by this technique; however, the determination of mercury vapor did, acquire a degree of importance [3].

In 1955, an Australian scientist Alan Walsh introduced the modern form of atomic absorption spectrometry (AAS). The introduction of this technique was timely, since the determination of elements in minerals, metals and alloys was a very important analytical issue. During those days, molecular spectra were usually obtained in absorption and atomic spectra in emission, and there was nothing like atomic absorption spectra. The method was received to offer many vital advantages over atomic emission spectra as far as spectrochemical analysis was concerned. Atomic absorption spectrometry offered the possibility of avoiding excitation interference, which at that time was thought by many to be responsible for some of the inter-element interferences experienced in emission spectroscopy when using an electrical discharge as light source both atomization and excitation source[4]. Furthermore, the technique was welcomed by many analytical chemists as a powerful alternative to spectrophotometric methods, which usually required some chemical pretreatment of samples, such as buffering, complexation, extraction and other operational steps, whereas dissolution of the sample into an aqueous medium was usually sufficient for using flame AAS.

### 1.3- Development of atomic absorption spectrometry

Atomic absorption spectrometry is one of the most popular spectroscopy techniques for qualitative and quantitative determination of up to70 elements at trace levels. The only elements that are not dealt with are the noble gases and several of the common gases whose resonance lines fall in the vacuum ultraviolet, for which commercial equipment is not designed.

In addition, some common nonmetallic elements, such as sulfur, phosphorus, and the halides, can be treated by indirect methods [5]. Alan Walsh is generally recognized as the ‘father’ of modern AAS. This privilege was given due to his campaign and untiring energy against the resistance to this new idea for more than a decade, spending much time to overcome the disinterest and misunderstanding from the scientists [3].

### 1.4- Principle of atomic absorption spectrometry

Atomic absorption technique is based on the measurement of selective absorption of light by free atoms created in an atomizer. By this process, the sample is converted into free atoms in the gaseous state by a process known as *atomization* and the free atoms absorb the optical radiation (light) from a source. The main components of an AAS are shown in Figure 1.1. The function of the instrument is as follows: (1) the radiation source, a hollow cathode lamp (HCL) or an electrodeless discharge lamp (EDL), emits a sharp line spectrum characteristic of the analyte atoms; (2) the emission beam from the radiation source is modulated; (3) the modulated signal passes through the atomic vapor where the atoms of the analyte absorb radiation of the line-like radiation source; (4) the desired spectral line (usually resonance line) is selected by the monochromator; (5) the isolated analyte line falls onto the detector (a photomultiplier) where the light signal is converted into the electrical signal; (6) the modulated signal is amplified by a selective amplifier; (7) the signal is finally recorded by a readout device (computer screen, strip chart recorder, or through data processing to a digital display unit or printer) [6].

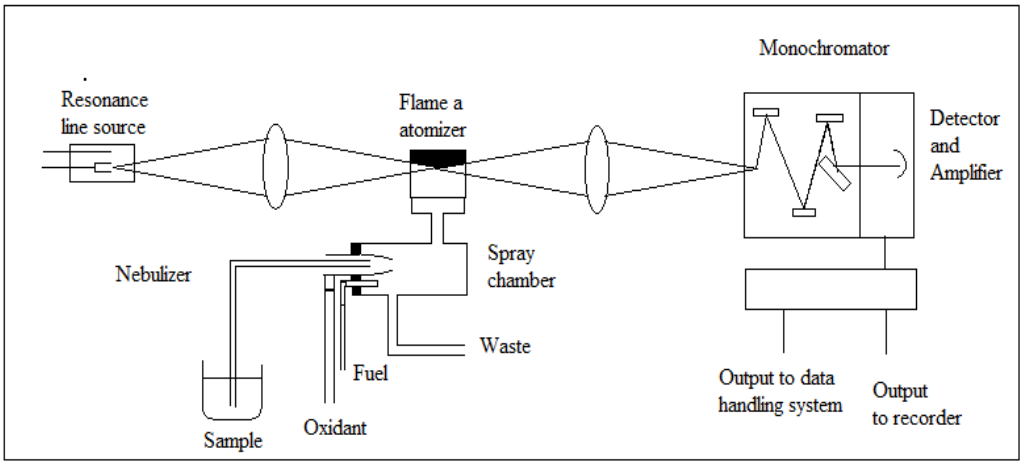


**Figure 1.1** The main components of an atomic absorption spectrometer [6]

### 1.5- Classification of AAS on the basis of atomizer and sample introduction

To obtain high sensitivity, low baseline noise, and high efficiency sample introduction, atomic absorption spectrometry technique can be classified into several categories depending on the atomization and sample introduction procedures:

#### 1.5.1- Atomizer units

The atomizer is the 'place' in which the analyte is atomized, its task is to generate as many free atoms in the ground state as possible and to maintain them in the absorption volume for as long as possible. The sensitivity of atomic absorption spectroscopy is directly proportional to the atomization degree of the analyte element (which also depends on temperature), which is in turn dependent on the effectiveness of the atomizer [7].

The common atomizers used in AAS includes: flame, graphite furnace (GF), flame-in-tube (FIT), quartz tube atomizer (QTA), and slotted quartz tube atomizer (SQTA).

For an ideal atomizer of volatile compounds with either AAS or AFS, the set of the following criteria should be fulfilled [7]:

1. Complete conversion of analyte to free atoms;
2. No reactions of free atoms in the observed volume;
3. Long residence time of free atoms in the observation volume to reach high atomizer-and-spectrometer sensitivity;
4. Minimum contribution to measurement noise to minimize the limit of detection (LOD);
5. Analyte preconcentration in the atomizer to reach high procedure sensitivity (this is not useful for some applications, e.g. ‘‘hyphenated’’ speciation analysis, which requires on-line signal detection);
6. User-friendliness including robustness of the atomizer functions;
7. Low running and investment cost.

In volatile compound determination, the atomizers can be either operated as on-line atomization or in-atomizer trapping technique. However, in order to improve sensitivity and to reduce interference coming from the liquid phases, the use of in-atomizer trapping, which is in line with the criteria 1, 2 and 3; became a widely used technique.

#### 1.5.1.1- Flame atomizers (FAAS)

The flame atomization technique is the oldest of the AAS atomizers and has been a workhorse for the determination of trace elements since 1960’s. In the monograph of B. Welz and M. Sperling [3], eight pre-requirements for an ideal flame have been elaborated, and among them, (1) the flame must have sufficient thermal energy to rapidly atomize the sample without causing ionization of the analyte. (2) it should allow both reducing and oxidizing conditions, (3) the flame should be transparent to the absorption radiation,

(4) it should allow atoms to remain in the absorption volume for long time, (5) it should produce a laminar combustion, so that distribution of the atoms in the absorption volume is constant, (6) the flame should be long to provide high sensitivity, (7) the flame gas and combustion products should not pose any health problems and (8) the flame operation should be inexpensive.

However there is no real flame atomizer that can meet all of the requirements. The temperature of the flame and thus the atomization efficiency depends on the types of fuel and oxidant as well as fuel to oxidant ratio. Nowadays, the air-acetylene flame is the most commonly used one and the less common one is the nitrous oxide-acetylene flame. These two flames are very close to the requirements of an ideal flame, and air-acetylene is more preferred because the oxidant (air) is less expensive.

In flame atomization technique, the analyte solution is converted to an aerosol and then introduced to the flame via a nebulizer at a flow rate of 5-10 mL/min. The function of nebulizer is to use pressurized gas flow to convert liquid phase into a mist composed of small droplets, called *aerosol*; the larger droplets are not allowed to reach the flame since they alter the temperature and thus atomization efficiency. The nebulization efficiencies of nebulizers commonly employed in flame atomic absorption spectrometry (FAAS) instruments does not exceed 10% [8]; Most of the sample is not transported to the atomizer and there is a great dilution of the sample by flame gases. The resulting analyte concentration in the measurement zone is relatively low where the source beam and atoms occupy the same volume for signal formation. The second deficiency is the short residence time of analyte atoms in the measurement zone; this value, considering flame velocities and beam geometry, could be calculated to be in the order of few milliseconds. Both of these deficiencies limit the sensitivity of the flame AAS Technique the most important drawbacks of FAAS [8].

### 1.5.1.2- Graphite furnace or electrothermal atomization

Graphite furnace technique was first developed by Boris L'vov, and it was made known only three years after the rediscovery of AAS. However the development of the first commercial GF AAS accessory onto the market took nearly ten years after FAAS. The reason for this delay was the improvement of the limits of detection by two to three orders of magnitude was not discernible until the end of the 1960s.
Two hot areas of investigation during the development of graphite furnace were the ideal dimensions and shape of the graphite tubes. Many investigations were made for the ideal length and the diameter of the graphite tubes. Güell and Holcombe [9-11] made a series of model calculations on the theme of tube dimensions and found that the geometry of the atomizer should be approximately 5 mm in diameter, and an optimum length of maximum 40 mm. However, another problem in graphite tubes was the non-isothermal absorption zone in the atomizer. To eliminate this problem, three solutions were used: (1) to atomize by capacitive discharge or (2) use of probe atomization, or (3) platform atomization [3]. Graphite furnace needs water cooling system, therefore rapid cooling cannot be achieved if online speciation analysis is to be performed. Although a wide variety of graphite tube designs have been used over the years, the dimensions nowadays are typically 20–25 mm in length and 5–6 mm inner diameter.

In principle, the graphite tube is operated by introducing a sample volume of usually 10-50 µL into atomizer of electrothermal atomization and the temperature is increased stepwise to remove the solvent and concomitants as completely as possible before atomization. Since the entire aliquot introduced into the graphite tube is atomized within a short time (typically 1 s), a peak-shaped, time-dependent signal is generated whose area (integrated absorbance) is proportional to the mass of the analyte in the measurement solution. Graphite furnace or electrothermal atomization (ETAAS), vapor generation techniques such as cold vapor (CVAAS) and hydride generation (HGAAS) provided a sensitivity improvement of 100–1000 fold over flame AAS.

### 1.5.1.3- Conventional quartz tube atomizer

The quartz tube atomizer, in principle is only use for the determination of gaseous/volatile compound of hydride forming elements. Different designs such as the L-shape quartz tube and T-shape quartz tube have been developed since its introduction. The most common design is the T-tube, and the L-tube is only used occasionally. In general, the design of the quartz tube normally contains an inlet arm where the gaseous sample passes through and a horizontal optical arm where the radiation from light source passes through. Narrow diameter of the inlet arm normally produces better sensitivity and the optical arm is often around 150 mm long with diameter typically around 10 mm [12]. The conventional quartz tube atomizer can be classified into two basic types: flame-in-tube atomizer (FIT) and conventional externally heated QTA (EHQTA).

In both types, the hydride generated under optimum conditions, is fully atomized in the cloud by reactions with extremely energetic H radicals. The free analyte atoms produced are stable within the H radical cloud, i.e., in the presence of a sufficient excess of H radicals. Even if free analyte atoms reacted to form molecular species, they should be re-atomized by the interaction with the excess of H radicals [7].

Various designs of FIT atomizers have been described in the monograph of J. Dědina, D.L. Tsalev, [12]. A convenient design [13] employs a capillary centered in the inlet arm of the T-tube to introduce a small flow of oxygen to the atomizer to support a highly fuel-rich, hydrogen–oxygen diffusion microflame, essentially invisible, burning at the capillary end. The capillary end is typically 2 to 10 mm upstream of the T-tube junction [12].

FITs do not require any external heating, however, the carrier gas must contain a large fraction of hydrogen to support the microflame. Since it is an oxygen–hydrogen flame, a temperature of around 2800 °C is expected within its body [7] with steep downward gradients occurring in its vicinity. H radicals are formed either in the

flame or by reactions between oxygen and hydrogen that took place at the entrance to the hot region of the tube. The heat produced by the microflame is controlled by the oxygen supply. For small flow of oxygen a very low amount of heat is produced and the volume of the microflame is small in size compared to the volume of the atomizer. Therefore, the temperature in the remaining part of the inlet arm and in the optical tube is rather low [14].

In conventional QTA, an external heating system is required. The external heating systems normally employ either an electrical resistance device or the acetylene-air flame to heat the optical tube of the atomizer to a temperature between 700 °C and 1100 °C. The carrier gas is usually argon. At least a small fraction of hydrogen in the atomizer atmosphere is required for hydride atomization; otherwise no free atoms are observed. Hydrogen is usually present since it is formed by decomposition of tetrahydroborate used for the hydride generation [7]. Conventional EHQTA atomizer do not employ a special tube to introduce oxygen but a certain oxygen content in the gas mixture is necessary for achieving optimum sensitivity.

At the beginning of the hot zone of the atomizer a cloud of H radicals, analogous to that in FITs, is formed by reactions between oxygen and hydrogen. The exact position of the cloud is controlled by the temperature profile within the atomizer, by the total gas flow rate and composition, and by atomizer design [12, 13]. For example, the cloud may be located well downstream in the inlet arm, in the T-tube junction or even in the optical tube of the atomizer depending on heating temperature and gas flow rate to the atomizer [12]. The same mechanism of hydride atomization in a conventional EHQTA as in a FIT indicates that these two types of conventional QTA are, in principle, identical. However, the main differences between conventional EHQTA atomizer and FITs are [7]:

(i) The technique of creating the H radical cloud: in FITs in a small self-supporting flame burning at the end of the oxygen delivery capillary; in conventional EHQTAs by external heating of the gases containing hydrogen and a small fraction of oxygen.

(ii) The mobility of the cloud in conventional EHQTAs compared to its fixed position by the capillary in case of FITs. The primary function of the elevated temperature in the conventional QTA is to start reactions between hydrogen and oxygen that generate H-radicals.

### 1.5.2- Sample introduction

#### 1.5.2.1- Liquid sample introduction

For liquid measurement, a nebulizer is used to transport the liquid solution into the spray chamber where it is turned into fine aerosol and then mixed with the flame gases. For efficient transfer of liquid and converting them to aerosol, several nebulizers have been introduced and these include: pneumatic, rotating disk, ultrasonic and electrostatic nebulizer. However, it is only the pneumatic nebulizer that has come into general use in AAS; because, it is cheap and energy of nebulization is provided by the nebulizing gas (the oxidant).

#### 1.5.2.2- Solid sample introduction

The introduction of solid samples to AAS for analysis involves the direct introduction of the solid sample in the absorption volume without prior digestion or dissolution. The method can reduce the time of analysis; it can lower the risk of contamination from reagents, apparatus, and the laboratory atmosphere in ultratrace analyses. It lowers the risk of loss of the analyte during sample preparation due to volatilization, sorption on the apparatus, or incomplete solubilization.

Nevertheless, the direct introduction of solid sample incorporates marked disadvantages and the technique places considerable requirements on the skill of the operator. For example it is more difficult to introduce a solid sample into the atomizer than a liquid sample. The inhomogeneity of the sample makes numerous replicate measurements necessary, which can be unacceptable for routine analyses [3].

### 1.5.2.3- Gaseous sample introduction

Gaseous sample introduction is achieved by vapor generation technique that is a wide- spread method used for the determination of metals, metalloids, and organometallic compounds. The two prominent forms of vapor generation are: cold vapor generation (CVG) and hydride generation (HG). Vapor generation is generally employed due to its inherent advantages that generally lead to an improvement in detection limit. These advantages are: (i) efficient separation of the analyte from the sample matrix, which often leads to a reduction of interferences and better detection limit (ii) high transport efficiency of gaseous analyte into the atomic absorption spectroscopy detector; (iii) extremely mild atomization conditions that can be used for the gaseous analyte forms, and can compete in achieving detection limits with the more expensive and complicated instrument such as inductively coupled plasma mass spectrometry (ICP-MS); (iv) high selectivity in some cases to permit differentiation of chemical species of a particular element; (v) simple analyte pre-concentration; and (vi) enabling used of gas phase separation method for speciation analysis of some elements.

The most popular techniques for the generation of volatile species are: chemical vapor generation, electrochemical vapor generation, photochemical vapor generation, and sonochemical vapor generation [15].

#### 1.5.2.3.1- Electrochemical vapor generation

Electrochemical hydride generation is performed in an electrolytic cell. The basic cell consists of two compartments, the anodic and cathodic spaces, separated by a semipermeable medium that enables electrical contact but limits the diffusion of reaction products between the compartments. On the cathode, water/hydronium ions are reduced to molecular hydrogen, a reaction which competes with the formation of the hydride, whereas on the anode water is oxidized to oxygen. Thus hydride is generated in the cathode space of an electrolytic cell with concurrent oxidation of water in the anodic compartment [16]. At least three sequential steps are involved in the process, including reduction and deposition of the analyte onto the surface of the cathode; stepwise reaction of the deposited metal with hydrogen co-generated on the electrode and desorption of analyte hydride. However, the design of the electrolyte generator is paramount to success of this approach.

#### 1.5.2.3.2- Photochemical vapor generation

This system involves the generation of volatile hydride from elements by UV irradiation in the presence of low-molecular-weight organic acids. The photochemical approach was first applied for volatile chemical generation (VCG) of selenium [17] and by using a low-pressure mercury lamp as the source of UV radiation volatile selenium hydride, selenium carbonyl, dimethyl selenide, and diethyl selenide were generated in the presence of formic, acetic, propionic, and malonic acids, respectively, and In acetic acid solution, the efficiency of generation was estimated to be 50±10%.

#### 1.5.2.3.3- Sonochemical vapor generation

This is a cold vapor generation technique within the context of green chemistry for the determination of mercury in liquid samples following high-intensity ultrasonication. The mechanism involved lies in the reduction of Hg(II) to Hg(0) by reducing gases formed upon sonication and subsequent volatilization of Hg(0) due to the degassing effect caused by the cavitation phenomenon. Even though the vapor generation of Hg can occur in ultrapure water, Carlos Bendicho *et al* [18] have reported that upon addition of a low molecular weight organic acid such as formic acid, favors better generation of volatile Hg.

#### 1.5.2.3.4- Chemical vapor generation

Chemical vapor generation is by far the oldest method used for vaporization of trace metals. In the 1830s James Marsh developed a method now called Marsh test for the chemical generation of arsenic hydride. In Marsh test, shown in Equation 1 and 2, a sample containing arsenic element is mixed with sulfuric acid and arsenic-free zinc, the resulting arsine gas was ignited and decomposed to pure metallic arsenic by passing it to a cold surface. This would appear as a silvery-black deposit. So sensitive was the test that it could detect as little as one-fiftieth of a milligram of arsenic [3]. The equation of Marsh test is as follows:

$$As_2O_3 + 6\ Zn + 6\ H_2SO_4 \rightarrow 2\ AsH_3 + 6\ ZnSO_4 + 3H_2O \quad (1)$$

The $AsH_3$ is passed through a heated tube where it is decomposed as arsenic and hydrogen, forming a black mirror film of arsenic in a cold zone.

$$2\ AsH_3 \rightarrow 2\ As + 3H_2 \quad (2)$$

Chemical vapor generation can also be classified into cold vapor technique and hydride generation technique.

### 1.5.2.3.4.1-The cold vapor technique

This method involves the determination of volatile compound without the use of atomizer. Mercury has a vapor pressure as high as 0.0016 mbar at 20 °C, which corresponds to a concentration of approximately 14 µg/L of atomic mercury in the vapor phase. The possibility thus exists of determining mercury directly by AAS without an atomizer.

Poluektov and Vitkun introduced the most successful technique for the determination of mercury by flame AAS, they discovered an unusually large increase in the absorbance, by one or two orders of magnitude, if tin(II) chloride was added to the sample being aspirated. This effect could be attributed to the reducing action of this reagent, which ensured that virtually all of the mercury being aspirated passed into the flame in the atomic state. They thereupon eliminated the nebulizer and flame, passed air through the sample after tin(II) chloride had been added, and then conducted the air through a 30 cm quartz cell mounted in the radiation beam of the atomic absorption spectrometer. The limit of detection (LOD) obtained by this technique amounted to 0.5 ng Hg [3].

Another element that can also form monoatomic vapor is cadmium. Sanz-Medel *et al.*[19] were the first to describe a highly sensitive Cd determination by the cold vapor technique AAS and by adding sodium tetrahydroborate, an unstable cadmium hydride ($CdH_2$) intermediate is formed, which then decomposes to atomic cadmium, permitting measurement by AAS. On the other hand, generation of atomic and molecular Cd species from aqueous media upon reaction with $NaBH_4$ was recently investigated by Yong-Lai Feng *et al* [20]. It is demonstrated that generated atomic species were stable in water, having a half-life of 2.2 min. The authors suggested that the initial products of the reduction reaction appeared to be free atoms, not the hydride, and subsequent interaction with nascent hydrogen gave rise to the molecular hydride.

### 1.5.2.3.4.2- Hydride generation technique

The aqueous-phase chemical hydride generation of volatile hydrides such as Ge, Sn, Pb, As, Sb, Bi, Se, Te, Hg, Cd, and, more recently, several transition and noble metals by acid derivatization of borane complexes is one of the most powerful and widely employed methods for determination and speciation analysis of these elements in trace and ultratrace levels [21].

In 1969, W. Holak [22] was the first to apply hydride generation for the determination of arsenic using AAS. Similar to that employed in the 'Marsh test', He generated hydrogen by adding zinc to the test sample solution acidified with hydrochloric acid and collected the arsine in a trap cooled in liquid nitrogen. At the end of the reaction he warmed the trap and conducted the arsine with a stream of nitrogen into an argon-hydrogen diffusion flame to measure the atomic absorption.

However the Zn-acid system for hydride generation was progressively replaced by the more convenient $NaBH_4$-acid reaction system following the first applications reported by R. Braman and co-workers who determined trace mercury [23], arsenic, and antimony [24] by atomic spectrometry. Subsequently, the $NaBH_4$-acid reaction system was successfully extended to all the other classical hydride-forming elements, Bi, Ge, Sn, Pb, Se, and Te [25], at trace level.

#### 1.5.2.3.4.2.1-Tetrahydroborate acid reduction system

The hydride formation by the tetrahydroborate reduction ($NaBH_4$/acid reaction) of analyte is usually performed in acidic (most often HCl) medium. Tetrahydroborate decomposes very rapidly in acidic media to form boric acid and hydrogen. The mechanism of chemical hydride generation by derivatization with tetrahydroborate (1–) ($BH^-_4$) salts such as $NaBH_4$ the most commonly used and less frequently used is

$KBH_4$ was initially based on the assumption of nascent hydrogen generation in the reaction of $NaBH_4$ with acid and Zn-acid systems [21] shown in Equation 3, 4 and 5.

$$[BH_4]^- + H^+ + 3H_2O \longrightarrow H_3BO_3 + 8H^\cdot \quad (3)$$

$$Zn + 2H^+ \longrightarrow Zn^{2+} + 2H^\cdot \quad (4)$$

The resultant atomic hydrogen reacts with aqueous ions of the element, $E^{(m+)}$, forming the volatile hydride.

$$E^{(m+)} + (m + n)\, H^\cdot \longrightarrow EH_n + m\, H^+ \quad (5)$$

The first authors that proposed this simple reaction mechanism were Robbins and Caruso [26], but it has never been proven.

However, the hypothesis of chemical hydride generation taking place according to the "nascent hydrogen" pathway has been a matter of debate inside the analytical community. An excellent synthesis of this debate was reported by Dědina in 1999 [27] who concluded that, at that time, there was no convincing evidence supporting or refuting the "nascent hydrogen" hypothesis.

In 2002, Laborda et al. [28] strongly criticized the possibility that atomic hydrogen could be formed during hydrolysis of $NaBH_4$, based on thermodynamic considerations. Considering that the estimated standard reduction potential for the $H^+/H$ couple is $E°(H^+/H) = –2.016$ V, neither THB [$E°(H_3BO_3/[BH_4]^-) = –0.482$ V], nor zinc [$E°(Zn^2/Zn) = –0.763$ V], would be able to perform the reduction of protons to atomic hydrogen.

In a recent review, the reaction mechanism of chemical hydride generation based on the direct transfer of hydrogen from boron to the element through analyte-borane complex intermediates has been critically studied by Alessandro D'Ulivo *et al* [21].

In pure aqueous solution, the THB and borane complexes decompose to give both dihydrogen and boric acid as the principal final products. This is a hydrolysis reaction formally consisting of two processes:

(i) A hydroxyl group replaces the hydride in the coordination sphere of boron, giving boric acid and (ii) a disproportion reaction between hydride and proton yields dihydrogen **as** shown in Equation 6

$$[BH_3X]^z + H_3O^+ + 2H_2O \rightleftharpoons H_3BO_3 + 3H_2 + [HX]^{z+1} \quad 6$$

Or in aqueous solution where the acid is $H_2O$ itself in Equation 7

$$[BH_3X]^z + 4H_2O \rightleftharpoons H_3BO_3 + 3H_2 + [HX]^{z+1} + [OH]^- \quad 7$$

Where X = $H^-$, $CN^-$, $OH^-$, $RS^-$, $NR_3$ etc., and the charge of the complex is z, the same as the ligand X.

However when X is $H^-$, the mechanism of acid hydrolysis of tetrahydroborate ion ($[BH_4]^-$), can be described as follows: The first step is the hydronium attack on the hydride, forming the $BH_3(H_2)$ intermediate, which then decomposes to give the first mole of dihydrogen as shown in Equation 8 and 9:

$$[BH_4]^- + H_3O^+ \rightleftharpoons BH_3(H_2) + H_2O \longrightarrow BH_3(H_2O) + H_2 \quad 8$$

$$[BH_4]^- + H_3O^+ \rightleftharpoons BH_3(H_2) + OH^- \longrightarrow BH_3(OH^-) + H_2 \quad 9$$

From Equation 6 to 9, the hydrolysis of the borane complex is simultaneously accompanied by direct transfer of the hydrogen from borane or from the reaction environment to the analytical substrate $[EY_n]^z$, in order to produce a volatile element hydride. The study of the mechanism using deuterated boranes in $H_2O/H_3O^+$, or hydrogenated boranes in $D_2O/D_3O^+$, a hydride generation system was coupled with GC-MS [29-31] and the elements such (E = As, Sb, Bi, Ge, Sn, etc.; Y = $H_2O$, $OH^-$, $Cl^-$, etc., and *z* is the charge) where converted into its volatile hydrides, $EH_m$. Although the reaction gave some isotopologues product, but the product such as $EH_{m-x}D_x$ was formed during the study, which result from the different processes through which H and D can be incorporated into the final hydrides. This study

evidently shows that during volatile formation, there is a direct transfer of hydrogen from boron to the hydride forming element as shown in equation 10.

$$[EY_n]^z + XBD_3 \longrightarrow \text{Reaction intermediates} \longrightarrow EH_{m-x}D_x \qquad 10$$

### 1.5.3-Atomization for volatile hydride compounds

The final step of the process of element determination or of speciation analysis employing volatile compound generation is atomization and detection. In principle, atomization methods can be either on-line or they can incorporate in-atomizer trapping to enhance the sensitivity of the determination.

#### 1.5.3.1- Online-atomization

On-line atomization means that hydride from the hydride generator is immediately introduced to the observation volume of the spectrometer and atomized there. The efficiency of analyte hydride delivered to the atomizer depends on the optimization condition of the hydride generation parameters. In AAS the signal produced by on-line atomizer is generally a time dependent and the temporary value of the signal is proportional to the supply of hydride [7], which gives the sensitivity of the whole analytical procedure.

Moreover, the sensitivity of the atomizer depends on the (i) the atomic absorption coefficient, (ii) atomizer temperature, (iii) atomization efficiency, (iv) gas flow rate, (v) atomizer dimensions, and (vi) extent of decay of free analyte atoms within the atomizer [12]. It should be stressed that the value of atomic absorption coefficient is, besides AAS instrument parameters such as spectral lamp emission profile and slit width, significantly influenced by the atomization temperature and the nature of the gas.

However, any on-line atomizer is characterized by two essential parameters such as: atomizer sensitivity and atomizer noise. The different type of atomizers used for on-line atomization of volatile hydrides is extensively reviewed by J. Dedina [7].

### 1.5.3.2- In-atomizer trapping or atom trapping

One of the inherent advantages of generation of volatile forms of analyte for analytical atomic spectrometry is that the analyte can be easily pre-concentrated. The principle of atom trapping operates by trapping the hydride species on the surface of an atom trap held at an optimized temperature and, finally, revolatilizing the analyte species by rapid heating of the trap and transporting them in a carrier gas to a heated quartz tube, as commonly used with hydride generation AAS systems

The trapping can take place on the surface of the atomizer segment which is aligned in the optical path of the instrument. In most of these systems the design is to provide a longer residence time for analyte atoms; therefore the term *trap* was occasionally used, mostly meaning a delay for atomic species in the measurement zone. The terminology "*in-situ*" trapping, also suggested in one of the first papers on in-atomizer trapping in GF [32], accurately reflects the nature of the process. In most recent review [8] the term atom trapping was used to reflect the trapping analyte hydride atoms on a pre-heated surface. Thus in-atomizer trapping offer a better sensitivity than on-line atomizer.
The procedure of in-atomizer trapping consists of two steps:
(i) trapping/collection and
(ii) volatilization/atomization.

In the first step, the analyte carried from a generator as hydride is trapped in the atomizer until its evolution is completed. For the optimum performance of the method it is highly desirable to trap the generated hydride completely. With incomplete trapping, not only the maximum sensitivity is not achieved but a small

deviation in an experimental parameter may lead to a significant change in trapping efficiency, and thus also in sensitivity.

The trapping efficiency is defined as the fraction of generated hydride trapped in the atomizer. It is sometimes useful to define the "overall efficiency of HG and trapping", as the fraction of the total analyte amount trapped in the atomizer [7].

In the second step, the trapped analyte is volatilized and atomized within typically less than 1 s. The volatilization efficiency is defined as the fraction of trapped analyte that are volatilized or atomized at the same time. In-atomizer trapping significantly enhances the procedure sensitivity. In-atomizer trapping could also be an effective tool for reducing interferences in the liquid phase by sample dilution or by slower addition of the reducing agent.

#### 1.5.3.3- Types of atom trapping

##### 1.5.3.3.1- In situ trapping in graphite furnaces

In-situ trapping in GF is still a popular atomization method for all analytically important hydrides [33-36] and for other elements such as Au [37], Ni [38], and Ag, Cu, Zn [39] as well.

In the first step of the procedure of in-situ trapping in GF, the atomizer is usually heated to approximately 200–600 °C to trap the analyte hydride carried from a generator. In the second step, the trapped analyte is volatilized and atomized at temperatures generally >2000 °C. A pre-atomization cleaning step (600 °C, 20 s) which extends the lifetime of the graphite tube is usually recommended to purge the graphite tube free of water vapor and hydrogen.

The geometry and quality of inner graphite surface, trapping temperature and flow rate of the carrier gas are the critical experimental parameters. The hydride should be introduced in to the furnace in a manner ensuring minimum losses and permitting convenient operation is required. The most convenient interface for introduction of hydride into the graphite furnace is the use of capillary tube most often made of quartz but also titanium has been used [40]. The tube is inserted through the sampling port of the furnace and is usually recommended to position the capillary tip as close as possible to the atomizer inner surface.

After hydride evolution from the generator is complete, the capillary is removed and the volatilization/atomization may be launched. The whole operation can be automated using the autosampler arm to insert and remove the capillary. This is usually performed in combination with permanent modifiers since the autosampler arm is not then required to inject modifier solution to the furnace before the trapping step. Both temporary modifiers such as Pd and permanent modifiers such as Ir can be used. However, permanent modifiers offer more advantages such as broad range of optimum trapping temperatures, and better sensitivity.

The trapping efficiency is most often estimated from the overall efficiency of HG and trapping by the comparison of the signal of trapped analyte with the signal obtained under analogous conditions for the liquid sampling [21]. The trapping efficiency is most often estimated from the overall efficiency of HG and trapping by the comparison of the signal of trapped analyte with the signal obtained under analogous conditions for the liquid sampling. Trapping efficiency is a critical parameter for the performance of the method. The trapping efficiency for a given analyte obviously depends on furnace design, modification of the surface where trapping takes place (graphite tube wall or platform), trapping temperature and the carrier gas flow rate.

#### 1.5.3.3.2- Trapping on quartz and atomization in quartz tube

Another promising approach for in-atomizer trapping is to collect the volatilized analyte in a quartz tube, which can be, in principle, integrated with the QTA. Unfortunately, trapping in quartz atomizers is by far not as straightforward as in GFs. The reason is the 3 orders of magnitude slower heating rate of the optical tube of the QTA [15].

A successful trapping of lead hydride in a bare quartz tube trap with subsequent volatilization and atomization in the conventional EHQTA was announced in 2002 by Korkmaz *et a*l. [41] who suggested that the same trap could also be used for other hydrides. In this study, some quartz particles obtained by crushing, were placed in the inlet arm of a quartz tube atomizer (QTA), near its connection point to the horizontal arm to serve as the trap. The trap location was heated externally using a resistively heated wire. Cold vapor generation (CVAAS) with a quartz trap has also been used for determination of Cd wherein the quartz atom cell was not heated [42].

Like graphite furnace trapping, the most critical analytical parameters for operation of the quartz trap are the temperature of the trap for collection and revolatilization, position of the trap and composition of the carrier gas for both collection and revolatilization.

#### 1.5.3.3.3- Slotted quartz tube atom trap

The slotted quartz tube (SQT) was introduced by Watling in 1977 [43, 44], and has been applied in the determination of As, Sb, Se and Hg [43] and Pb, Zn, Cd, Bi, Co, Mn and Ag [44]. This device provides a sensitivity enhancement of 2-5 folds as compared to FAAS.

The device was a simple hollow quartz tube that was positioned on the laminar flame so that the lower slot coincided with the flame; another slot was made on the tube at an angle of 120° with respect to the lower slot that accepted the analyte atoms from the flame.

In the study made by O.Y. Ataman group [45] SQT was used in an atom trapping (AT) mode where the enhancement in sensitivity is much higher as compared to SQT-FAAS, in the range of 50 to few thousands depending on conditions. In order to effect volatilization of the trapped analyte species, different organic solvents such as iso-octane, n-hexane, acetonitrile, acetone, methyl ethyl ketone, were successfully used; however, isobutyl methyl ketone (IBMK) was chosen after some evaluation [45].

In principle, the operation of SQT-AT can be summarized as follows [8]:

**(i)** Using an optimized flame, sample solution is aspirated while the SQT is positioned above the flame. Analyte atoms are trapped on the inner surface of the SQT. This step usually takes a few minutes and is called collection.

**(ii)** At the end of the collection stage, a rather low volume, 10–50 μL, of an organic solvent is introduced to the flame. This alters the flame composition for a very short period of time, sufficient to release analyte species from quartz surface; this stage is called revolatilization.

**(iii)** Revolatilization is followed by rapid atomization and a transient signal is obtained.

#### 1.5.3.3.4- W-coil for Trapping and Atomization

Tungsten devices have been employed in analytical atomic spectrometry for approximately 30 years [46]. In a recent review of the technique the authors suggest that the characteristics of an ideal electrothermal atomizer material might include: high melting point, high purity, ease of manufacturing into desired shapes, fast heating rate, chemical and physical stability and inertness at high temperature, and durability [46].

Tungsten has the highest melting point (3422 $^{0}$C) among all metals in the periodic chart. While being a good electrical conductor, tungsten is also ductile and may be formed into different shapes reproducibly. Chemically, tungsten is relatively inert, stable in both air and water, and resistant to high concentrations of many common acids, such as hydrochloric, sulfuric and nitric acid. Tungsten is also relatively inexpensive and these combined properties make tungsten a valuable material for the production of common lamp filament [46]. As a result, a variety of tungsten wires can be reproducibly twisted into many shapes and sizes. Many of these could be employed for atomic spectrometric applications. It can be electrically heated up to 3000 $^{0}$C at very high heating rates, with a simple power supply (15 V and 150 W). Unlike graphite furnace, it rapidly cools down without the need of water coolant. Initially W-coil was used only as an electrothermal atomizer in an inert atmosphere, such as Ar. Sampling is similar to that in GFAAS; 5-50 µL of sample solution is injected on W-coil and usual stages such as drying, ashing, atomization and cleaning are then applied.

The analytical figures of merit for W-coil AAS are comparable to those for traditional GFAAS. Both peak height and integrated absorbance have been used for quantification. Generally, peak height provides better sensitivity and lower LODs, while integrated absorbance may give better linearity and improved reproducibility. Berndt *et al* [47] measured sensitivities for 13 elements using a W-coil AAS

instrument and found them to be comparable to those of GFAAS, in most cases. For barium, sensitivity was higher by one order of magnitude with W-coil AAS.

In all such comparisons, there are many atomizer-dependent factors that affect the sensitivity, including the optical length of the atomizer, heating rate, use of chemical modifier and use of open or closed types of atomizers. In W-coil AAS, for example, one of the most important factors is the coil position, including the viewing height (typically 1–3 mm above the coil) and viewing angle [46].

It is also noteworthy that tungsten has also been used as a tube atomizer [48] where the application was for Se and As determination using bare and Pt coated surfaces. In a W-tube atomizer, platinum, iridium and rhenium have been successfully used as chemical modifiers for the determination of Se and As. The platinum-treated tubes were very efficient at collecting hydrides in the low temperature range of 100–200 $^{0}$C, reaching efficiency close to 100%. Iridium- and rhenium-treated tubes were capable of trapping hydrides in the high temperature range of 700–900 $^{0}$C, approaching an overall efficiency of 10%, however palladium modifier caused fatal deterioration of the tungsten tube [48].

The first studies involving atom trapping on a W-coil were reported almost simultaneously for Bi [49] and Se [50]. In this approach volatile analyte species were formed by hydride generation and trapped on a W-coil held at an optimized temperature for trapping; at the end of the trapping period, W-coil is heated to a higher temperature and peak shaped signal is obtained with enhanced sensitivity. Other applications of this technique were reported for determination of Cd [51], Se [52], Sb [53, 54], As [54] and inorganic As species [55].

The use of a chemical modifier has been a common practice in GFAAS since the inception of the modern stabilized temperature platform furnace (STPF) technique by Slavin *et al.*, in 1981 [8]. However, the application of chemical modifiers has been reported far less frequently for metallic atomizers.

Using chemical modifier in W-coil has several advantages that include: increased tungsten coil lifetime by over 400 heating cycles); reduced background levels and eliminated condensed/liquid phase interferences caused by concomitants. Moreover, iridium, thermally-coated onto a W-coil, has also been used as a permanent chemical modifier for the determination of Se in water samples by Xiandeng Hou *et al.* [56]. Each iridium coating lasted for 300–400 firings and the coil could be re-coated for further use. The lifetime of the coil was extended up to 1600 firings. Coating of tungsten coil with chemical modifier also increases the sensitivity and linear dynamic range of the method. Recently the used of Rh-coated tungsten coil has been reported for As determination and for 400 µg Rh coated, the signal remains stable for about 300 firings [55].

In VG tungsten coil can be used ETA for nonvolatile elements too as in ETA-AAS in which the sample vapor is atomized and probed directly in the absorption zone, or as ETV to ICP in which produces a sample aerosol that is then carried by gas to a separate atomizer for analysis. In Figure 1.2 the two modes of operation of tungsten atomizer with hydride generation are shown.

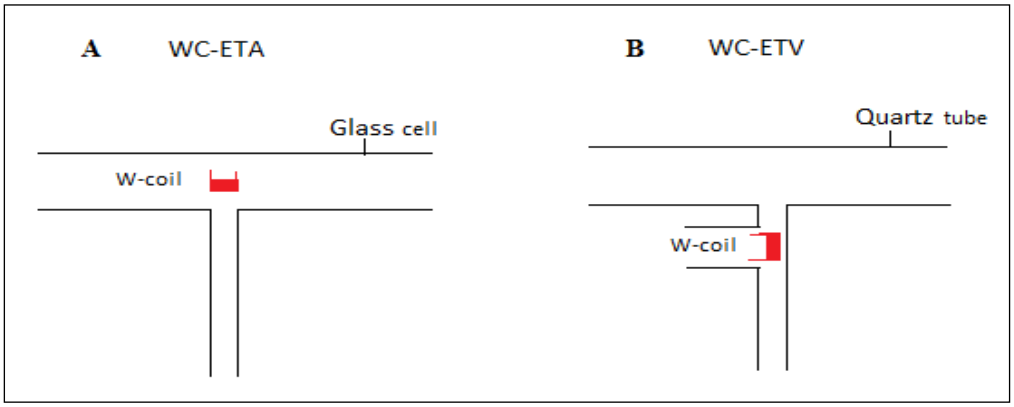


**Figure 1.2** The arrangement of tungsten coil use in analytical atomic absorption spectrometry. **A**-is the ETA coil is in absorption zone and **B**- is the ETV coil vaporized the sample analyte after trapping and atomization take place in the externally heated quartz tube

## 1.6- Arsenic element

Elemental arsenic (As) is a member of Group 15 of the periodic table, with nitrogen, phosphorus, antimony and bismuth. It has an atomic number of 33 and an atomic mass of 74.91 g/mol.

### 1.6.1-Physical properties of arsenic

Arsenic is a semimetallic element and exists in allotropes of as; *metallic gray*, *yellow* and *black arsenic*, with gray being the most common. The gray arsenic is brittle, and a semiconductor with a bandgap of 1.2–1.4 eV at its amorphous structure. It is also the most stable form allotrope. The yellow arsenic is a soft, waxy, and unstable allotrope. Being a molecule, it is the most volatile, least dense and most toxic form. Solid yellow arsenic is produced by rapid cooling of arsenic vapor, and is rapidly transformed into the gray arsenic by light. The black arsenic is a poor electrical conductor and can also be formed by cooling vapor at around 100–220 °C. It is glassy and brittle [57].

When heated in air, arsenic oxidizes to arsenic trioxide; the fumes from this reaction have an odor resembling garlic. This odor can be detected on striking arsenide minerals such as arsenopyrite with a hammer. Arsenic (and some arsenic compounds) sublimes upon heating at atmospheric pressure, converting directly to a gaseous form without an intervening liquid state at 887 K (614 °C).

### 1.6.2- Chemical properties

Naturally occurring arsenic is composed of one stable isotope, $^{75}As$ and pure arsenic is seldomly found in nature. The compounds of arsenic resemble in some respects those of phosphorus which occupies the same group in the periodic table. Arsenic exists in four valency states: –3, 0, +3, and +5. In strongly reducing environments, elemental arsenic and arsine (–3) can exist. Under moderately reducing conditions, arsenite (+3) may be the dominant form, but arsenate (+5) is generally the stable oxidation state in oxygenated environments. Arsenic also bonds readily to itself as seen in the square $As_4^{3-}$ ions in the mineral Skutterudite (cobalt arsenide mineral). In the +3 oxidation state, arsenic is typically pyramidal owing to the influence of the lone pair of electrons [58].

### 1.6.3- Arsenic and arsenic compounds

There are many arsenic compounds in both marine and terrestrial environments. Although the nomenclature and abbreviations of the arsenic species have been a matter of concern to Kevin A. Francesconi and Doris Kuehnelt [59], the nomenclature and abbreviations provided here is the common method found in literature. The names, abbreviation and molecular structures of some these arsenic species are shown in Table 1.1.

**Table 1.1** Names, abbreviations and structures of As species [59]

| **Name** | **Abbreviation** | **Structure** |
|---|---|---|
| Arsenite | As(III) | 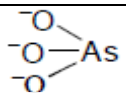 |
| Arsenate | As(V) | 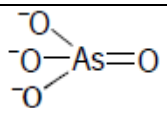 |
| Monoethylarsonite | MMA(III) | 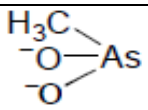 |
| Monoethylarsonate | MMA(V) | 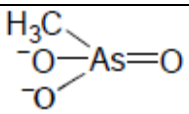 |
| Dimethylarsinite | DMA(III) | 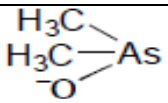 |
| Dimethylarsinate | DMA(V) | 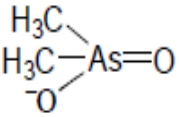 |
| Trimethylarsine oxide | TMAO | 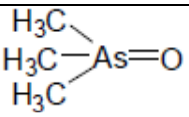 |
| Trimethylarsine | TMA | 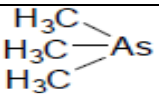 |
| Dimethylarsine | $DMH_3As$ | 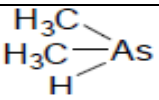 |
| Monoethylarsine | $MMH_3As$ | 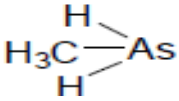 |
| Arsine | $H_3As$ | 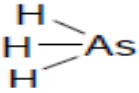 |
| Arsenobetaine | AB | 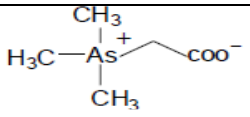 |

**Table 1.1** Names, abbreviations and structures of As species (continued)

| | | |
|---|---|---|
| Arsenocholine | AC | 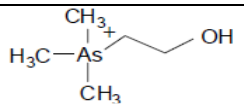 |
| Trimethylarsoniopropionate | TMAP | 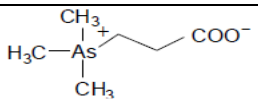 |
| Dimethylarsenoylethanol | DMAE | 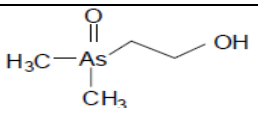 |
| Dimethlyarsinothioylacetate | | 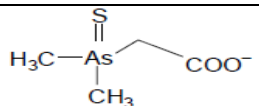 |
| Dimethylarsinoylacetate acid | DMAA | 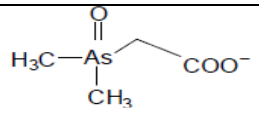 |
| Tetramethylarsonium ion | TETRA | 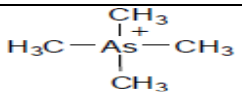 |
| Dimethylated Arsenosugars | | 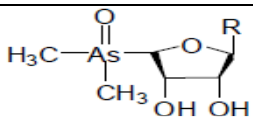 |
| Trimethylated Arsenosugars | | 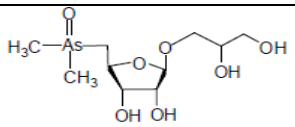 |

### 1.6.4- Sources and occurrence of arsenic

Arsenic is present in more than 200 mineral species, the most common of which is arsenopyrite. It is estimated that about one-third of the atmospheric flux of arsenic is of natural origin. Volcanic action is the most important natural source of arsenic, followed by low-temperature volatilization. Inorganic arsenic of geological origin is found in groundwater used as drinking-water in several parts of the world. Organic arsenic compounds such as arsenobetaine, arsenocholine and tetramethylarsonium salts, arsenosugars and arsenic containing lipids are mainly found in marine organism and some in terrestrial species.

Elemental arsenic is produced by reduction of arsenic trioxide ($As_2O_3$) with charcoal. $As_2O_3$ is a by-product of metal smelting operation. Mining, smelting, of non-ferrous metals and burning of fossil fuels are the major industrial processes that contributes to anthropogenic arsenic contamination of air, water and soil. Historically the use of arsenic-containing pesticides has left large tracts of agricultural land contaminated. The use of arsenic in the preservation of timber has led to contamination of the environment [60].

#### 1.6.4.1- Arsenic in soil

Arsenic occurs mainly as inorganic species but also can bind to organic materials in soils. Under oxidizing conditions, in aerobic environments, arsenates, iAs(V), are the stable species and are strongly sorbed onto clays, iron and manganese oxides/hydroxides and organic matters. Arsenic precipitates as ferric arsenate in soil horizons rich in iron. Under reducing conditions arsenites, iAs(III), are the predominant arsenic compounds.

Inorganic arsenic compounds can be methylated by microorganisms, producing under oxidizing conditions, monomethylarsonic acid (MMA), dimethylarsinic acid (DMA) and trimethylarsine oxide (TMAsO) [60].

Under anaerobic conditions these can be reduced to volatile and easily oxidized methylarsines. The forms of arsenic present in soils depend on the type and amounts of sorbing components soil, such as pH and redox potential. Arsenates of Fe and Al ($AlAsO_4$, $FeAsO_4$) are the dominant phases in acid soils and are less soluble than calcium arsenate, $Ca_3(AsO4)_2$, which is the main chemical form in any alkaline and calcareous soils [60]. The adsorbed arsenate fraction in soils is closely related to soil pH and redox potential (Eh). It also varied with soil type under the same pH conditions, increasing in order from sierozem to brown soil to chestnut soil [60].

Arsenic gets biomethylated (i.e. addition of $CH_3$ to arsenic through biological activity) in the soil–water, sediment water interfaces through the activity of bacteria (such as *Escherichia coli*, *Fla_obacteriun* sp, *Methanobacterium* sp) and fungi (such as *Aspergillus glaucus*, *Candida humicola*). In the course of biomethylation, iAs(III is oxidized to iAs(V) and $CH_3^+$ is reduced to $CH_3^-$ and stable arsenic oxy-species are formed [61].

#### 1.6.4.1.1- Factors influencing arsenic content in soil

The principal factors influencing the concentration of elements in soils are the parent rock and human activities. Factors such as climate, the organic and inorganic components of the soils and redox potential status also affect the level of arsenic in soils. When rocks are weathered, arsenic may mobilize as salts of arsenous and arsenic acids ($H_3AsO_4$) [60].

### 1.6.3.2- Arsenic in water

In natural waters, arsenic is commonly found as inorganic arsenic (iAs), while organic arsenic (oAs) species occur in marine and biological samples. iAs is more toxic than its organic counterparts. iAs is found in water in the form of As(V) and As(III), as $H_3AsO_3$ and $H_3AsO_4$, respectively. Depending on the $pK_a$ values and pH of the medium, different species are predominant in solution. The As(III) forms are more toxic than the As(V) forms. The maximum permissible concentration (MPC) of total arsenic in drinking water is set at 10 µg/L [61], while the limit values for arsenic species are not established.

The major chemical form in which arsenic appears to be thermodynamically stable is arsenate ion. A wide range of relative proportion of dissolved arsenate and arsenite is present in groundwater. The concentration of arsenic in unpolluted fresh waters

typically ranges from 1-10 µg/L, rising to 100–5000 µg/L in areas of sulfide mineralization and mining [60].

At moderate or high redox potentials arsenic can be stabilized as a series of pentavalent (arsenate) oxyanions, $H_3AsO_4$, $H_2AsO_4^-$, $HAsO_4^{-2}$ and $AsO_4^{-3}$. However, under most reducing (acid and mildly alkaline) conditions and lower redox potential, the trivalent arsenite species ($H_3AsO_3$) predominate. As(0) and As(-III) are rare in aquatic environments. Complex organic arsenic compounds such as tetramethylarsonium salts, arsenocholine, arsenobetaine, dimethyl(ribosyl)arsine oxides and arsenic containing lipids are identified in the marine environment [62]. Only a very minor fraction of the total arsenic in the oceans remains in solution in seawater, as the majority is sorbed on to suspended particulate materials.

Various geological and geochemical conditions can control the concentrations of arsenic in ground water. These factors include leaching of geological material; factors such as pH, Eh, solution composition, sediment chemistry/mineralogy, grain size distribution of aquifer sediment, competing and complexing ions, aquifer mineralogy, reaction kinetics, and hydraulics of the groundwater system [63].
Normally groundwater does not contain methylated form of arsenic but lake and pond waters contain arsenite, arsenate as well as methylated forms, i.e. MMA and DMA.

#### 1.6.3.3- Arsenic in air

In air, arsenic exists predominantly absorbed on particulate matters, and is usually present as a mixture of arsenite and arsenate, with the organic species being of negligible importance except in areas of arsenic pesticide application or biotic activity [64]. The human exposure of arsenic through air is generally very low and normally arsenic concentrations in air ranges from 0.4 to 30 ng $m^{-3}$ [65].

### 1.6.5- Metabolisms and toxicity of arsenic

#### 1.6.5.1- Metabolism

Humans are exposed to many different forms of inorganic and organic arsenic species (arsenicals) in food, water and other environmental media. Each of the forms of arsenic has different physicochemical properties and bioavailability and therefore the study of the kinetics and metabolism of arsenicals in animals and humans is a complex matter.

Routes of arsenic intake in vivo are considered to be via the respiratory tract for arsenic in dust and fumes, and through oral means for arsenic in water, beverages, soil, and food. Few investigations of dermal absorption rates for arsenicals are undertaken. The bioavailability of ingested inorganic arsenic varies depending on the matrix in which it is ingested (i.e. food, water, beverages or soil), the solubility of the arsenical compound itself and the presence of other food constituents and nutrients in the gastrointestinal tract [60]. Tissue distributions of arsenic depend on blood perfusion, tissue volumes, diffusion coefficients, membrane characteristics, and tissue affinities. The fate of ingested arsenic in vivo depends on: (1) oxidation and reduction reactions between iAs(V) and iAs(III) in the plasma; and (2) consecutive methylation reactions in the liver [59]. Inorganic arsenic is methylated in vivo in human. Arsenate is rapidly reduced to arsenite, which afterwards is partly methylated. The main site of methylation appears to be the liver, where arsenic methyltransferase enzymes mediate the methylation process with *S*-adenosylmethionine as the methyl donor and glutathione (GSH) as an essential co-factor. Studies on humans suggest that methylation may begin at limiting dose of about 0.2–1 mg/kg (0.003–0.015 mg As $kg^{-1}$ per day) [66]. R. M. Raie [67] compared tissue arsenic levels in infants (aged 1 day to 5 months) and adults from Glasgow, Scotland using neutron activation analysis (NAA).

Mean levels of arsenic (mg $kg^{-1}$ dry weight) in liver, lung and spleen in infants versus adults are 0.0099 versus 0.048, 0.007 versus 0.044, and 0.0049 versus 0.015, respectively. These data suggest that arsenic accumulates in tissues with age, a finding that is wholly consistent with observations in laboratory animals [68].

In most animal studies DMA is the main metabolite, while in human the urinary excretion consists under normal conditions, (i.e. without excessive ingestion of inorganic arsenic) of about 20% inorganic arsenic, 20% MMA and 60% DMA. Because, inorganic arsenic gets methylated to MMA and DMA in vivo and during circulation in plasma MMA is partly absorbed and this absorbed MMA is further methylated to DMA, while DMA is excreted mainly in an unchanged form [69, 70]. Moreover in more recent studies, the reduction of both MMA(V) and DMA(V) to their trivalent analogues monomethylarsonous acid, MMA(III) and dimethylarsinous acid, DMA(III) respectively and excreted through urine was also reported. However, similar studies are unavailable for other organoarsenicals [71, 72].

Studies with radioactively labeled ($^{74}As$) arsenate in human showed that 38% of the dose was excreted in urine within 48 h and 58% of the total within 5 days [73]. In the subjects who ingested 500 µg As in the form of arsenite, 33% of the dose was excreted in the urine within 48 h and 45% within 4 days [70]. It is estimated that about 60–70% of the daily-ingested inorganic arsenic is excreted in the urine [74].
Excretion of arsenic via other routes than via urine and feces (e.g. in sweat), are in generally minor amounts. Since arsenic can accumulate in keratin-containing tissues [60], skin, hair and nails can also be considered as potentially minor excretory routes. The three most commonly employed biomarkers used to identify or quantify arsenic exposure are total arsenic in hair or nails, blood arsenic, and total or speciated metabolites of arsenic in urine. Because arsenic (as the trivalent form) is accumulated in keratin-rich tissues such as skin, hair and nails, they are used as indicators of past arsenic exposure. Recently, Bin Hu and Fei Zheng [75] developed a method of dual-column capillary microextraction combined with ETV-ICP-MS for the speciation of arsenic in human hair extracts.

Normally inorganic arsenic is very quickly cleared from human blood. For this reason blood arsenic is only used as an indicator of very recent and/or relatively high level exposure, for example, in poisoning cases [76] or in cases of chronic stable exposure (i.e. from drinking water). Studies show that in general blood arsenic does not correlate well with arsenic exposure in drinking water, particularly at low levels.

As common with any other biomarkers of arsenic exposure, arsenic levels in urine may result from inhalation exposure as well as ingestion from food and water, thus provide a measure of the total absorbed dose. However, since arsenic is rapidly metabolized and excreted into the urine, the levels of arsenic in urine are best suited to indicate recent arsenic exposure. Hence total arsenic: inorganic arsenic and the sum of arsenic metabolites (inorganic arsenic + MMA + DMA), in urine are all used as biomarkers of recent arsenic exposure. This approach becomes increasingly uncommon because certain organoarsenicals (for example, the practically non-toxic compound arsenobetaine) present in substantial amounts in certain foodstuffs are excreted mainly unchanged in urine [77]. Therefore using total urinary arsenic under these conditions will result in overestimation of inorganic arsenic exposure.

To avoid the potential for over-estimation of inorganic arsenic exposure inherent in using total urinary arsenic, most studies now measure speciated metabolites in urine, and used either inorganic arsenic or the sum of arsenic metabolites (inorganic arsenic + MMA + DMA) as an index of arsenic exposure. However, this can give misleading results unless a careful diet history is taken and/or seafood consumption is prohibited for at least 3 days prior to urine collection. There are two reasons for this. First, some seafoods contain the arsenic metabolites MMA and DMA, particularly DMA, in fairly high amounts. Secondly, arsenosugars present in seaweeds and some bivalves are extensively metabolized to DMA (either by the body itself or the gut microbiota), which is then excreted in urine [60].

### 1.6.5.2- Toxicity

With regards to toxicity of arsenic, the chemical forms and oxidation states are virtually very important. In addition to chemical form and oxidation states, the toxicity of arsenic also depends on other factors such as physical state: gas, solution, or powder particle size, the rate of absorption into cells, the rate of elimination, the nature of chemical substituents in the toxic compound, and the pre-existing state of the patient. The toxicity of arsenicals decrease in the order, arsines > iAs(III) > arsenoxides (org As(III)) > iAs(V) > arsonium compounds > As [78].

Studies in laboratory animals have demonstrated that the toxicity of arsenic is dependent on its form and its oxidation states. It is generally recognized that the soluble inorganic arsenicals are more toxic than the organic ones, and the iAs(III) are more toxic than iAs(V) [63, 79].

In a study the British Geological Survey *et al* [80], the arsenic-affected areas of Bangladesh the modal proportion of iAs(III) appears to be between 50 and 60% of the total arsenic. Because ingested iAs is extensively metabolized in humans, chronic exposure to iAs results in chronic exposure to methylated and dimethylated arsenicals. MMA(III), a biotransformant of inorganic arsenic, is up to 26 times more toxic than inorganic arsenite in Chang human hepatocytes [81]. According to Lin et al. [82], MMA(III) is over 100 times more potent than iAs(III) as an in vitro inhibitor of thioredoxin reductase. So, formation of MMA(III) appears to represent toxification of both iAs(V) and iAs(III). Also, in vitro studies have shown that MMA(III) and DMA(III), like iAs(III), can form GSH complexes, and that these are at least as toxic as iAs(III) [83, 84] and in vitro study showed that MMA(III) was more cytotoxic to human cells (hepatocytes, epidermal keratinocytes, and bronchial epithelial cells), compared to iAs(III) and iAs(V) [84]. The authors concluded that high methylation capacity did not protect these cells from the acute toxicity of trivalent arsenicals.

Generally, the most common toxic mode-of- action for an element is the inactivation of enzyme systems, which serves as biological catalyst [60] Trivalent arsenic interferes with enzymes by bonding to -SH and -OH groups, especially when there are two adjacent HS-groups in the enzyme. The enzymes, which generated cellular energy in the citric acid cycle, are adversely affected. The inhibitory action is based on inactivation of pyruvate dehydrogenase by complexation with iAs(III), whereby the generation of adenosine-5-triphosphate (ATP) is prevented. The enzyme system comprises of several enzymes and cofactors, one protein molecule of enzyme having one lipoic acid. In the presence of iAs(III), it replaces the two hydrogen atoms from the thiol groups and attaches with a sulfur molecule and form a dihydrolipoylarsenite chelate complex, which prevents the reoxidation of the dihydrolipoyl group that is necessary for continued enzymatic activity, and this pivotal enzyme step is blocked. As a result, the amount of pyruvate in the blood increases, energy production is reduced, and finally the cell damages slowly [85, 86]. The reactions are shown in Figure 1.3.

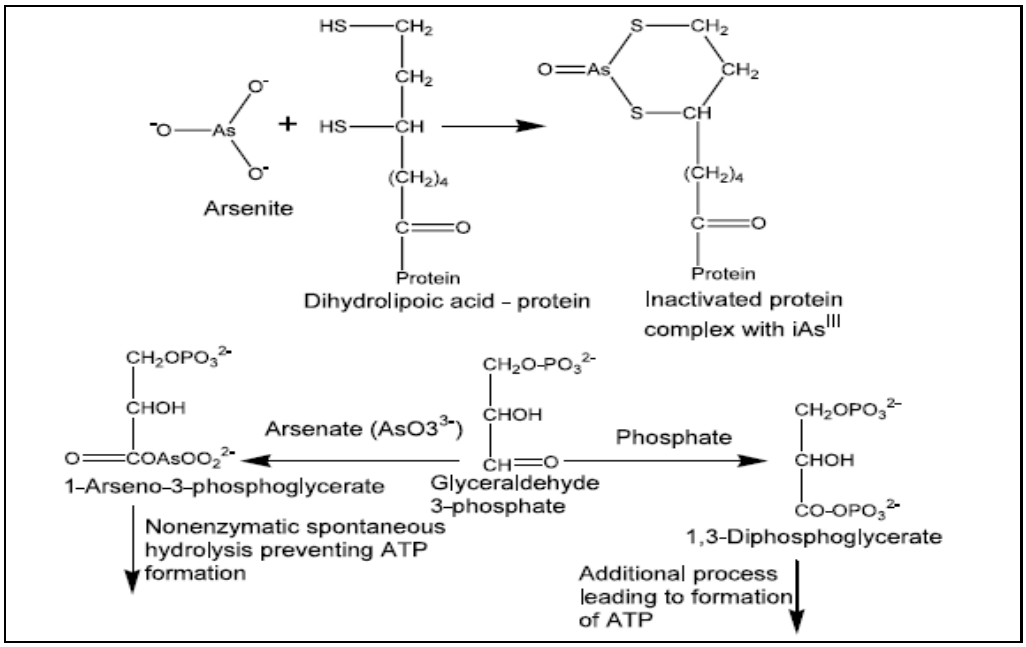


**Figure 1.3** The mode-of- action of iAs(III) in preventing the generation of adenosine-5-triphosphate (ATP) [60, 85, 86]

As a result of the strong bond between iAs(III) and sulfur may be the reason why arsenic accumulates in the keratin tissues hair and nail. It is proposed that trivalent arsenic form a stable ringed structure with vicinal dithilols of keratin in hair [60]. Arsenic inhibits enzymes, such as the pyruvate oxidase, *S*-aminoacid oxidase, choline oxidase and transaminase. Although iAs(III) is regarded the more toxic form of the element, iAs(V) as arsenate can be disruptive by competing with phosphate. For example, arsenate uncouples oxidative phosphorylation. Oxidative phosphorylation is the process by which ATP is produced, while at the same time reduced nicotinamide adenine dinucleotide (NADPH) is oxidized [87] as shown in Equation 11 and 12.

$$3ADP + 3H_3PO_4 \rightarrow 3ATP + 3H_2O \quad (11)$$

$$NADPH + H^+ + 1/2O_2 \rightarrow NADP^+ + H_2O \quad (12)$$

The arsenate disrupts this process by producing an arsenate ester of ADP, which is unstable and undergone hydrolysis non-enzymatically. This process was termed as arsenolysis. Hence the energy metabolism is inhibited and glucose-6-arsenate is produced rather than glucose-6-phosphate [60].

Arsenate may also replace the phosphorous in DNA and this appears to inhibit the DNA repair mechanism. Such an action may explain the clastogenicity of arsenic, because an arsenodiester bond will most likely be weaker than the normal phosphodiester bond. However, no direct evidence is located to show that arsenate is incorporated into DNA. In environments where phosphate concentrations are high, arsenate toxicity to biota is generally reduced. Arsenic-contaminated environments are characterized by limited species abundance and diversity. If levels of arsenate are high enough, only species, which exhibited resistance, may be present [88].

Chronic exposure to inorganic arsenic may give rise to several health effects including effects on the gastrointestinal tract, respiratory tract, skin, liver, cardiovascular system, hematopoietic system, nervous system etc.

However there is no published information concerning toxicological effects in human exposed orally to organoarsenicals. Some of the health effects of arsenic exposure to various internal and external organs are summarized in Table 1.2

**Table 1.2** Some of the health effects of arsenic exposure to various internal and external organs [60]

| Health effect | Condition |
|---|---|
| Respiratory | laryngitis, tracheae bronchitis, rhinitis, pharyngitis, shortness of breath, chest sounds (crepitations and/or rhonchi), nasal congestion and perforation of the nasal septum |
| Pulmonary | chronic cough and lung disease |
| Cardiovascular | Abnormalities in heart and peripheral arteries such as cardiovascular abnormalities, Raynaud's disease, myocardial infarction, myocardial depolarization, cardiac arrhythmias, thickening of blood vessels and their occlusion |
| Gastrointestinal | Manifestation of dry mouth and throat, heartburn, nausea, abdominal pains and cramps, and moderate diarrhea and Anorexia, malabsorption and weight loss may be present |
| Hematological | Anemia (normochromic normocytic, aplastic and megaloblastic) and leukopenia (granulocytopenia, thrombocytopenia, myeloid, myelodysplasia) are common effects of poisoning |
| Hepatic | Since the liver tends to accumulate arsenic with repeated exposures, hepatic involvement is reported most commonly as a complication of chronic exposures over periods of months or years. |

**Table 1.2** Some of the health effects of arsenic exposure to various internal and external organs (continued)

| | |
|---|---|
| Renal | The kidneys are the major route of arsenic excretion, as well as a major site of conversion of pentavalent arsenic. Sites of arsenic damage in the kidney includes capillaries, tubules and glomeruli, which leaded tohematuria and proteinuria |
| Dermal | Arsenic toxicity produce a variety of skin insignia such as diffused and spotted melanosis, leucomelanosis, keratosis, hyperkeratosis, dorsum, Bowen's disease, and cancer |
| Neurological | Acute high exposure (1 mg As $kg^{-1}$ per day or more) often causes encephalopathy with symptoms as headache, lethargy, mental confusion, hallucination, seizures and coma |
| Reproductive | Inorganic arsenic readily crosses the placental barrier and affects fetal development which result to increased fetal, neonatal and postnatal mortalities, and elevations in low birth weights, spontaneous abortions, still-birth, pre-eclampsia and congenital malformations. |
| Mutagenetic | Mutagenesis includes the induction of DNA damage and a wide variety of genetic alterations, these changes may cause genetic damage transmissible to subsequent generations, and/or some may cause cancer |
| Carcinogenic | Arsenical skin cancers commonly occur in the presence of dermatologic manifestations of arsenicism, and some has internal neoplasms that are regarded as arsenical in origin and the cancer risk sites are notably the lung, skin, bladder, kidney and liver |

### 1.6.6- Uses of arsenic

Some of the potential usages of arsenic compounds are given in the following sections.

#### 1.6.6.1- Insecticides

Arsenic is a widely used element for the preparation of insecticides and pesticides. Some of the form of pesticides, are: lead arsenate, $Ca_3AsO_4$, copper acetoarsenite, Paris-Green (copper acetoarsenite), $H_3AsO_4$, MSMA (monosodium methanearsonate), DSMA (disodium methanearsonate) and cacodylic acid are used in cotton production as pesticides [89].

#### 1.6.6.2- Herbicides

The inorganic arsenicals, primarily, sodium arsenite, were widely used since about 1890 as weed killers, particularly as non-selective soil sterilants [90].

#### 1.6.6.3- Feed additives

Many arsenic compounds are used for feed additives. These compounds includes: $H_3AsO_4$, 3-nitro-4-hydroxy phenylarsonic acid, 4-nitrophenylarsonic acid etc [60].

#### 1.6.6.4- Poison

Arsenic compounds are infamous as very potent poisons and are preferred as homicidal and suicidal agents [57].

### 1.6.6.5- Desiccants and wood preservatives

Arsenic acid in the form of $H_3AsO_4$ is used extensively as a cotton desiccant in the U.S. since in 1964 [60].

The first wood preservative was Fluor–Chrome–Arsenic–Phenol (FCAP), which was used as early 1918 in USA. Chromated Copper Arsenate (CCA) and Ammonical Copper Arsenate (ACA) in combination were used in 99% of the arsenical wood preservatives. Wolman salts and Osmosalts, zinc and chromium arsenate are also used as wood preservative [57, 90].

### 1.6.6.6- Drug

Large quantities of arsenic have been used for softness and cleanliness of the skin, to give the plumpness to the figure, beauty and freshness to the complexion and also to improve the breathing problem Common medicinal preparations, which contained arsenic, includes: Fowler's solution (potassium arsenite), Donovan's solution (arsenic and mercuric iodides), Asiatic pills (arsenic trioxide and black pepper), de Valagin's solution (liquor arsenic chloridic), sodium cacodylate, arsphenamine (Salvarsan), neoarsphenamine, oxophenarsine hydrochloride (Mapharsen), arsthinol (Balarsen), acetarsone, tryparsamide and carbarsone [57].

## 1.6.7- Speciation analysis

As has become apparent for studies of the biogeochemistry of many of the elements, especially those that enter the human food chain, the information about chemical composition needed is not just the concentration of the total element, but about the concentrations of all the different compounds that contain the element of interest [90]. This distribution of an element among various different chemical forms is known as "speciation".

The International Union of Pure and Applied Chemistry (IUPAC) define speciation analysis as the analytical activities of identifying and/or measuring the quantities of one or more individual chemical species in a sample. The definition of species is based on several different levels of atomic and molecular structure where chemical forms of a same element are manifested. The different chemical forms are: (1) isotopic composition, (2) electronic or oxidation state, (3) inorganic and organic composition of their complexes, (4) organometallic species, and (5) macromolecular compound and complexes.

Fractionation is the process of classification of an analyte or a group of analytes from a certain sample according to physical (e.g. size, solubility) or chemical (e.g. bonding, reactivity) properties [91].

Speciation studies are of interest to chemists doing research on the evaluation and chemical treatment of waters, soils, and sediments, to biologists inquiring about the influence of species on animals and plants, and to geochemists investigating the transport of elements in the environment. However, the most important reason for speciation analysis is to identify the metal species that have adverse effects on living organisms. The interaction of metals with biota is highly dependent on their chemical forms, being the impact of some metals strongly related to their oxidation state and/or organic or inorganic structure, rather than to their total concentration [92].

Consequently, biotransformation of elements in aquatic systems, quantification of individual species of an element should be well known for the real analysis of the toxicity of the element. The fundamental requirement in element speciation is the need to determine each of the forms of a given element quantitatively, independently and without interference from the other forms. From this point of view, "an ideal element speciation method is one that can provide the desired information without altering the original sample and the quantification of different metal species is rather difficult because the concentration of heavy metals in the environment is generally very low relative to the detection limits of the available analytical techniques" [93].

### 1.6.7.1- Arsenic speciation analysis

Arsenic speciation is an important consideration, since the different forms of arsenic having different properties and different toxicity; and as mentioned above, arsenic is generally toxic in both arsenite and arsenate forms, but is nontoxic in some highly methylated organic forms, such as arsenobetaine and arsenocholine. Therefore, the speciation of As seems absolutely necessary mainly for toxicity species-dependent which does not well correlate with the total As concentration. Therefore, determination of total As in a sample is of limited value because the result does not usually reflect the true level of hazard of that element. Hence, speciation of As is highly relevant in providing meaningful risk assessment data to assess the appropriate hazard level [92].

Distribution of an element among its various species will affect the behavior of a particular element greatly. And this is accepted by many by science fields and authorities. Now by means of new developments in analytical instrumentation and methodology make us to identify and measure the species present in a particular system. Thus IUPAC recommends that the term speciation should be used to indicate "the distribution of species in a particular sample or matrix" [91].

### 1.6.7.2- Analytical techniques in arsenic speciation

In speciation analysis of arsenic, both chromatography and non-chromatographic methods are used.

Non-chromatographic method is used for inorganic species of elemental speciation and the respond obtained from the active hydride forming chemical species of the element, is used to determine the other chemical species by subtracting the total respond from the active species after pre-reduction process (i.e. total inorganic arsenic $As_t$ = As(III) + As(V)). Non-chromatographic chemical speciation is still

growing because they can offer simple and inexpensive ways to made speciation or, at least, for the determination of specific or toxic forms of trace elements [92].

The method of cryogenic trapping involves the collection hydride in a cold trap. The hydride is then most often purged into an atomizer simultaneously with evaporation after heating the trap. The marked advantage of cryogenic trapping is that the hydride can be collected from a very large volume of sample and the collected hydride can be subsequently evolved and transported to the atomizer/detector very rapidly. The sample volume with cryogenic trapping is limited by the capacity of the apparatus to handle water vapor and aerosol formed in the reaction vessel. However, pronounced losses should be expected for less stable hydrides (plumbane, tellurium hydride, stannane, and bismuthine). A further disadvantage of the cryogenic collection is that it is time consuming and involves considerable effort [15].

Nowadays, the combination of chromatography, in its various modes, with sensitive spectroscopic detection methods has coalesced into hyphenated techniques. The evolution and advantages (mainly a high degree of automation, a good reproducibility and a short analysis time) of the hyphenated techniques have become the method of choice.

### 1.6.7.3- Procedures in chromatographic speciation method of arsenic

#### 1.6.7.3.1- Sampling and sample pretreatment for speciation

The most practical difficulty encountered in speciation is to preserve the integrity of the sample and the species of interest during sampling, storage and pretreatment and because of that, procedures which result in a modification of equilibria or in a transformation of the different species must be avoided [93]. The weather conditions and nature and seasonal affects should be considered during sample collection from

natural media. The sampling itself needs to be planned, designed for the specific sample, documented and controlled to assure quality effectively.

Biological samples should be kept at low temperatures as bacteria can deform the structure of the tissue or the sample to be analyzed, so protection of the sample is an important issue.
Another way of preservation is by freeze drying in which water is removed from the sample. The mass of the wet and dry sample before and after freeze-drying respectively is very important as this will allow us to calculate the moisture content in the sample. After freeze-drying process, the sample is dry and is ready to be homogenized. The sample should be homogeneous because it is important to minimize errors resulting from moisture in calculations [94].

#### 1.6.7.3.2- Extraction

The extraction of arsenic species from sample matrices requires efficient procedure with efficient extraction solvent. It should be highlighted that the risk of producing a wrong result increases with the number of analytical steps and with their complexity therefore minimizing the extraction period and steps is also important in extraction procedures. Water samples can generally be analyzed without any extraction procedure [95] but arsenic in solid samples must be extracted prior to speciation analysis, because ″in situ″ determination of As is currently impossible at low concentrations. The extraction step is very crucial to make sure that no transformation of species occur during extraction, moreover one should be sure that all As species present in a sample is extracted [96]. Since no chemical extraction is currently ideal, a combination of various extractants aliquot is often recommended to reach this efficient extraction.

In solid matrices it is more difficult to extract analyte. Hence optimization of extraction is a need. Commonly methanol/water mixture is used as an extractant. The analyte is often difficult to extract; it is necessary to optimize the procedure for each matrix investigated. Almost certainly, methanol was used because it extracts fewer non-arsenical compounds and it is easy to remove by evaporation. Methanol, however, is a poor solvent for extracting inorganic arsenic species and hence is not suitable for samples containing such species. Trifluoroacetic acid has been used for the extraction of organic and inorganic arsenic species in cooked rice and vegetable [97]. In general it is thought that organic arsenic species will prefer methanol to water as an extra extraction solvent because they are organic. But the organic arsenicals are polar so they can prefer water too.

#### 1.6.7.3.2.1- Various methods of extraction

In an elaborated review, Christian Dietz *et al* [98] gave the various extraction technique for tin and arsenic. Some of the extraction methods are given below:

##### 1.6.7.3.2.1.1-Solvent extraction

Liquid–liquid extraction (LLE) is an easy and provides robust method and has been employed for speciation purposes. In this case a selective complex of one of the species considered is extracted in an organic solvent, being separated from the rest of species of the element considered. In some cases an additional back-extraction step is necessary [98].

#### 1.6.7.3.2.1.2- Solid phase extraction

Solid phase extraction (SPE) is similar with liquid–liquid extraction. The basic approach involves passing the liquid sample through a column, cartridge, tube or disk containing an adsorbent that retains the analytes and subsequent recovery upon elution with an appropriate solvent then the mechanism of retention depends on the nature of the sorbent. The extraction columns is normally filled with anion or cation exchanger, complex forming resin, activated or modified alumina among others. Nonpolar stationary phases such as C18 silica, have also been used in combination with a previous complexation step of some species in order to separate the different chemical forms of an element. Unlike liquid-liquid extraction, solid-phase extraction of species can apply in flow injection analysis (FIA) and connected on-line to the detector [98, 99].

#### 1.6.7.3.2.1.3- Enzymatic extraction

Enzymes can be used to determine a bioavailable fraction of species by mimicking living environments, such as gastric digestion processes proteases, lipases and amylases are examples of extraction material used in this type of extraction [98].

#### 1.6.7.3.2.1.4- Microwave assisted extraction

Microwave is an efficient method for analyte extraction. It can be applied to various matrices during sample preparation. A low power microwave system can be applied for the extraction of organometallic compounds. The aim of using low power is not to break carbon-metal bond during the process. This method can be coupled with separation systems and online procedures can easily be applied [98].

#### 1.6.7.3.2.1.5- Ultrasound processor extraction

In order to fasten the mixing process, ultrasonic probe extraction method can be used. This method provides removal of particles from the substrate itself. At first glance it is simple and efficient but it has disadvantages too. This method has the main disadvantage of non-uniformity in mixing resulted from bubbling in water. The other disadvantage is high local temperature and pressure [98].

#### 1.6.7.3.2.1.6- Sonication extraction

Sonication is the act of applying sound energy to agitate particles in a sample. Maria Ines Soares Melecchi et al. optimized the parameters of sonication extraction such as extraction time, solvent polarity, sample amount, solvent volume and sample particle size and found that the most influential variables were extraction time and solvent polarity [100].

### 1.6.7.3.3- Chromatographic separation techniques

Traditionally, the most common separation technique for the separation of target analytes are separated into their constituent chemical forms or oxidation states before elemental analysis high performance separation technique such as gas chromatography (GC), capillary zone electrophoresis (CE), and several liquid chromatographic (LC) methods like ion ex-change chromatography (IEC) and ion pair chromatography (IPC) on reversed phase HPLC columns are used in the separation of arsenic species in speciation analysis.

Volatile arsenicals found under natural conditions were separated highly efficient by GC. Arsenolipids were determined in fish oil [101]. Several mixed arsenosulfur compounds which were produced by intestinal micro-organisms [102] were

analyzed. Typically, volatile arsenicals are produced in derivatization steps like hydride generation and methyl thioglycolate derivatives were extracted into hexane and determined by GC atomic emission [103]. However, many naturally occurring arsenicals are not volatile and not stabile at the temperature required to keep them in the gas phase. For these compounds liquid separation methods like CE and LC are better suited [104].

High separation efficiencies made CE an attractive method [105]. However, its low amount of analyte mass applied in combination with low sensitivity detectors provides insufficient LOD. CE coupled to more sensitive detectors requires special interfaces and attention to some particular issues.

*HPLC and Ion Chromatography:* chromatographic separations, except size exclusion (SEC), used for arsenic speciation is ion-exchange chromatography. The different types of IC methods are: anion exchange (AEX), cation exchange (CEX), ion exclusion (IEC), ion pair chromatography (IPC).

Since arsenic species cover a whole range of molecule polarities, e.g. anions (As(V), MMA, DMA), cations (AC, TMA) and, depending on the pH, neutral molecules (AB, As(III)), the diverse polarities, the growing number of different types of As-compounds still poses a permanent challenge to IC. Therefore IC method employed for the chromatographic separation should be robust in routine speciation analysis [104].

#### 1.6.7.3.4-Inorganic As(III)/As(V) speciation

The fact that the two most toxic As-compounds are the inorganic As(III) and As(V) justify this fractionation for samples influenced by pure geochemical processes (e.g. groundwater) where no or very minor fraction of organic arsenicals occur.

#### 1.6.7.3.5- Some detection techniques for arsenic determination

The atomic spectroscopy methods that are employed most often for the analysis of arsenic are: AAS, ICP-AES, ICP-MS, and AFS. The inherent part of ICP-AES and ICP-MS is the ICP torch that works as the atomizer. In contrast to ICP-based methods, AAS and AFS have to employ an atomizer. The atomizer used in AAS or AFS can be either online-atomization or in-atomizer trapping of the VC. It should also be noted that atomization interferences in the case of VCG for ICP-based methods are generally insignificant.

##### 1.6.7.3.5.1- Atomic absorption spectrometry

AAS is relatively an inexpensive technique terms of investment as well as running costs. It is a well-established and robust method. It is the most popular atomic spectroscopy method and convenience for volatile compound sample introduction. It is also easily hyphenated with HPLC. However its detection capability for arsenic is less than AFS instrument. But with a suitable pre-concentration method, and using hydride generation as sample introduction, it is possible to improve the sensitive of AAS for arsenic to two orders of magnitude compared with conventional solution introduction. As the noise is not adversely affected, the greatly increased signal-to-noise ratio makes the limit of detection for arsenic by HG-AAS with a quartz tube atomizer similar to that of ETAAS (about $0.05 \mu g L^{-1}$) [90].

##### 1.6.7.3.5.2- Atomic fluorescence spectrometry

The other relatively simple and cheap method is AFS. It generally offers higher sensitivity than AAS, but it is useful for a limited number of elements, such as Hg, As, Se, Sb, Bi and Te. The instrument can be interfaced with continuous flow separations and thus HPLC-AFS (with HG as the interface) is a viable technique for

speciation analysis, and represents something of a niche market as a less expensive alternative to ICP-MS [90].

#### 1.6.7.3.5.3- Inductive coupled plasma atomic emission spectrometry

ICP-AES is, in contrast to AAS and to AFS, a virtually multielemental method. However, it requires more complicated apparatus compared to AAS and its sensitivity cannot compete with that of ICP-MS [7].

#### 1.6.7.3.5.4- Inductive coupled plasma mass spectrometry

ICP-MS is also multielemental, and provides by far the best detection power. However, it is also the most complicated and expensive technique regarding both in investment and running costs. It is well known by all laboratories operating ICP-MS instruments that the determination of arsenic is subject to some particular interferences. The presence of chlorine in the sample, most likely as the chloride ion, gives rise to the formation of $^{40}Ar^{35}Cl^{+}$ at m/z 75 and in many instruments with quadrupole mass analyzers this ion cannot be distinguished from $^{75}As^{+}$ and so the signal is enhanced [90].

Most manufacturers of ICP-MS instruments offer the option of a collision/reaction cell in which unwanted molecular species, such as $^{40}Ar^{35}Cl^{+}$, may be dissociated by collision with a bath gas, such as helium. Alternately, by introducing a gas, such as $O_2$ or $CH_4$ to react with $^{75}As^{+}$, detection can be shifted to m/z 91, in the case of $^{75}As^{16}O^{+}$ or m/z 89 in the case of $^{75}As^{14}CH^{2+}$. Yet a third option is to use a spectrometer with sufficient resolving power to be able to differentiate between the species at the nominal m/z of 75 [90].

### 1.6.7.3.6-Arsenic hydride generation with tetrahydroborate

The conversion of arsenic species such as arsenite As(III), arsenate As(V), methylarsonic MMA and dimethylarsonic DMA, to their corresponding arsines by sodium tetrahydroborate is pH dependent. For arsines to be formed, the acidity of the reaction must be controlled to ensure that the arsenic species are fully protonated. The yield of arsine from each individual species therefore depends on the $pK_a$ values of the corresponding arsenic acids; finding common reaction conditions which can simultaneously satisfy the conditions necessary for the efficient reduction of As(III), As(V), MMAA and DMAA has been difficult [106].

The pre-reductant reagents used for iAs(V), such as potassium iodide in ascorbic acid [107–109], or thiourea in ascorbic acid solution [55] have low stability and take at least 30 min with high concentration for reaching complete pre-reduction. The –SH group, namely L-cysteine (L-cys) became more popular [110]. These agents reduce pentavalent arsenicals to trivalent and react with trivalent arsenicals forming arsinothiol derivates.

It has also been suggested that L-cys is enhancing the HG performance by forming borane complexes with tetrahydroborate [111]. By means of L-cys treatment uniform signals can be obtained from iAs(V), MAs(V) and DMAs(V) [112].

Nevertheless, optimum conditions must be carefully maintained when HG is performed from HCl media, because HG is efficient in a very narrow range of acid concentration (0.01 – 0.1 mol/L) only [113]. This has been solved by the use of buffered media (TRIS·HCl buffer) proposed by Tomáš Matoušek *et al* [112]. The buffer also ensures selective HG only from trivalent As species without pre-reduction.

However in a study reported by A. G. Howard and C. Salou [106], except L-cys, thioglycolic acid (TGA) and other similar compounds with –SH group were tested as the pre-reducing agents. TGA performed well, others such as 2-mercaptoethanol, 3-mercapropropionic acid reduced only one of the three species completely, thiourea commonly used for reduction of Se(VI) to Se(IV) could not reduce MAs(V) at all.

Nowadays, in automation of any analytical methods minimum sample pretreatment is required. Therefore, replacement of the time-consuming off-line pre-reduction by a method with integrated pre-reduction step (on-line pre-reduction) is desirable [110]. No loss of sensitivities, low consumption of all reagents and simplicity are the main requirements. The general limiting factor is reaction rate of pre-reductant with As species which mostly affects analysis time and sample throughput. It was proved that L-cys needs about 1 hour to complete the reaction with iAs(V), MAs(V) and DMAs(V) at room temperature [112]. To achieve on-line pre-reduction of pentavalent arsenicals by means of L-cys, the reactor must be heated [113]. On-line pre-reduction by means of TGA was suggested by A.G. Howard and C. Salou [106], for its short reaction time with inorganic and methylated pentavalent As species.

### 1.7- Aim of study

The aim of this study is to develop a chromatographic on-line speciation of As(III) and As(V) using a W-coil atom trap with AAS. Thioglycolic acid pre-reductant reagent for on-line pre-reduction of As(V) will be used so that the generation of arsine by reaction with sodium tetrahydroborate can be achieved at the same time from both the inorganic arsenic species, As(III) and As(V). The generated arsine will be pre-concentrated or trapped on Ir-coated tungsten coil so that the relatively broad chromatographic peaks will be converted to a transient signal with peak half width of less than 0.5 s. Thus the sensitivity for arsenic determination would be increased to the ng/L level.

# CHAPTER 2

# EXPERIMENTAL

## 2.1- Instrumental

Atomic absorbance measurements were performed using a Thermo Scientific SOLAAR 32 Ice 3000 SERIES AA spectrometer (USA) equipped with a deuterium ($D_2$) background corrector. A PHOTRON Lamps (USA) arsenic hollow cathode lamp was used for arsenic atomic absorption and operated at 8 mA. The wavelength and the spectral band pass were set to 193.7 nm and to 0.2 nm respectively, this small spectral band was chosen so that energy radiation is obtained and to easily focus the beam on the surface of the tungsten coil. Measurements were based on peak height absorbance.

For hydride generation, two flowmeters (Cole Parmer Instrument Co. USA) were used to measure the flow rate of argon and hydrogen gases (99.9% pure) (Linde, Turkey). Two BT100-2J two-way channels peristaltic pumps (LongerPump-Shanghai China) were used to pump sample and reduction reagent solutions and to drain waste solution from gas liquid separator. Two home-made cylindrical gas-liquid separators (GLS) similar to the one described by Matousek *et al.* [114] were constructed in the Glass Shop of Chemistry Department, METU, Ankara and used to separate the arsenic hydride gas from the solution. A 6-port injection valve-040 from IDEX Health and Science LLC (USA) was used for the flow injection sample introduction. Color coded Tygon tubings (Cole Palmer USA) were used in hydride generation system; the red coded tube has internal diameter (ID) of 1.14 mm and the blue coded tube has ID of 1.65 mm.

The Tygon tubes were connected to peristaltic pumps to transport the solutions to reaction coil and then stripping coils. Polytetrafluoroethylene (PTFE) tubes with ID of 0.8 mm were obtained from Cole Parmer, USA) for preparing the reaction and stripping coils. The meeting points of the solutions were made of PTFE T-connectors from Cole Parmer (USA) and nylon knots (Cole Parmer) were used to connect PTFE tubes with T-connectors.

The HPLC pump used was CECIL 1100 SERIES (Cambridge, United Kingdom). An IC-Pak Anion exchanger column (4.6 mm x 5 cm) was bought from Waters (USA).
For microwave oven digestions, Ethos Plus Milestone microwave laboratory system (USA) was used. HP 500 Teflon microwave vessels were used during total arsenic digestion. VWR standard analogue shaker (USA) was used in procedures.

Vortex mixing was performed using an NM 110 vortex mixer from NÜVE (Turkey). For sonication, Elma S40 H sonication bath was employed (Germany). For centrifugations, a bench top centrifuge, NF 200 from NÜVE (Turkey) was used. Filtrations were done using 0.45 µm Metricel membrane filters from Pall Corporation (Mexico).

Freeze drying was performed using the CHRIST ALPHA 2-4 Freeze Dryer (Germany). Measurements for pH were done by using pH meter PHM210 from MeterLab (Ankara, Turkey).

## 2.2- Reagents

All stock and standard working solutions were prepared in deionized water (0.273 µS/cm) which was obtained from TKA-Pacific, Germany. All reagents were of analytical grade. The daily working standards were prepared from standard stock solutions of As(III) (99.32 mg/L) and As(V) (32.9 mg/L) which were prepared by weighing 0.0172 g of solid stock from $NaAsO_2$ (Fisher Scientific USA) and 0.0137 g from $Na_2HAsO_4.7H_2O$ (Fisher Scientific USA) respectively. The solid is then dissolved in 0.8 mol/L nitric acid (Merck Germany) and the resulting solution was appropriately diluted to 100 mL with deionized water. The working solutions were prepared in hydrochloric acid (Merck Germany) with concentration indicated. For the reduction of arsenic species into arsenic hydride, $NaBH_4$ (96% purity, Merck, Germany) was dissolved in 0.3% (w/v) NaOH (CARLO ERBA, France) was used, concentration was adjusted as required.

Thioglycolic acid (TGA) (Merck, Germany) and potassium iodide (KI) (Riedel-de Häen) with L(+)ascorbic acid (Carlo Erba, Italy) were used as pre-reduction agents. In order to improve the trapping efficiency of W-coil, 20 µL of 1000 mg/L of Ir and 1000 mg/L Rh were used for coating and compared on the basis of increasing the efficiency and sensitivity of the method.

Certified reference materials of Waste Water EU-L-2 from Enviro MAT SCP-SCIENCE (Canada), Trace Elements in Water 1643e from NIST (Gaithersburg, MD, USA), Trace Elements in Spinach Leaves 1570a from NIST (Gaithersburg, MD, USA) and Tuna Fish Tissue BCR627 from IRMM (Geel, Belgium) were used to validate the accuracy of the methods.

## 2.3- Procedures

The experimental procedure in this work consist of the constructing of hydride systems shown above and this was followed by alignment radiation of the hallow cathode lamp through the optical arm of either the QTA or the glass cell. For the WC-ETA, the radiation passes on the surface of the coil which was indicated by the signing of the W-coil. Coating of either the newly extracted tungsten coil or the inner QTA was carried out. In WC-ETA, during coating, both hydrogen and argon gas are sent to the system, however for QTA coating, only argon is being sent. Following the coating of the W-coil, the coil is heat to clean the surface and gas trapping was perform and in this study, only the carrier gases are sent and trapped. This was to make sure that the hydrogen and argon gas are free of arsenic contamination. The blank solution was then sent and a calibration study was study for each of the methods used in this research work.

### 2.3.1- The hydride generation manifolds used in this study

Three types of hydride generation manifolds were used in this study. These were
(i) Continuous flow hydride generation (CF-HG) and (ii) Flow injection hydride generation (FI-HG) for total As determination and nonchromatographic speciation and (iii) High performance liquid chromatography with anion exchange column hydride generation (HPLC-HG) for chromatographic speciation of inorganic arsenic species. Outputs of these systems were directed to first gas liquid separator (GLS) and then to atomizer.

### 2.3.1.1- The manifold of continuous flow hydride generation (CF-HG)

The continuous flow hydride generation system consists of two solution compartments; one contains the acidified arsenic sample and the other contains the sodium tetrahydroborate solution that was stabilized in sodium hydroxide. It contains Tygon tubes connected to peristaltic pump and PTFE tubes, used for reaction and stripping coils. The set-up of the CF-HG manifold is shown Figure 2.1.

The important parameters optimized in the technique of hydride generation for inorganic arsenic speciation are the flow rate and composition of sample solution, flow rate and concentrations of the reductant sodium tetrahydroborate solution, the length of the reaction and stripping coils, the flow rate, composition and concentration of pre-reduction reagent to convert As(V) to As(III), and flow rates of argon gas that was introduced between the reaction and stripping coils.

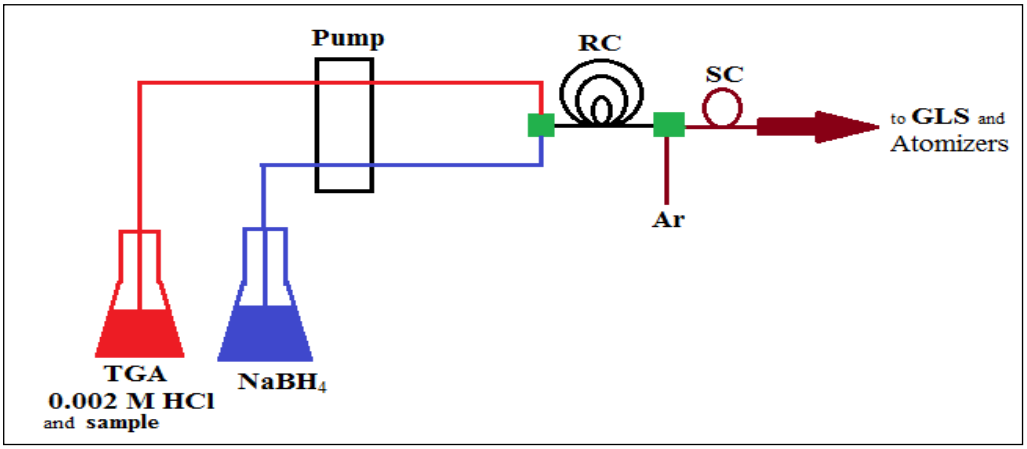


**Figure 2.1** The CF-HG manifold with TGA in 0.002 mol/L HCl for the pre-reduction of As(V) and $NaBH_4$ compartments. Argon gas is introduced between the reaction and stripping coil to strip arsenic hydride. RC: reaction coil, SC: stripping coil.

### 2.3.1.2- The manifold of flow injection hydride generation (FI-HG)

The arrangement of flow injection hydride generation for the online determination As(III) and As(V) is shown in Figure 2.2. The system consists of a sample carrier solution which was made up of a 0.05 mol/L buffer solution of pH 5.8, consisting of ammonium dihydrogenphosphate ($NH_4H_2PO_3$) and phosphoric (V) acid ($H_3PO_4$). The carrier solution transports the sample from the sample loop (SL) to the pre-reduction coil where the As(V) is reduced to As(III) by 1.0% (v/v) thioglycolic acid (TGA) in 0.002 mol/L HCl.

The resulting solution is then mixed with sodium tetrahydroborate solution in the reaction coil (RC) to form arsenic hydride or arsine ($AsH_3$). Arsine is then stripped by argon gas in the stripping coil (SC). The arsenic hydride is again carried by argon to the gas liquid separator(s) for further separation of gaseous arsenic hydride with the solution phase. The analyte vapor is directed by gas flow to electrically heated quartz tube atomizer (EHQTA) or to tungsten coil electrothermal atomizer (WC-ETA) where atom trapping takes place.

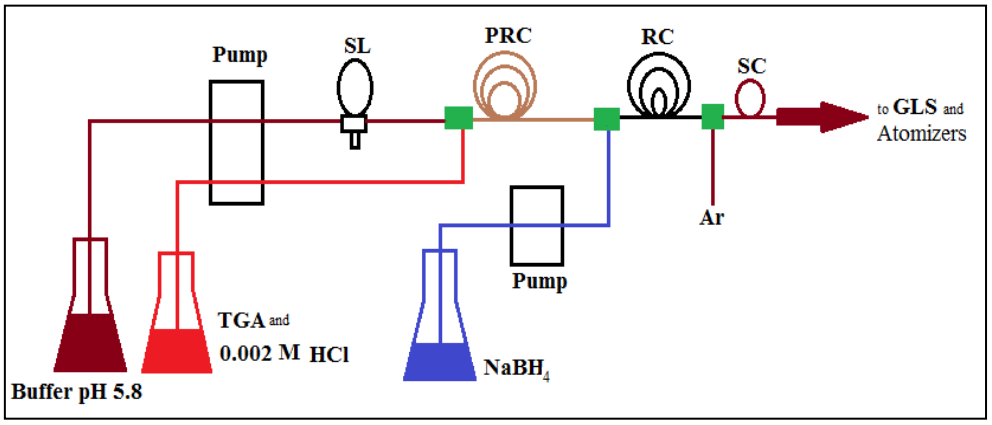


**Figure 2.2** The setup of FI-HG used for online inorganic arsenic speciation. $NH_4H_2PO_4/H_3PO_4$ buffer as sample carrier solution and TGA for online pre-reduction of As(V). SL: sample loop, PRC: pre-reduction coil, RC: reaction coil, SC: stripping coil.

### 2.3.1.3- The manifold of high performance liquid chromatography and hydride generation

The set-up for high performance liquid chromatography hydride generation, consist of a mobile phase reservoir that contains the phosphate buffer solution of pH 5.8, the HPLC pump with injection port and sample loop, a guard column and a strong anion exchanger column. After elution of the analyte from the analytical column, the eluate was made to pass through the pre-reduction coil where it was mixed with TGA solution. The solution mixture is further transported to reaction coil (RC) to react with sodium tetrahydroborate to produce arsine ($AsH_3$).

The arsine gas is then stripped by argon gas in stripping coil, and transported to gas liquid separator where the liquid is sent to waste and the gaseous analyte phase is directed to the atomizer. The arrangement of the HPLC-HG is shown in Figure 2.3.

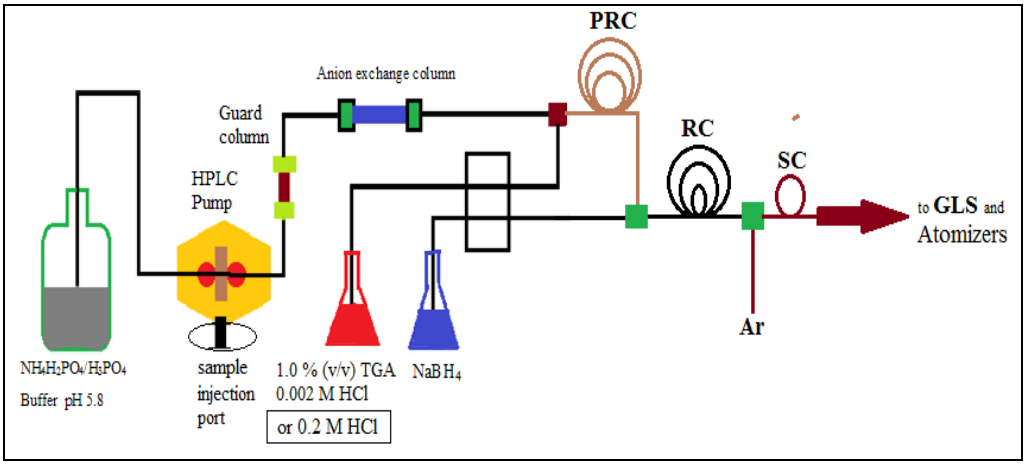


**Figure 2.3** The manifold of HPLC-HG, allowing online pre-reduction of As(V) and the generation of $AsH_3$ which is transported to atomizer. PRC: pre-reduction coil, RC: reaction coil, SC: stripping coil.

#### 2.3.1.3.1- Preparation of HPLC mobile phase

The mobile phase was a buffer solution prepared from ammonium dihydrogen phosphate ($NH_4H_2PO_4$) (Merck, Germany) and 85% pure phosphoric acid ($H_3PO_4$) (Sigma-Aldrich Laborchemikalien, GmbH Germany) at pH 5.8. The Henderson–Hasselbalch equation was used to calculate the amount of $NH_4H_2PO_4$ salt and the volume of $H_3PO_4$ solution needed for 1.00 L to make a concentration of 0.05 mol/L of the buffer solution; thus 0.2202 g of $NH_4H_2PO_4$ was dissolved in deionized water and 3.252 mL of $H_3PO_4$ were added. The pH of the solution was then adjusted with $NH_3$ solution until the pH of 5.8 was obtained. The contents were placed in a 1.00 L volumetric flask and the volume was made up using deionized water. The buffer solution was degassed for 1 hour using sonicator.

#### 2.3.1.3.2- Calculation of buffer solution concentration

The components of the buffer solution used are $NH_4H_2PO_4$ and $H_3PO_4$. The selected pH was 5.8 so the p$K_{a2}$ value of the ammonium dihydrogen phosphate which is 7.2 was selected. To prepare the concentration of 0.05 mol/L, the following calculation was undertaken using from 13 to 17: The molecular weight of $NH_4H_2PO_4$ is 115.03 g/mol and with the Henderson–Hasselbalch equation which is

$$pH = pK_{a2} + \log [NH_4H_2PO_4]/[ H_3PO_4] \quad (13)$$

substituting pH = 5.8 and p$K_{a2}$ = 7.2 in Equation 13

$$5.8 = 7.2 + \log[NH_4H_2PO_4]/[ H_3PO_4] \quad (14)$$

Rearranging Equation 14

$$\log [H_3PO_4]/ [NH_4H_2PO_4] = 1.4 \quad (15)$$

Taking Antilog and further rearrangement of Equation 15

$$[H_3PO_4] = 25.119[NH_4H_2PO_4] \quad (16)$$

To prepare the concentration of 0.05 M, the sum of the two buffer species was taken

$$[NH_4H_2PO_4] + [H_3PO_4] = 0.05\ M \quad (17)$$

by substituting 25.119[$NH_4H_2PO_4$] in Equation 17 and calculating for [$NH_4H_2PO_4$]
[$NH_4H_2PO_4$] = 0.0019143152 M
From the molecular mass the amount to weight can be calculated by multiplying them which gives 0.2202 g.
For the acid, substitute in Equation 16 and [$H_3PO_4$] = 0.048085683 M
By using the dilution equation $M_1V_1 = M_2V_2$ where $M_1$ for [$H_3PO_4$] = 14.76 M
$M_2$ is 0.048085683 M and $V_2$ is 1000 mL then solved for $V_1$ and taking that volume and dissolving it in 1 L deionized water, solution was prepared. Adjust the pH of the solution to 5.8 using aqueous $NH_3$.

### 2.4-The types atomizers used in this study

Two types of atomizers were employed in this study. They are i) electrically heated quartz tube atomizer (EHQTA), and ii) tungsten coil atom trap electrothermal atomizer (WC-ETA). The electrically heated quartz tube atomizer was convenient for direct atomization of the analyte species and therefore it was utilized also to determine the timing of peaks in flow injection and high performance liquid chromatography hydride generation studies. The tungsten coil was used as an atom trap in electrothermal atomization mode, where the coil surface functioned as a trapping and atomization platform.

### 2.4.1- The electrically heated quartz tube atomizer (EHQTA)

The EHQTA, consist of a home-made electrical furnace for heating, a quartz T-tube, also named as quartz tube atomizer (QTA) and one gas liquid separator. The furnace was constructed from electrical resistance Ni-Cr wire curled inside the two ceramic parts molded in semi-cylindrical form. The QTA was made of quartz and was constructed in usual T-shape. It has an inlet arm with length of 9.0 cm and 0.5 cm id, 13 cm long optical arm with 1.5 cm internal diameter. The gas liquid separator

(GLS) was cylindrical in shape and was made from glass. The arsenic hydride from the stripping coil is separated from the liquid in GLS. The block diagram of the GLS and EHQTA is shown in Figure 2.4. The picture of the electrical furnace and the quartz T-tube are given in Figure 2.5.

To improve the sensitivity of quartz tube atomizer, it was necessary to coat the inner surface of the quartz at the optical arm or the absorption volume with arsenic atoms. The coating of a newly constructed QTA was carried as follows: 100.0 ng/mL of As(III) was prepared in 0.2 mol/L HCl in a 100 mL volumetric flask and by using the continuous flow mode of hydride generation, the arsenic hydride formed after hydrolysis with sodium tetrahydroborate, was sent to the electrically heated quartz tube atomizer until the whole of 100 mL solution is consumed. The completion of the coating was indicated by a stable continuous signal.

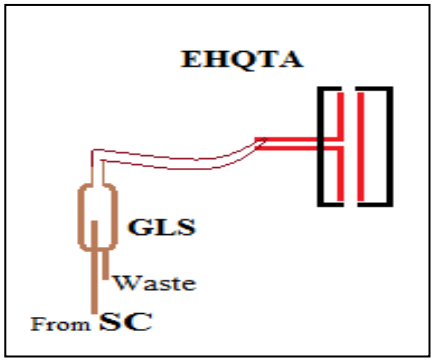


**Figure 2.4** The block diagram of the gas liquid separator and the electrically heated quartz tube atomizer


**Figure 2.5** The pictures of (A) quartz T-tube, (B) inner area of the electrical furnace with the two semi-cylindrical ceramic parts and (C) the closed electrical furnace

### 2.4.2- The tungsten coil atom trap electrothermal atomization (WC-ETA)

The tungsten-coil atom trap electrothermal atomization comprises of a double layer tungsten coiled filament with surface area of 12 $mm^2$. The W-coil was obtained from a 150 W, 15 V Philips Focusline (Germany) projection lamp, Type 6550. It was fixed in two copper electrodes supported by a PTFE fitting which was inserted into a glass joint and glued with hot silicon. The coil temperature was manually controlled by a variable potential power supply (Variac) connected to main electricity and a 750 W transformer was connected between the Variac and the tungsten coil. The input voltage of the variable potential power supply was 220 V. The temperature of the tungsten coil was measured using a thermocouple together with an infrared thermometer from TIME GROUP INC (China). The projector lamp bulb and the tungsten coil filament are shown in Figure 2.6 A and B.

The atomization cell of the tungsten coil electrothermal atomization is made of glass and has an optical arm of 13 cm long and internal diameter of 1.5 cm, it contains an inlet arm (9 x 0.8 cm) and two gas outlets. The ends of the optical arm were closed with quartz windows. The design of the atomization cell is shown in Figure 2.6 C. Two gas liquid separators were used with the tungsten coil atomizers. In the first gas liquid separator (GLS-1), the arsenic hydride is separated from the liquid phase. The gaseous analyte and some water vapor are then transported by argon to mix with hydrogen gas that was introduced between the two gas liquid separators. The argon and hydrogen gases carry the arsenic hydride and water vapor to the second gas liquid separator (GLS-2) where further separation of the water vapor and hydride takes place. The waste outlet of GLS-2 was connected with Tygon tubing that was connected to a peristaltic pump so the water vapor was drained to the waste. Droplets of water were observed in GLS-2 and inside the Tygon tubing. The arsine was then carried to the iridium-coated tungsten coil.

The introduction of hydrogen gas in this system served three importance functions: i) to transport arsine to the coil, ii) to protect the coil from oxidation by oxygen, and iii) to increase the efficiency of atomization of the analyte atom. The block diagram of the two GLS and the W-coil electrothermal atomizer are shown in Figure 2.7.

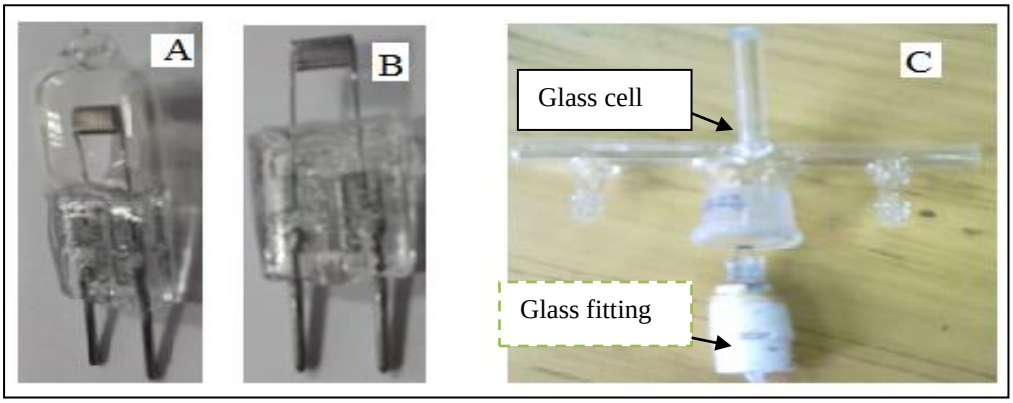


**Figure 2.6** The pictures of the A- the projector lamp bulb, B-the extracted tungsten filament and the design of the glass cell

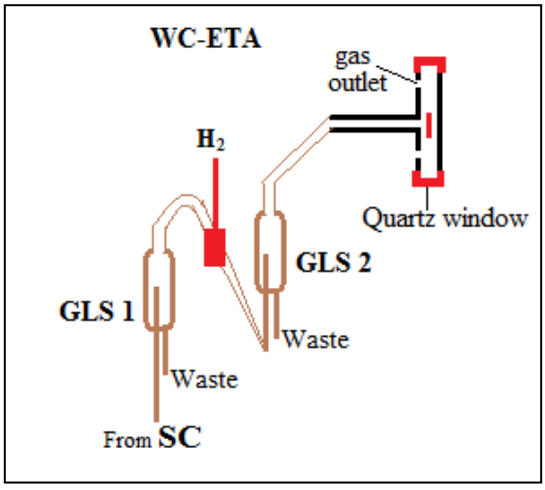


**Figure 2.7** The block diagram of the arrangement of the two gas liquid separator and the tungsten coil inside the glass cell, the glass has two quartz window and two gas outlets.

### 2.4.2.1- Coating of tungsten coil

For the coating of the tungsten coil with chemical modifiers such as iridium or rhodium, manual injections of 20 µL aliquots taken from 1000 mg/L stock solution of Ir or Rh were performed on the surface of bare W-coil surface in 10 consecutive replicates. The heating program during the coating was: 1.500 Volt for 10 s for drying stage, 3.640 Volt for 30 s for the coating stage and 7.500 Volt for 2 s followed by 9.800 Volt for 2 s for cleaning stages. During the coating procedure $H_2$ and Ar flow rates were 175 and 150 mL/min respectively and the peristaltic pumps were not operating.

### 2.4.2.2-Determination of W-coil temperature

The temperature of the tungsten coil was measured with a thermocouple and an optical pyrometer (IRCON Pyrometer, Model 20 USA). The temperature reading was simultaneously taken from the devices and the pyrometer was given higher reading than the thermocouple with differences of almost 200 °C.

To use the thermocouple, the tip was coated with ceramic so that electrical conduction between the thermocouple and coil was avoided, and by increasing the voltage of the variac potential supplier, the temperature of the coil read from the two devices was also increasing. The thermocouple has maximum temperature measurement of 1020 °C, therefore at higher voltage, only the pyrometer measurement was utilized for high temperature measure. As shown Figure 2.8, the results of the experiment showed an exponential relationship between applied voltage and temperature. The voltage at the trapping temperature used was 2.6 Volt gave 720 °C from the thermocouple, and for the atomization temperature (1920 °C) with potential of 10.9 Volt was calculated using the exponential equation generated from the thermocouple and corrected using pyrometer reading at that voltage. During measurement, both the optimum flow of argon and hydrogen were sent into system.

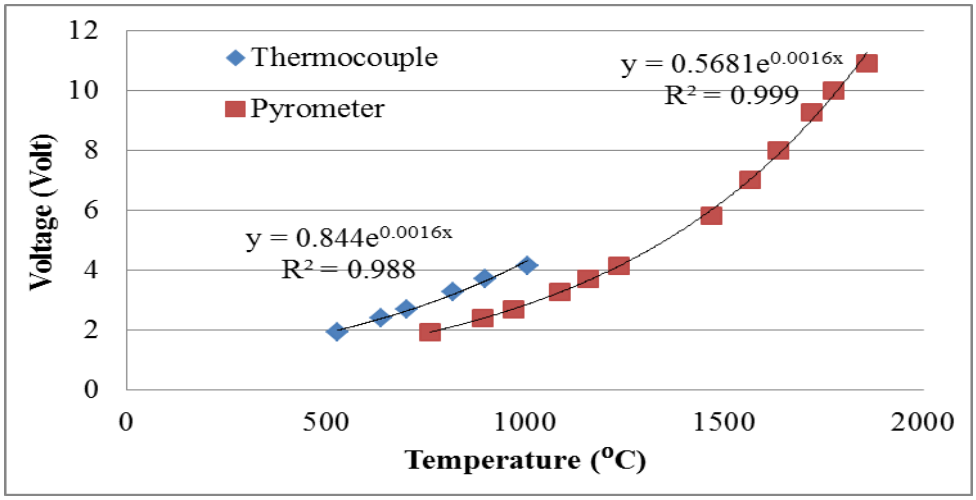


**Figure 2.8** The calibration plot of temperature reading from the thermocouple and optical pyrometer versus the voltage applied to the tungsten coil with an AVO meter. The voltage was control by a variac potential supplier connected to transformer.

## 2.5- Experimental studies on CRMs and real samples

### 2.5.1- Total arsenic determination in water CRMs

Total arsenic determination was carried out to the certified reference material of Waste Water EU-L-2 and Trace Elements in Water 1643e. For the EU-L-2 CRM, the procedure described in the certificate of the certified reference material was followed. For this, the concentration of the stock solution of 80.0 ± 0.002 ng/mL was prepared by making 1:100 dilutions (i.e. taking 1.0 mL from CRM bottle and diluting it to 100.0 mL with deionized water). 160 folds dilution was performed from this stock solution to make 0.5 ng/mL. For 1643e CRM, 120 folds dilution was made to prepare a solution of 0.5 ng/mL. The selected method of analysis was then applied.

### 2.5.2- Total arsenic determination in CRM 1570a Trace Elements in Spinach Leaves

A total of 0.1 g of 1570a CRM sample was weighed accurately, transferred into PTFE microwave vessel and 3.0 mL of 25% $HNO_3$ and 1.0 mL of 30% $H_2O_2$ were added to contents before performing total arsenic digestion using microwave digestion. The contents were heated from room temperature to 100 °C for 5 min and held at this temperature for 10 min, heated to 150 °C in 5 min and held at this temperature for another 10 min, with a maximum potency of 800 W. Finally, the digested sample and the digested blank solutions were made up to 30 g with deionized water and measured with the selected method of analysis.

### 2.5.3- First extraction procedure of arsenic from 1570a CRM

A solution of 1/3 (v/v) MeOH/$H_2O$ prepared in 0.1 mol/L NaOH was used for the solvent of extraction. An amount of 0.20 g of the 1570a CRM was weighed and added into 10.0 mL of the solvent in two 15 mL plastic containers to have a parallel study. The solution was left for overnight shaking with VWR standard analogue shaker. The following day, the samples were further mixed for 5 min with a vortex mixer and then placed in a sonication bath for 20 min. The samples were centrifuged for 15 min over 5000 rpm and then filtered with 0.45 µm Metricel membrane filters; 4.0 mL portion of the filtrate was placed into HP 500 microwave Teflon vessel and 3.0 mL of 25% $HNO_3$ and 1.0 mL of 30% $H_2O_2$ was added to the filtrate and then digested with the microwave along with a blank using the same program as the spinach leaves CRM. The remaining filtrate was then used for chromatographic speciation of As(III) and As(V). Finally, the digested sample and the digested blank were made up to 30.0 g with deionized water and measured with continuous flow hydride generation tungsten coil electrothermal atomization atomic absorption spectrometry (CF-HG-WC-ETAAS) or the selected method of analysis.

### 2.5.4- Second extraction procedure of arsenic from 1570a CRM

Two parallels with an amount of 0.20 g of 1570a CRM of Spinach Leaves was treated with 10.0 mL of 1.0% (v/v) trifluoroacetatic acid (TFA) in 15.0 mL plastic container and mechanically shaken for 12 h with the VWR standard analogue shaker. The samples were then further mixed with a vortex mixer for 5 min, and then placed into the sonication bath for 20 min., centrifuge for 15 min at 5000 rpm was applied and filtered with 0.45 µm Metricel Membrane Filter.

An amount of 4.0 mL aliquot was taken from filtrated sample and was subjected for total arsenic determination by adding 3.0 mL of 25% $HNO_3$ and 1.0 mL of 30% $H_2O_2$ to the filtrate and then digested with the microwave along with a blank using the same program as the spinach leaves CRM. The remaining filtrate was then used for chromatographic speciation of As(III) and As(V). Finally, the digested sample and the digested blank were made up to 30.0 g with deionized water and measured with continuous flow hydride generation tungsten coil electrothermal atomization atomic absorption spectrometry (CF-HG-WC-ETAAS).

### 2.5.5- Total arsenic determination in BCR 627

A total amount of 0.050 g of BCR 627 Tuna Fish Tissue sample was placed in PTFE microwave vessels after 3.0 mL concentrated $HNO_3$ was added, the solution was allowed to stand for 12 hours in order to dissolve the matrix. Following this, 1.0 mL $H_2O_2$ was added to the solution and total arsenic digestion was carried out using microwave digestion. The contents were first heated at 90 °C for 10 min to warm the sample, using a power of 205 W. Then a power of 465 to 705 W (150 °C) was applied for another 15 min. The samples were then cooled down after one cycle of microwave digestion. After this step, the samples were treated again suing the programme above to achieve the complete digestion of the organic compounds.

The digested sample and digested blank solutions were then diluted with 30.0 g using deionized water and measured with flow injection hydride generation electrically heated quartz tube atomizer atomic absorption spectrometry (FI-HG-EHQTA) Arsenic content in the samples was quantified by means of an external calibration plot for the standards.

### 2.5.6- Pretreatment for real samples

Vegetable samples were in two different places in Turkey: the first place was at the Beypazari local market in Ankara where Dill, Garden rocket, Lettuce, Parsley and Spinach were bought and the second place was in backyard gardens in Balikesir. Water sample was also collected in Balikesir from the gardens where the vegetables were collected. Upon arrival at the lab, the roots of the vegetables were cut and the leaves were thoroughly cleaned with tap water to remove the dirty soil. The clean leaves were then rinsed with deionized water and then dried by allowing them on the lab bench to stand for 1 hour. They were then sorted out into groups of 1 and 2; thus group 1 leaves contain the light color leaves or the fresh one and group 2 contained dark color leaves. However for Dill vegetable, the sorting was based on the lower and upper part of the leaves. The samples were chopped into smaller pieces and kept in plastic containers that were labeled as 1 and 2 according to the groups and again put them into plastic back before placing them in the refrigerator.

In order to obtain a homogenized powdered leaves in dry form, the leaves were treated by dry freezing process so that while water is removed, the chemical status of the analyte composition of the leaves are intact. However in order to obtain the water content of each leave, a separate set of the leaves were weighed before and after dry-freezing. After subjected to dry-freezing, samples were then crushed into powder manually using plastic gloves and again placed in 50 mL plastic bottles. In order to avoid moister entering into the samples, the cover of the bottles were all kept covered

with parafilm, placed in zippered plastic bags and then kept in refrigerator until the time of analysis.

The same procedure of microwave digestion of Trace Elements in Spinach Leaves CRM 1570a were applied to the leave samples for total arsenic determination. The continuous flow hydride generation tungsten coil atom trap electrothermal atomization technique (CF-HG-WC-ETAAS) was used for the determination. Because the Dill leaves contain relatively high concentration of arsenic, about 65 times more than the limit of quantification, these samples were further subjected to extraction procedure using trifluoroacetic acid for determination of iAs.

# CHAPTER 3

# RESULTS AND DISCUSSION

## 3.1- Heating performance of the electrically heated quartz tube atomizer

In order to electrically heat the quartz T-tube atomizer, a homemade furnace was constructed from two semi-cylindrically molded ceramic parts that fit on the optical arm of the QTA. The ceramic parts were electrically heated by Ni-Cr resistance wire that was coiled inside the body. The temperature of the furnace along the length of optical arm of the QTA was cross-examined by using the set-up shown in Figure 3.1 (A). In preliminary studies, it was observed that the flow of argon causes a decrease by 5 °C of the internal temperature of the furnace; Ar was passed through the inlet arm with a flow rate of 300 mL/min.

The arrangement of the setup was as follows: The center of the T-tube is the inlet arm and was marked as the zero point. So from the zero point to the ends of the tube along the optical arm make a distance of 6.5 cm in both right and left directions. The measurement of temperature were realized by inserting the tip of the thermocouple inside optical arm of the tube beginning from outer point (6.5 cm) towards the zero point at the center of the tube. The tip of the thermocouple was carefully positioned at the center of horizontal arm, inside the tube in such a way that it does not touch the inner surface of the QTA. This was necessary because atomization of the arsenic hydride can only happen in the absorption volume and when the atoms touches the inner surface of the tube, they either decay or trapped on it [12].

To compare the temperature of the electrically heated ceramic and the temperature of inner space of the tube along the optical arm, another thermocouple was placed inside a hole bored in the ceramic body; the temperature readings of the two thermocouples were taken simultaneously. It was observed that the difference in two temperatures 20 $^{\circ}$C, cooler part being inside. Therefore during further studies, the temperature of the furnace was set to 1020 $^{\circ}$C. The result of the experiment given in Figure 3.1 (B) indicates that the entire optical arm of the quartz tube atomizer was symmetrically heated along the distance of 4.0 cm at both sides. Even when the temperature was varied from 800 to 1000 $^{0}$C, the heating profile of the tube remained nearly the same.

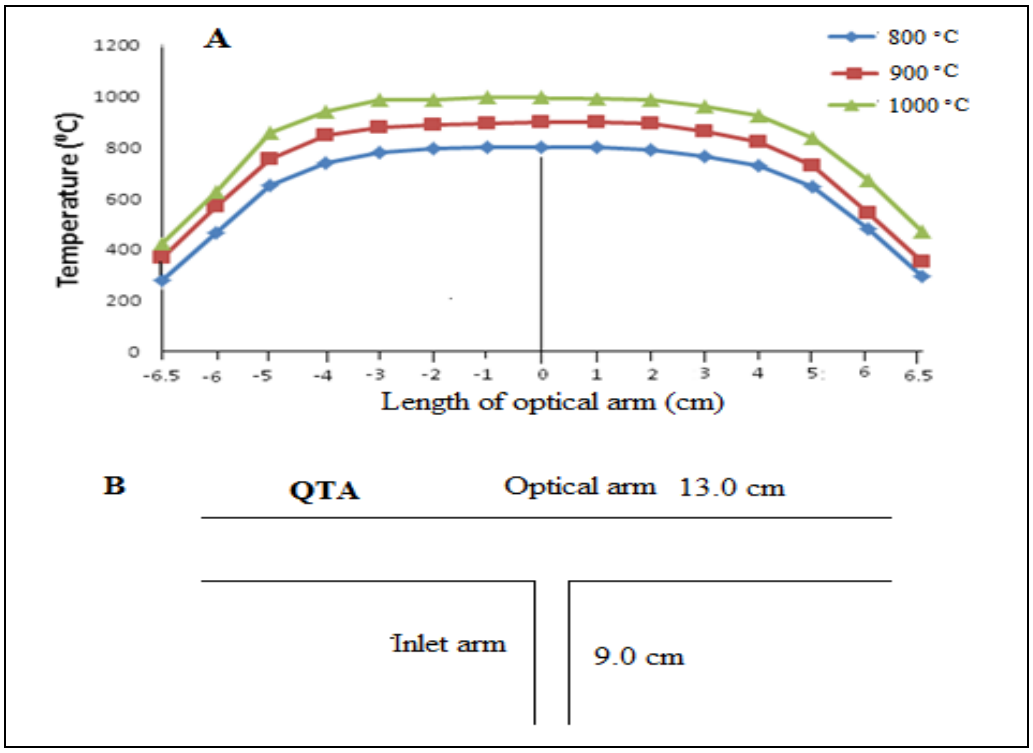


**Figure 3.1** The temperature profile of QTA studied along the distance of the optical arm while argon flow rate was 300 mL/min. **A-** Plot of the distance versus temperature for different set of temperatures and **B-** Electrically heated quartz tube atomizer (EHQTA) that comprises of electrical furnace and QTA.

### 3.2- The atomization temperature of arsenic hydride using EHQTA

Among the criteria of an ideal atomizer, is that the atomizer should completely convert all analyte to free atoms [15], this would imply that, the atomizer temperature play an important role in the atomization of arsenic hydride ($AsH_3$) to free arsenic atoms. The atomization signal was investigated for 700, 800, 900, to 1000 °C. In this study, arsenic hydride was generated from 25 ng/mL of As(III) solution by continuous flow mode (Figure 2.1). As shown in Figure 3.2, almost a linear relationship was observed between the atomic absorption signal and atomizer temperature as it was increased from 700 to 900 °C. Between 900 and 1000 °C, a plateau was formed, and the repeatability of the signals was also observed to be improving from 6 to 2% RSD with the increase in temperature. The selected atomization temperature for further study was 1000 °C.

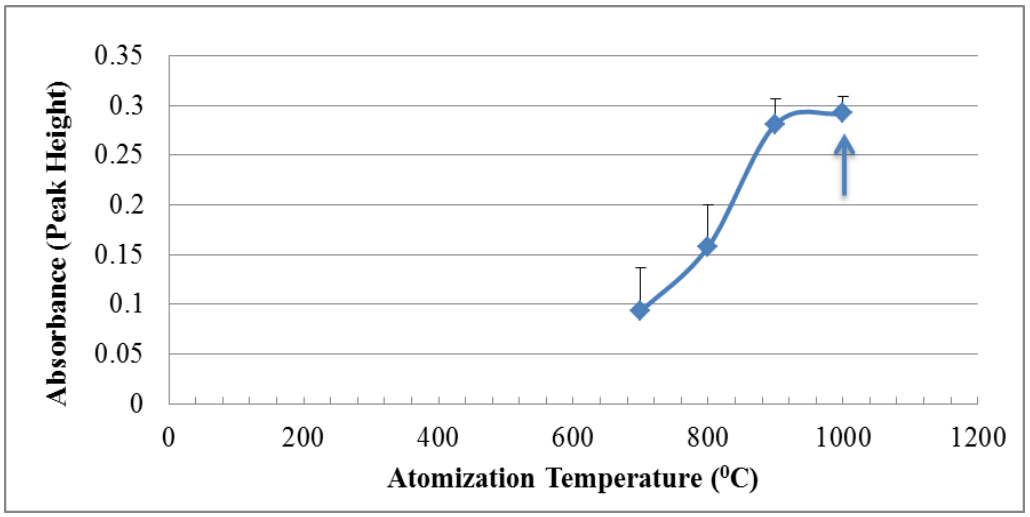


**Figure 3.2** Atomic absorption signal of As(III) of when furnace temperature was varied from 700 to 1000 °C. HCl and sample flow rates were 3.0 mL/min, Ar flow rate was 250 mL/min. concentration of $NaBH_4$ was 1.0% (w/v) and its flow rate was 1.5 mL/min.

### 3.3- Optimizations and measurements

Optimization studies were carried out in the following systems used during this study. These three systems are:

1. Continuous flow hydride generation with electrically heated quartz tube atomizer (CF-HG-EHQTA) or atom-trap tungsten coil electrothermal atomization (CF-HG-WC-ETA),
2. Flow injection hydride generation with electrically heated quartz tube atomizer (FI-HG-EHQTA) or atom-trap tungsten coil electrothermal atomization (FI-HG-WC-ETA),
3. High performance liquid chromatography hydride generation with electrically heated quartz tube atomizer (HPLC-HG-EHQTA) or atom-trap tungsten coil electrothermal atomization (HPLC-HG-WC-ETA).

During optimization studies, one parameter was varied while the others were kept constant and optimization cycles were repeated until a stable and repeatable signal was obtained. The absorbance measurements were based on peak height and the *error bars* indicate the %RSD of three measurements.

#### 3.3.1- Continuous flow hydride generation with EHQTA

A preliminary calibration study was performed in order to establish the working concentration of As(III) during optimization study. From the result of the calibration plot, 5.0 ng/mL was the selected concentration for optimization studies. In the optimization study of CF-HG-EHQTA, the following parameters such as, concentration of hydrochloric acid, flow rate of sample and HCl, concentration and flow rate of $NaBH_4$, length of reaction and stripping coil and flow rate of argon as carrier gas were investigated.

### 3.3.1.1- Concentration of hydrochloric acid in As(III) sample solution using CF-HG-EHQTA-AAS

For arsenic hydride generation hydrochloric acid is widely used for the hydrolysis of $NaBH_4$. In order to find the optimum HCl concentration, the concentration of HCl in the analyte solution was varied between 0.05 and 2.0 mol/L. As shown from Figure 3.3, when the concentration was 0.05 mol/L, the atomic absorption signal was lower; however, from 0.1 to 0.75 mol/L the signals remain constant and decrease when HCl concentration was further increased to 1.0 mol/L or more. The selected concentration was 0.25 mol/L because it produced a stable and constant continuous signal.

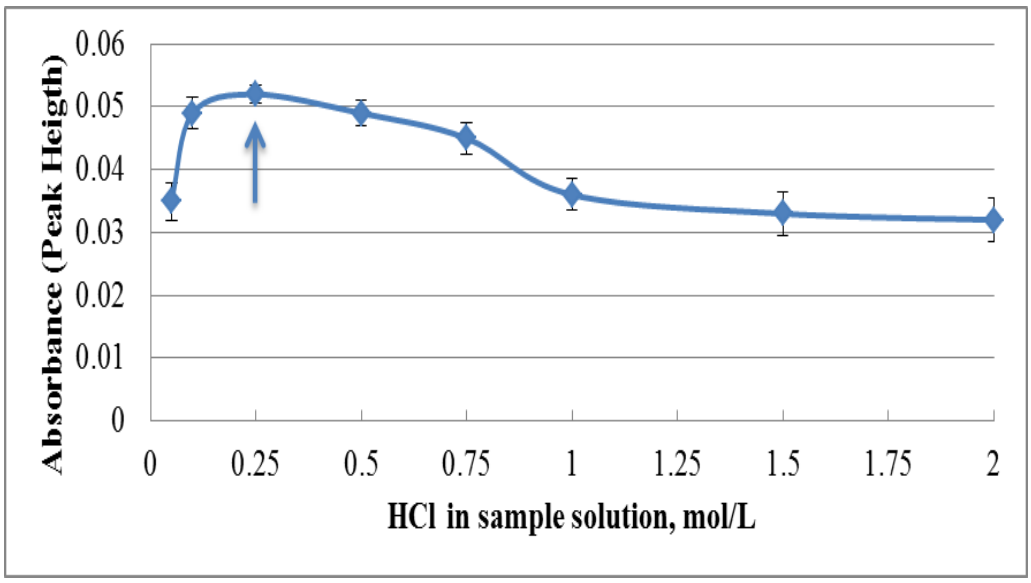


**Figure 3.3** The effect of HCl concentration in sample solution when argon flow rate was 250 mL/min, $NaBH_4$ flow was 1.5 mL/min and 1.0% (w/v). HCl flow was 3.0 mL/min and using 5.0 ng/mL As(III)

### 3.3.1.2- The effect of hydrochloric acid and sample solution flow rate using CF-HG-EHQTA-AAS

After optimizing the concentration of HCl in analyte solution, working standard solution of 5.0 ng/mL of As(III) was prepared in 0.25 mol/L hydrochloric acid. The flow rate of the acidic solution was varied from 1.0 to 8.0 mL/min and the results of the experiment are shown in Figure 3.4. As seen from the figure, when the flow was varied from 1.0 to 5.0 mL/min the signal gradually increases. By increasing the flow to 6.5 mL/min, a smooth stable continuous signal was obtained with 2% RSD. However by further increasing the flow rate from 6.5 to 8.0 mL/min, the signals started to decrease. The optimum flow rate selected was 6.5 mL/min.

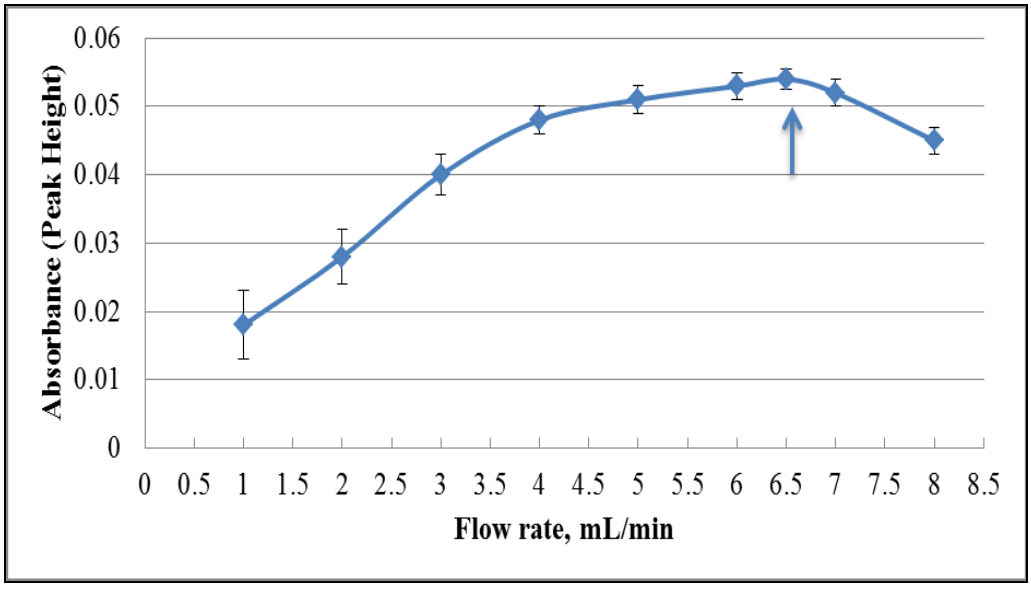


**Figure 3.4** The influence of HCl and analyte solution flow rate on the signal of 5.0 ng/mL of As(III), when argon flow rate was 250 mL/min, $NaBH_4$ flow was 1.5 mL/min and 1.0% (w/v).

### 3.3.1.3- The effect of sodium tetrahydroborate ($NaBH_4$) concentration using CF-HG-EHQTA-AAS

For the generation of arsenic hydride volatile species from 5.0 ng/mL As(III), $NaBH_4$ was used as the reductant. The effect of $NaBH_4$ concentration on $AsH_3$ generation was investigated by varying the concentration between 0.10 and 2.5% (w/v). From the experimental results shown in Figure 3.5, it is observed that the absorbance signal increases when the concentration of $NaBH_4$ increases from 0.10 to 1.0% (w/v) and then level-off at 1.5% (w/v), however the signal decreases when the amount was increase between 2 and 2.5. The optimum concentration of $NaBH_4$ selected was 1.5% (w/v).

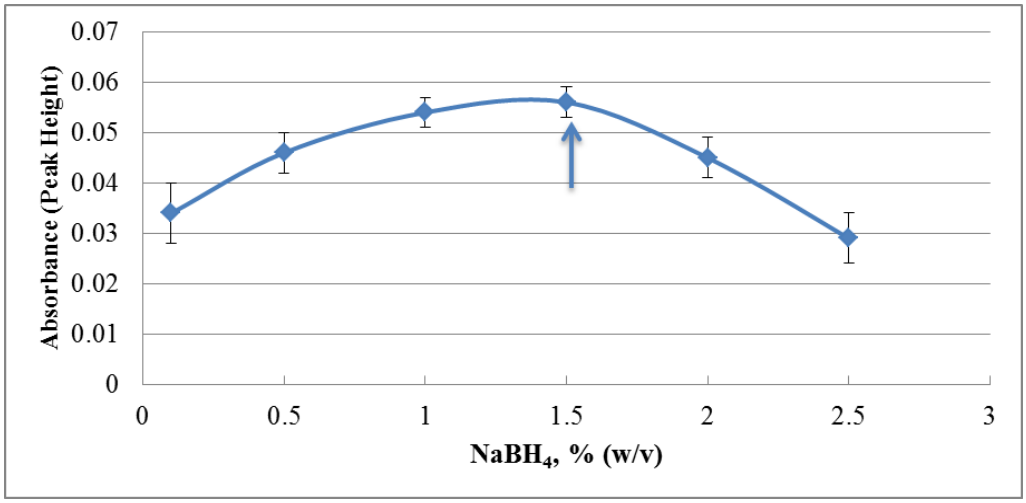


**Figure 3.5** The effect of $NaBH_4$ concentration on 5.0 ng/mL of As(III) signal. The flow of $NaBH_4$ was 3.0 mL/min, HCl concentration was 0.25 mol/L and its flow rate was 6.5 mL/min. Other parameters are given in Table 3.1.

### 3.3.1.4- The effect of $NaBH_4$ flow rate on the absorbance signal using CF-HG-EHQTA-AAS

The efficiency in the generation of As hydride species is directly related with both the flow rates of carrier and reductant solutions. The effect of reductant solution flow rate was investigated by varying its flow between 1.0 and 3.5 mL/min. The optimum value was found to be 2.0 mL/min. For the higher and lower flow rates of $NaBH_4$, the peak height of As(III) signal decreased as shown in Figure 3.6.

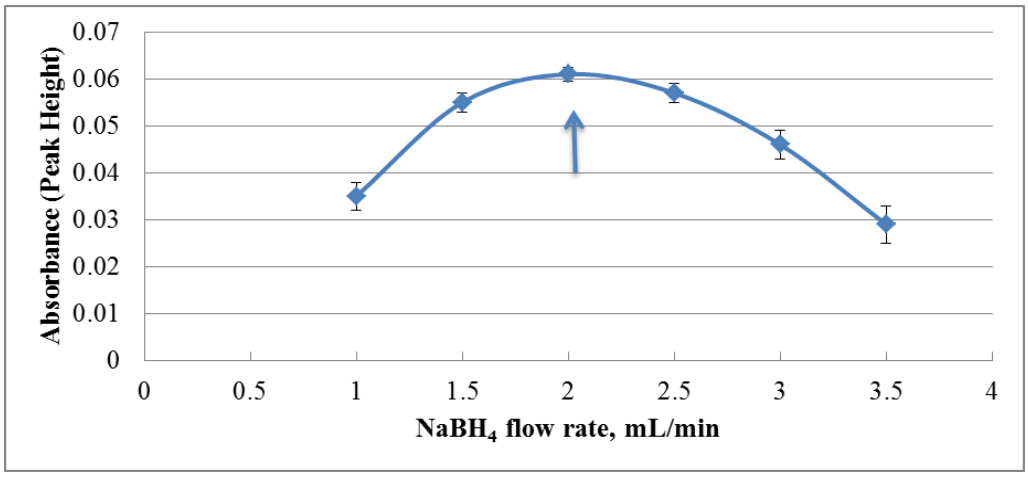


**Figure 3.6** The effect of $NaBH_4$ flow rate on signal of 5.0 ng/mL As(III). $NaBH_4$ was 1.5% (w/v), HCl and analyte solution flow was 6.5 mL/min. Ar flow was 250 mL/min and other parameters are given in Table 3.1.

### 3.3.1.5- Effect of argon flow rate on As(III) signals while $NaBH_4$ is 2.0 mL/min using CF-HG-EHQTA-AAS

The importance in the optimization of the carrier gas in hydride generation is to have an efficient stripping of arsenic hydride in the stripping coil and transporting the analyte hydride through the gas liquid separator to the atomizer. To find the optimum flow of argon, the flow rate was varied from 100 mL/min to 375 mL/min.

The optimum flow was found to be 200 mL/min; the results are shown in Figure 3.7. At higher flow rates from 300 to 375 mL/min, the high transportation of the arsenic hydride was achieved but their residence time in the absorption zone was shorten; in addition analyte vapor is diluted by excess Ar, causing a decrease in signal.

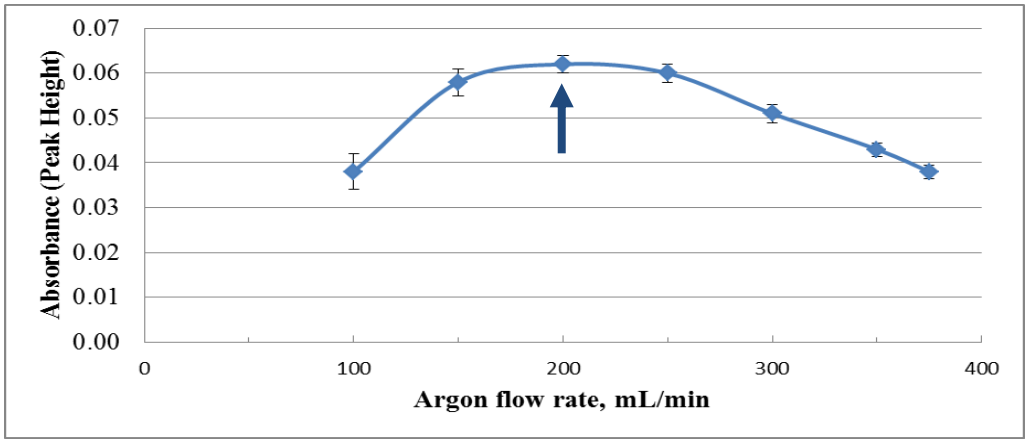


**Figure 3.7** The effect of Ar flow rate on 5.0 µg/L of As(III) signal, the length of reaction coil was 60 cm and the length of stripping coil was 30 cm. 200 mL/min was selected as the optimum value. Other parameters are given in Table 3.1.

### 3.3.1.6- Length of reaction and stripping coil (CF-HG-EHQTA-AAS)

The reaction coil provides the medium where arsenic hydride is generated by the hydrogen transfer mechanism from sodium tetrahydroborate that is hydrolyzed by hydrochloric acid. The stripping coil is the medium were argon strips the volatile arsenic hydride from the solution, and transport it to the atomizer. The plots of the optimization study for the reaction and stripping coils are given in Figure 3.8. The length of the reaction coil was varied from 30 cm to 180 cm. The optimum reaction coil length was found to be 120 cm when a 20 cm stripping coil was used. In the case of the stripping coil, the lengths from 5 to 30 cm, were investigated, the optimum stripping coil was found to be 10 cm when 120 cm reaction coil was used. Further experiments were carried out by employing 120 cm reaction coil and a 10 cm stripping coil.

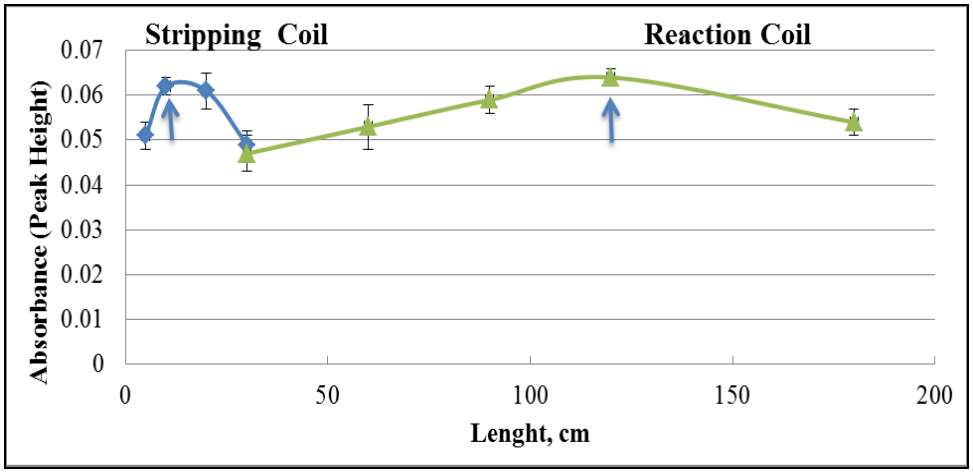


**Figure 3.8** Effects of reaction and stripping coil lengths on the analytical signal As obtained by conventional CF-HG-EHQTA. The signals were obtained using of 5.0 ng/mL As(III) in 0.25 mol/L HCl. Other parameters are given in Table 3.1.

**Table 3.1** The optimized parameters of CF-HG-EHQTA with their optimum values using 5.0 ng/mL of As(III). (n =3)

| **Parameters** | **Optimum Value** |
|---|---|
| HCl in sample solution | 0.25 mol/L |
| Flow rate of HCl | 6.5 mL/min |
| Concentration of $NaBH_4$ | 1.5% (w/v) |
| Flow rate of $NaBH_4$ | 2.0 mL/min |
| Carrier gas flow rate | 200 mL/min |
| Length of reaction coil | 120 cm |
| Length of stripping coil | 10 cm |
| Atomization temperature | 1000 $^0$C |

### 3.3.1.7- The effect of hydrochloric acid concentration on As(V) signal without TGA using CF-HG-EHQTA-AAS

By using the optimum parameters in Table 3.1, the influence of hydrochloric acid concentration on As(V) hydride formation was investigated. The concentration of HCl was varied from 0.01 to 4.0 mol/L and 50 ng/mL of As(V) was used. The experimental results obtained in Figure 3.9 are similar to the results obtained by Amjad Shraim *et al.* [115]. They studied the variation of absorbance signal with concentration of hydrochloric acid for arsine generation and found the same relationship. In conventional According to A.G. Howard and C. Salou the direct reduction of arsenate [As(V)] requires it to be fully protonated by the use of strong forcing acidic conditions [106], and this means that high concentration of HCl is required if As(V) is to be converted to arsine. This explanation was also observed during study; as the HCl concentration was increased from 0.1 to 3.0 mol/L, the signals were also increasing. Therefore in order to make a non-chromatographic speciation analysis of inorganic arsenic, lower HCl concentration of around 0.005 to 0.1 mol/L so that arsine generation from As(V) is suppressed.

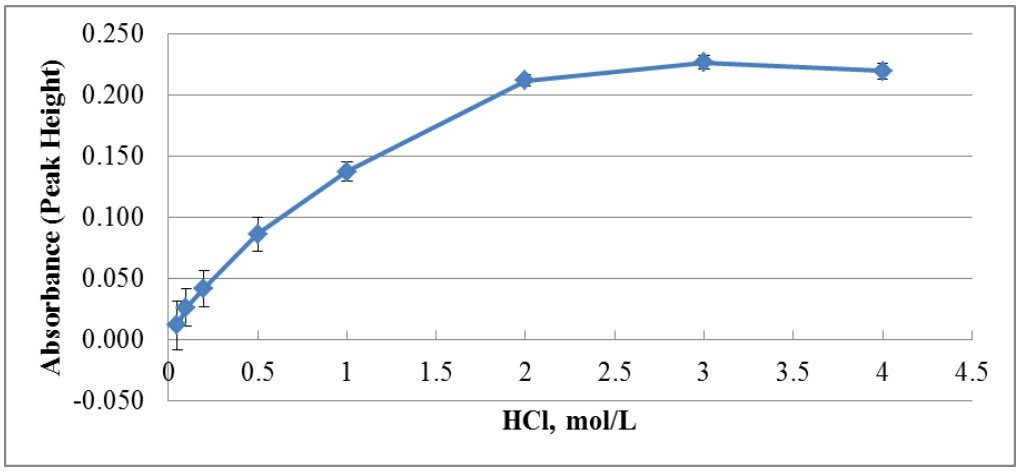


**Figure 3.9** The effect of HCl on the analytical signal of 50 ng/mL As(V), obtained using the optimized parameters of CF-HG-EHQTA, given in Table 3.1.

### 3.3.1.8- The pre-reduction time of TGA for As(V) using CF-HG-EHQTA-AAS

By using CF-HG-EHQTA system, the pre-reduction effect TGA on As(V) was investigated on the basis of the time needed for the pre-reduction reagent to completely reduce As(V) to As(III). To study pre-reduction time of TGA, 10.0 ng/mL As(V) in 0.002 mol/L HCl was prepared and as soon as the solution was running in the continuous flow hydride generation system, 1.0 mL of TGA solution was added to the 100 mL As(V) solution. The plot of absorbance signal against pre-reduction period is shown in Figure 3.10; the generated continuous flow signal is shown in Figure 3.11. The absorption signal of As(V) was observed to start emerging after 45 s and then remain constant to 300 s. The result of this experiment is the same as what was found by Stanislav Musil and Tomáš Matoušek [110] and A.G. Howard and C. Salou [106]. According to the hypothesis of A.G. Howard and C. Salou, in the presence of TGA the extreme acidity conditions are unnecessary as the arsenic species are pre-reduced from As(V) to As(III) prior to the tetrahydroborate step given in Equation 18.

$$2\text{T-SH} + \text{R}_n\text{As O(OH)}_{3-n} \rightarrow \text{T-S-S-T} + \text{R}_n\text{As(OH)}_{3-n} + \text{H}_2\text{O} \qquad 18$$

The reaction of TGA with the arsenic species is proceeded by the dimerization of TGA with then react with the As(V) species to form a coordinated arsenic-thiol ($\text{R}_n\text{As(-ST)}_{3-n}$ ) complex and then reduced it to As(III). The reaction is fast and upon forming, it is uncharged and less sterically hindered to the attack of tetrahydroborate. The As(III) species produced, could then react with TGA to give As(III)-thioglycollate complexes as shown in Equation 19, that react with the tetrahydroborate to give arsine. (R is a methyl group and *n* is 0 or 3).

$$\text{R}_n\text{As(OH)}_{3-n} + (3-n)\text{T-SH} \rightarrow \text{R}_n\text{As(-ST)}_{3-n} + (3-n)\text{H}_2\text{O} \qquad 19$$

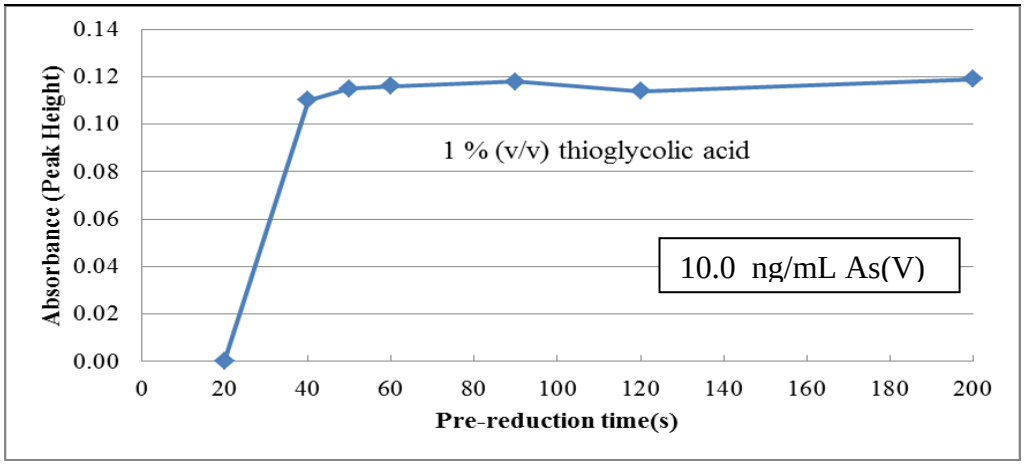


**Figure 3.10** The pre-reduction time for As(V) by TGA using the optimized parameters of CF-HG-EHQTA given Table 3.1, except that the concentration of HCl was 0.002 mol/L.

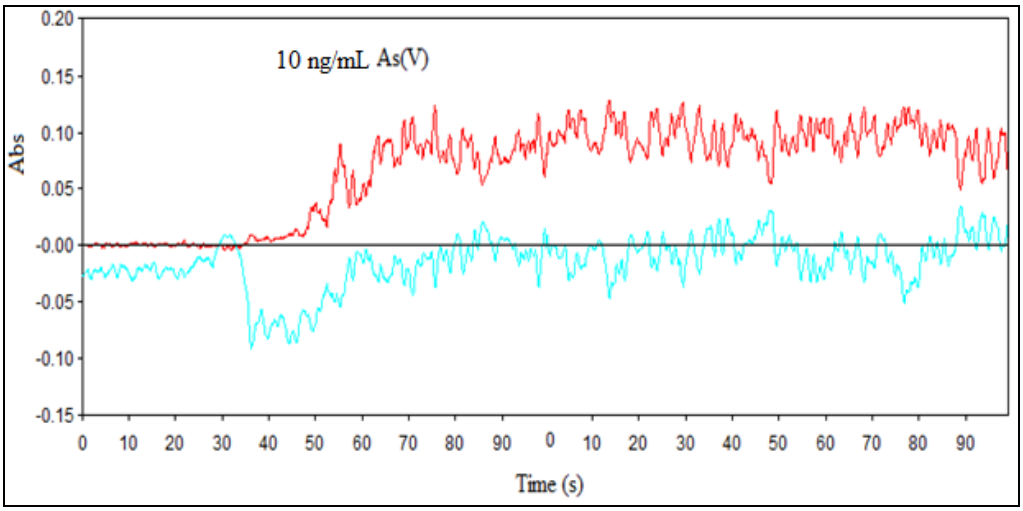


**Figure 3.11** The continuous flow signal of As(V) after the pre-reduction with TGA using the optimized parameters of CF-HG-EHQTA except that the concentration of HCl was 0.002 mol/L.

### 3.3.1.9- The pre-reduction time of potassium iodide in ascorbic acid using CF-HG-EHQTA-AAS

In order to study the pre-reduction time of As(V) by KI in ascorbic acid (AA), 8 volumetric flasks were used and the optimized values of 0.5%(w/v) KI in 0.5%(w/v) L(+) ascorbic acid for As(V) studied in our lab were utilized. In all the volumetric flask, KI and AA were first dissolved, and then As(V) and HCl were added so that the final concentrations were 10 ng/mL and 0.002 mol/L, respectively. The total volume was 100 mL made up using deionized water. The solution in the first volumetric flask was placed for analysis immediately after preparation using the CF-HG-EHQTA system. However no signal was observed for this solution, corresponding to zero min waiting periods. The second, third, fourth to the seventh flasks were kept for 10, 20, 30, 40, 50 and 60 min prior to analysis. The results are in Figure 3.12. It was observed that a complete reduction of As(V) was achieved after to 30 min. Since 30 min waiting time is not proper for an on-line prereduction in a flow system, efforts were concentrated on TGA as a pre-reduction agent for the conversion of As(V) to As(III).

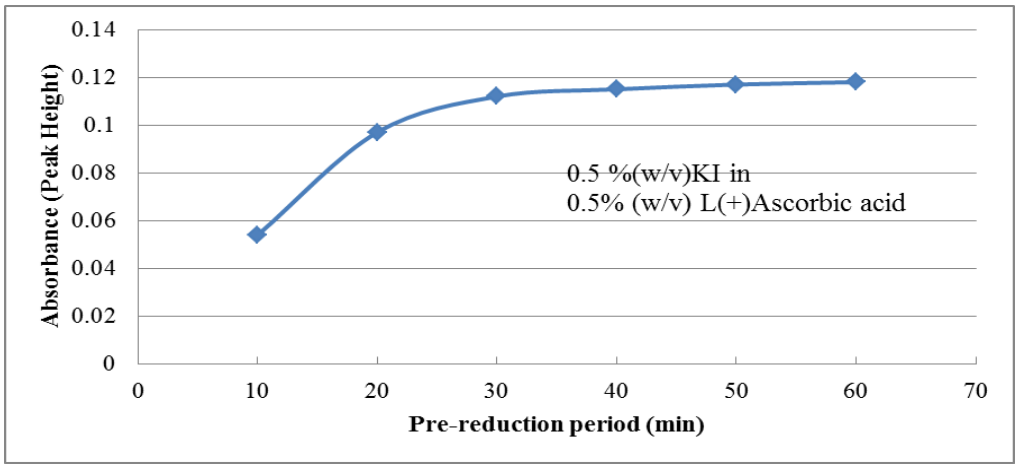


**Figure 3.12** The pre-reduction time of As(V) by KI in ascorbic acid. The optimum parameters of CF-HG-EHQTA given Table 3.1 were used except that the HCl concentration was 0.002 mol/L.

### 3.3.1.10- Calibration plot for As(III) and As(V) with CF-HG-EHQTA-AAS

By using the optimized parameters of CF-HG-EHQTA given in Table 3.1, the calibration plots of As(III) and As(V) were produced without the use of pre-reductant reagent. The calibration plot of As(III) and As(V) are shown in Figure 3.13 and Figure 3.14, respectively. Peak height of the analytical signal was used for absorbance measurements. For As(III), the linearity was found between the concentrations of 1.0 ng/mL and 50.0 ng/mL and above the concentration of 50.0 ng/mL, deviation from linearity was observed. However for As(V), the linearity was observed between 10 ng/mL and 100 ng/mL.

The calibration of As(V) using 1.0%(v/v) TGA as pre-reductant reagent is shown in Figure 3.15, and the analytical plot was linear was between the concentrations of 1.0 ng/mL and 50.0 ng/mL. The pre-reduction was very fast, less than one minute, and the analytical signal of As(V) had the same sensitivity as the analytical signal of As(III). It was also observed that TGA does not affect the sensitivity of As(III) under the same conditions as As(V). This was a very positive achievement that can be used for online speciation of inorganic arsenic species.

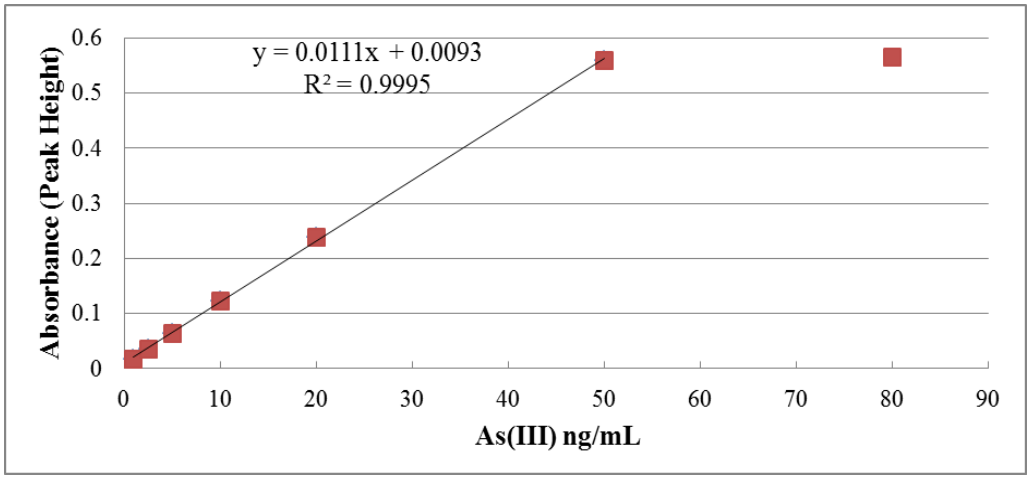


**Figure 3.13** Calibration plot of As(III) obtained by using the optimized parameters of CF-HG-EHQTA in Table 3.1.

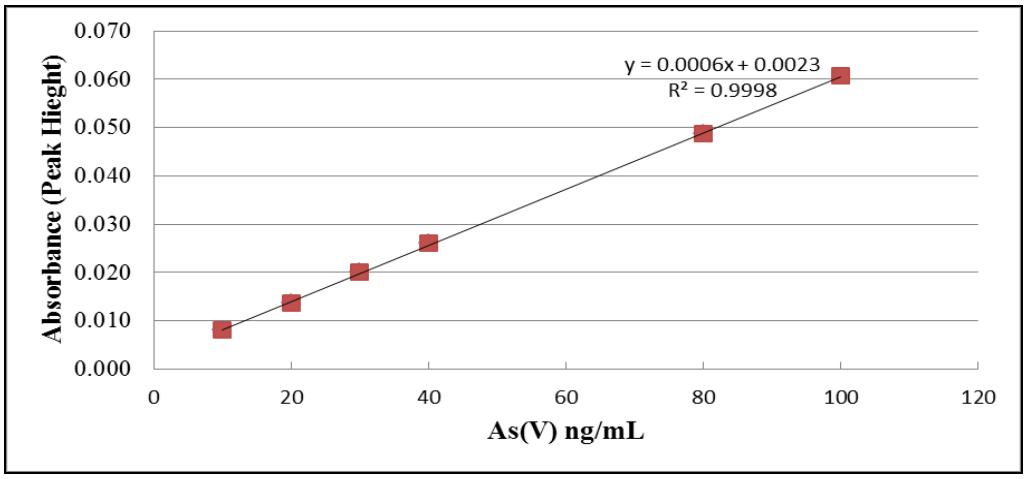


**Figure 3.14** Calibration plot of As(V) obtained by using the optimized parameters of CF-HG-EHQTA in Table 3.1. HCl concentration was 0.25 M

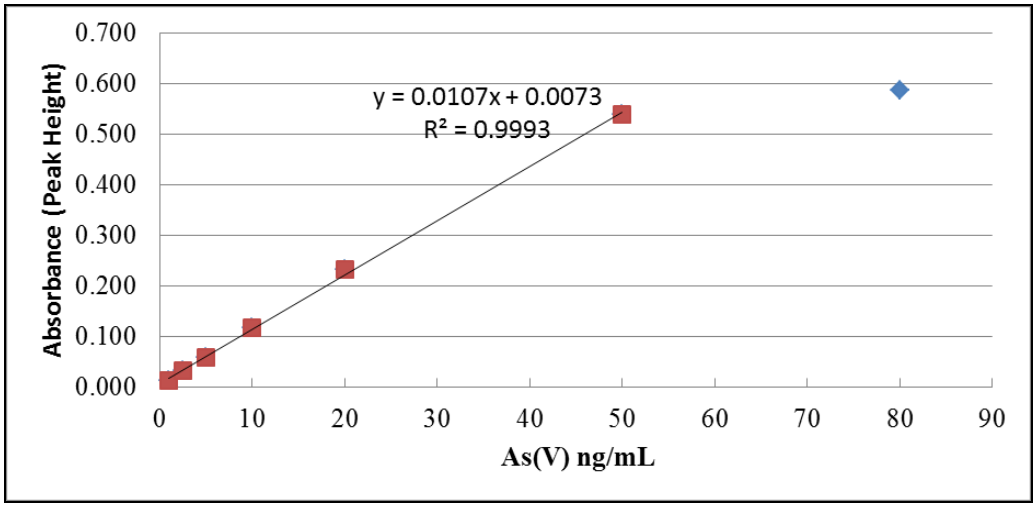


**Figure 3.15** Calibration plot of As(V) pre-reduced in 1.0%(v/v) TGA. The optimized parameters of CF-HG-EHQTA shown in Table 3.1 were used except that HCl concentration was 0.002 mol/L; the pre-reduction lasted less than one minute.

### 3.3.1.11- Analytical figures of merit for CF-HG-EHQTA-AAS

The analytical signal of 1.0 ng/mL As(III) obtained by CF-HG-EHQTA is given Figure 3.16. The reproducibility of the measurements was 5.3% RSD for 10 replicates (N=10). The % RSD was better at higher concentrations. The sensitivity of the CF-HG-EHQTA was calculated in terms of characteristic concentration ($C_0$) and limit of detection. The results of the analytical figures merit are given in Table 3.2. The LOD was calculated from 3 times the standard deviation of the signal obtained by a standard at or slightly above the limit of quantitation.

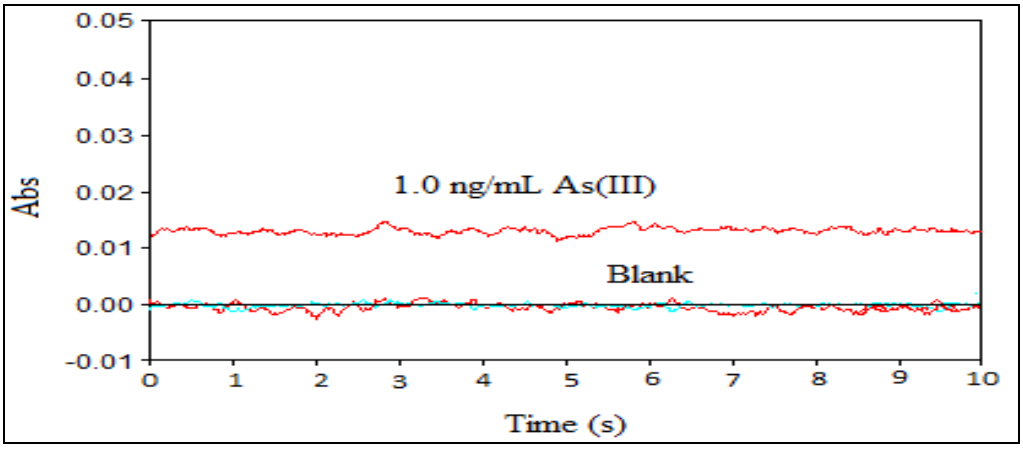


**Figure 3.16** The analytical signal of 1.0 ng/mL As(III), obtained by the optimized parameters of CF-HG-EHQTA. The continuous flow signal was acquired for 10 s

**Table 3.2** Analytical figures of merit for CF-HG-EHQTA technique. Calculations were based on peak height of the analytical signal.

| **Figures of merit** | **Values** | | |
|---|---|---|---|
| | As(III) in 0.25 mol/L HCl | As(V) in 0.25 mol/L HCl | As(V) in 1.0%(v/v) TGA and 0.002 mol/L HCl |
| LOD (ng/mL) | 0.2 | 3.8 | 0.3 |
| LOQ (ng/mL) | 0.7 | 13 | 1.1 |
| Range (ng/mL) | 1 to 50 | 10 to 100 | 1 to 50 |
| $C_0$ (ng/mL) | 0.4 | 6.4 | 0.4 |

### 3.3.2-Continuous flow hydride generation tungsten coil atom trap electrothermal atomic absorption spectrometry (CF-HG-WC-ETAAS)

In the optimization study of CF-HG-WC-ETAAS, the following parameters such as, trapping and atomization temperature of tungsten coil coated with iridium or rhodium that were used as chemical modifier, and trapping time; the amount of hydrogen and argon flowing through the system; the use of pre-reduction reagents for As(V) and the concentration of HCl in TGA; and concentration and flow rate of $NaBH_4$, were investigated using 1.0 ng/mL of As(III). The optimum parameters of CF-HG-EHQTA given in Table 3.1 were utilized in the initial stages of optimization study.

#### 3.3.2.1- Optimization of trapping and atomization temperatures using As(III) without TGA using CF-HG-WC-ETAAS

Permanent chemical modifier was firstly introduced to tungsten coil hydride trapping by Barbosa *et al*., for selenium hydride trapping [50, 116]. The trapping of arsine with rhodium-coated coil was also reported [55, 116]. Generally the use of permanent chemical modifiers in tungsten coil trapping was inherited from the knowledge of hydride trapping in graphite furnace. Bare tungsten coil can trap bismuth hydride [49, 117], as tungsten is also an important chemical modifier in graphite furnace. However, this is not applicable for Se, As and Sb and thus coating of the tungsten coil with a thin layer of noble metal was indispensable [55]. Preliminary experiments in this work showed that trapping of arsine on bare tungsten coil was not successful and the reproducibility of the signal was between 18 and 20% RSD. A comparison study for the performance of Rh and Ir chemical modifiers was undertaken using their trapping and atomization temperatures and as well as the maximum number of useful firings that can be obtained from them.

For this optimization study, 200 µg Rh was coated on a newly extracted tungsten coil and the optimum trapping and atomization temperatures were determined. By using trapping time of 60 s, the optimum trapping temperature of rhodium for As atoms was evaluated. The trapping temperature of the W-coil was varied from 611 to 957 °C, and it was found out that Rh was not trapping As at temperatures lower than 611 °C. The optimum trapping temperature for Rh was found to be 720 °C. In the determination of the optimum atomization temperature of Rh, the temperature of the W-coil was varied from 1620 to 2770 °C and the optimum atomization temperature was found to be 1920 °C (10.9 V). The results of the experiment are shown in Figure 3.17. The number of useful firings measured for Rh was 300 to 350, before the analyte signal decreased by 20%.

In the case of Ir, 200 µg of iridium was coated on a newly extracted tungsten coil, and by using 60 s trapping time, the optimum trapping temperature was determined by varying the coil trapping temperature from 575 to 957 °C. The optimum trapping temperature for Ir was found to be also 700 °C (2.63 V). The trapping temperatures obtained in this experiment are in agreement with the results of Docekal and Marek [48] who found values between 700 and 900 °C using tungsten tube atomizer. *R. Liu et al* [55] also found 640 °C for As trapping on Rh-coated tungsten coil and an atomization temperature of 1930 °C was found. For the investigation of the optimum atomization temperature for Ir-coated tungsten coil, the atomization temperature of the coil was varied from 1620 to 2770 °C and the optimum temperature was also found to be 1920 °C (11.0 V). Moreover, the number useful firings measured for Ir was at least 400 before the analyte signal decreased by 20 %. The error bars indicate the %RSD of 3 measurements.

From the experimental investigation of trapping and atomization temperature Ir was selected as the best chemical modifier. From the result shown in Figure 3.17, Ir-coated W-coil results were about 1.5 times higher than those of Rh-coated W-coil. In a comparison of chemical modifiers such as Pd, Rh, Ir by C.G. Bruhn *et al*. [118], it

was shown that Rh-coated W-coil was more stable, but the result from Rh was comparable with Ir. However in the technique used by C.G. Bruhn *et al*, a temperature programming method was used in a way similar to GFAAS consisting of drying, ashing, and atomization and cleaning steps; these did not involve any atom trapping.

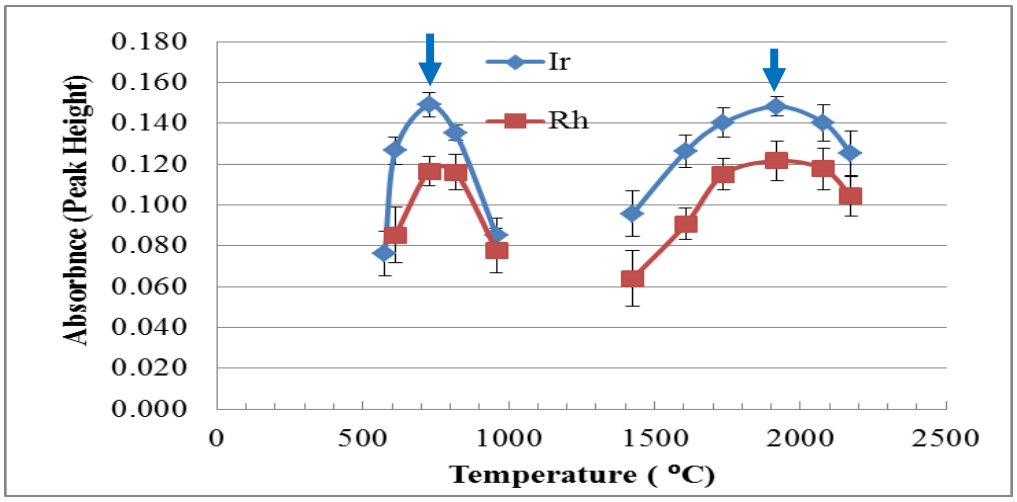


**Figure 3.17** The responses of Ir-coated and Rh-coated W-coil using 60 s trapping time, 1.0 ng/mL of As(III) in 0.2 mol/L HCl was used, 1.5%(w/v) $NaBH_4$, hydrogen flow was 50 mL/min and argon was 150 mL/min. optimum atomization and trapping temperature were 1920 ˚C and 720 ˚C

### 3.3.2.2- Amount of Ir used for coating using As(III) without TGA using CF-HG-WC-ETAAS

The optimum amount of Ir coated on the surface of the tungsten coil to give an efficient, stable and long life time of the coil was examined by changing the mass from 100 to 400 µg. 1.0 ng/mL of As(III) was used in this study and the results are shown in Figure 3.18. It was observed that at low mass of the chemical modifier, the signal was lower but reproducible with 5% RSD, however from the mass of 200 to 400 µg, the signal remained the same. The life-time of the coated iridium was determined by calculating the number of firings before the signal decreased by 20%.

The optimum mass of the chemical modifier selected was 200 µg and the coated W-coil signals were stable for at least 400 firings.

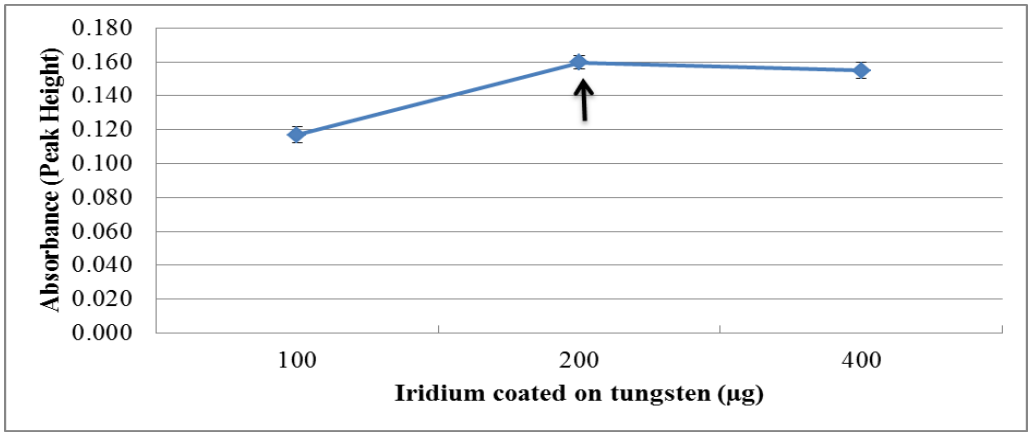


**Figure 3.18** The mass of Ir-coated on tungsten coil, trapping temperature 720 °C and atomization temperature 1920 °C, flow rate of $H_2$ 73 mL/min and Ar 75 mL/min.

### 3.3.2.3- The effect of hydrogen flow during trapping and atomization steps using As(III) without TGA using CF-HG-WC-ETAAS

The role of hydrogen on W-coil atomizer is to provide a reducing environment thus protecting the tungsten coil from oxidation. From Equations 20 to 22 it is apparent that any oxygen generated during hydride generation would react with hydrogen to form water and even if some oxidation products of tungsten were momentarily formed, they would be reduced immediately by hydrogen gas [119]. Hydrogen gas has thermal conductivity of 4.46 x $10^{-4}$ cal $s^{-1}$ $cm^{-1}$ at 26.7 °C, therefore it also has the role of cooling the temperature of the W-coil. It should be remembered that thermal conductivity of Ar is about 10 time lower, 4.3 x $10^{-5}$ cal $s^{-1}$ $cm^{-1}$ at 26.7 °C. In order to avoid the oxidation of the W-coil a further precaution was implemented by using two gas liquid separators. In this design, water vapor that passes through the first GLS is further separated from volatile arsenic hydride in the second GLS [55]. In order to obtain the optimum flow rate of hydrogen during trapping and atomization

stages, the flow of the gas was varied from 0, 22, 33, 53, 73, and 103 mL/min. but because of the danger in hydrogen gas, high flow rates were avoided.

$$WO(g) + H_2(g) \longrightarrow W(s,g) + H_2O(g) \quad (20)$$

$$WO_2(s,g) + 2H_2(g) \longrightarrow W(s,g) + 2H_2(g) \quad (21)$$

$$WO_3(s,g) + 3H_2(g) \longrightarrow W(s,g) + 3H_2O(g) \quad (22)$$

In the first study, the trapping of As atoms on Ir-coated W-coil without the flow of hydrogen was tried and the flow of hydrogen gas during atomization stage was varied between 22 and 103 mL/min. It was found that, when the flow was less than 22 mL/min during atomization, the coil rapidly oxidized during the atomization step, and it was visibly observed by blue powder of tungsten oxide, $W_2O_5$ and/or $W_4O_{11}$ formed on the surface of the glass cell. The oxidation process of the tungsten coil is also indicated by a popping sound. Since $H_2$ is produced during the hydride generation, this minimum amount of hydrogen was also able to protect the tungsten during the trapping stage. From the experimental results shown in Figure 3.19, it is clear that during trapping without $H_2$, the analytical signal was 2 times less sensitive for all the flow rates of hydrogen during atomization. In order to determine the optimum hydrogen gas flow during trapping and atomization stage, the flow rates between 22 and 103 mL/min were investigated for both trapping and atomization. The results of this experiment are shown in Figure 3.19 and the optimum hydrogen flow rate selected for both the trapping and atomization stages, was 73 mL/min.

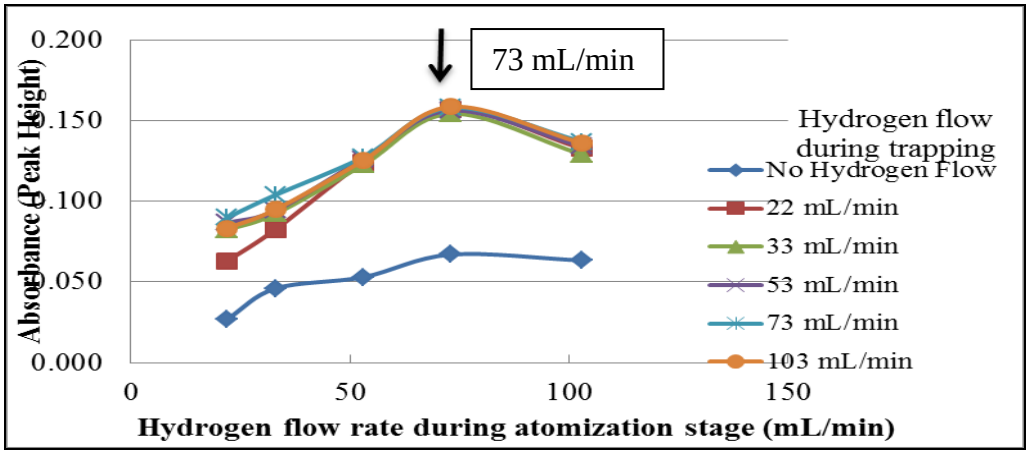


**Figure 3.19** The influence of $H_2$ flow rate during trapping and atomization processes using 1.0 ng/mL of As(III) for 60 s trapping. Trapping and atomization temperatures were 720 and 1920 °C, respectively. 0.25 mol/L HCl and 1.5% (w/v) $NaBH_4$, and argon flow rate was 150 mL/min was used.

### 3.3.2.4- Evaluation of argon gas flow rate for 73 mL/min $H_2$ flow using As(III) without TGA using CF-HG-WC-ETAAS

Argon was used as the carrier gas and it was introduced upstream the stripping coil. In the stripping coil, $AsH_3$ is separated from the liquid phase and transported through the first GLS after which it meets with hydrogen flowing at 73 mL/min. The two gases now carry $AsH_3$ through the second GLS to the pre-heated tungsten coil in the glass cell. During the evaluation of the argon flow, the flow rate remained the same for both trapping and atomization processes. The optimum flow of argon was investigated by varying the flow from 5 to 200 mL/min. As it is shown in Figure 3.20, from 5 to 50 mL/min, the analytical signal was increasing with increase in flow rate. However from 75 to 200 mL/min, the analytical signal almost remained constant and maximum absorbance signal was obtained at 75 mL/min. The optimum selected flow was 75 mL/min.

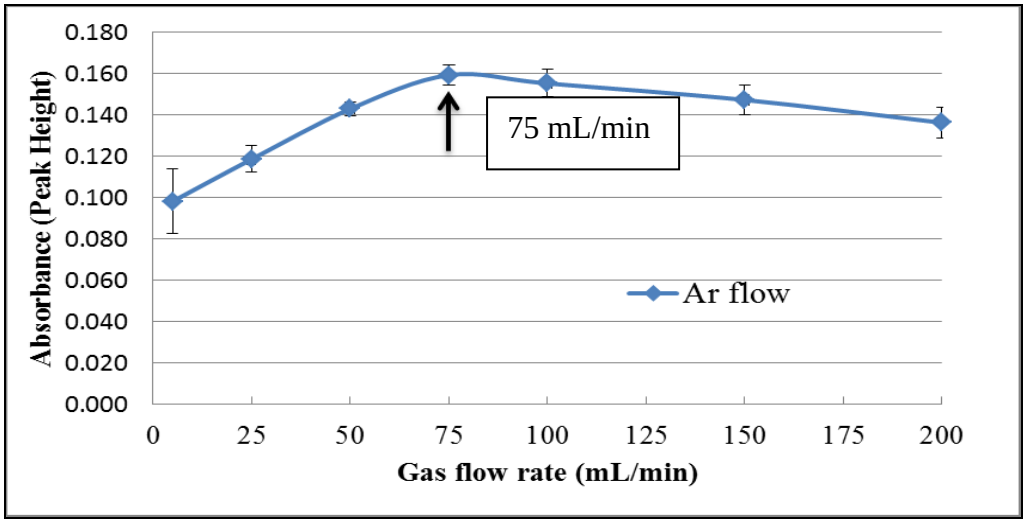


**Figure 3.20** The response of 1.0 ng/mL of As(III) signal in 0.25 mol/L HCl using 1.5% $NaBH_4$ with Ar variation. Trapping period was 60 s. Trapping and atomization temperature were 720 ˚C and 1920 ˚C, respectively

### 3.3.2.5- The influence of HCl on As(III) and As(V) analytical signal without TGA using CF-HG-WC-ETAAS

The influence of HCl concentration on As(III) and As(V) hydride generation using the Ir-coated W-coil atom trap was again investigated. The HCl concentration was varied from 0.05 to 2.0 mol/L and the results are shown in Figure 3.21. For As(V) hydride generation, the oxy-anion ($R_nAs(O)(OH)_3$, where R is a methyl group and n ranges from 0 to 3); must be fully protonated if they are to be converted to arsine [106]. As $pK_1$ for As(V) ($H_3AsO_4$) 2.3, the reaction must therefore be carried out at very low pH around 1 to 3 M hydrochloric acid. For As(III), ($H_3AsO_3$) on the other hand, is fully protonated under all acidic conditions ($pK_1$ is 9.2) and will therefore react with the THB under mild acid conditions. However since the acid hydrolysis of THB is in micro seconds [21], the amount of hydrogen gas produced will cause dilution in the system. Thus the absorbance signals of As(III) started to drop at high acid concentration. The absorbance signals of As(V) remains constant (similar to what was seen in CF-HG-EHQTA).

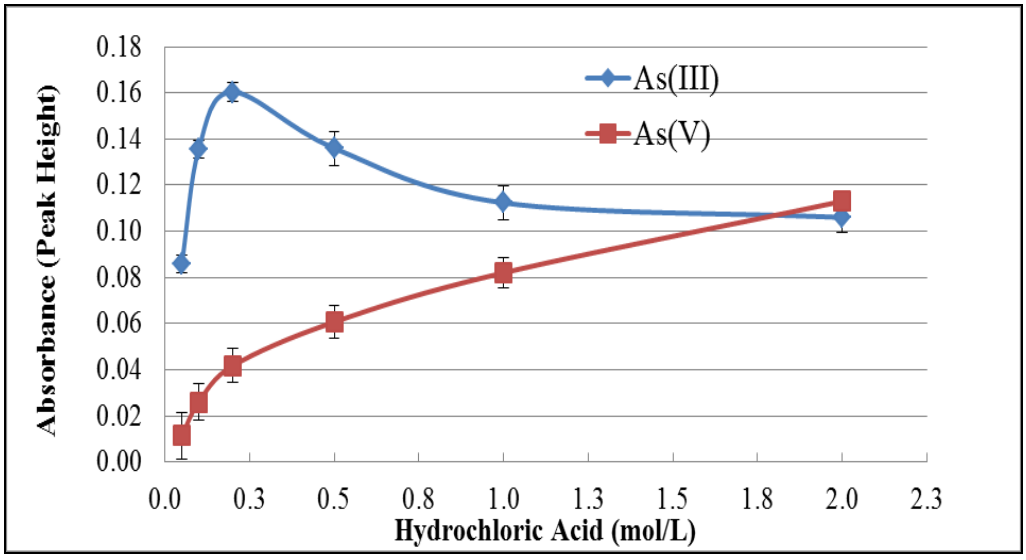


**Figure 3.21** The influence of HCl concentration on 1.0 ng/mL of As(III) and 5.0 ng/mL As(V) hydride formation, the trapping time was 60 s, the trapping and atomization temperatures were 720 $^{0}$C and 1920 $^{0}$C, respectively.

### 3.3.2.6- The effect of $NaBH_4$ concentration on As(III) and As(V) signals without TGA using CF-HG-WC-ETAAS

The effect of $NaBH_4$ concentration on the absorption signal of As(III) and As(V) was investigated first without the use of pre-reduction reagents for As(V). The concentration of $NaBH_4$ was varied from 0.1 to 2.0% (w/v) and the solutions were stabilized in 0.3% (w/v) NaOH. By increasing the concentration of $NaBH_4$ from 0.1 to 1.0% (w/v) an increase in signal intensity of As(III) was observed; however for As(V) there was lower increase in the signal intensity. For As(III) the signal intensities decreases when the concentration of $NaBH_4$ was increased to 2.0% w/v, and for As(V) the signal remains almost constant. The results of the experiment are shown in Figure 3.22. The concentration of 1.5% w/v of $NaBH_4$ was selected as the optimum value and was used for other optimization studies.

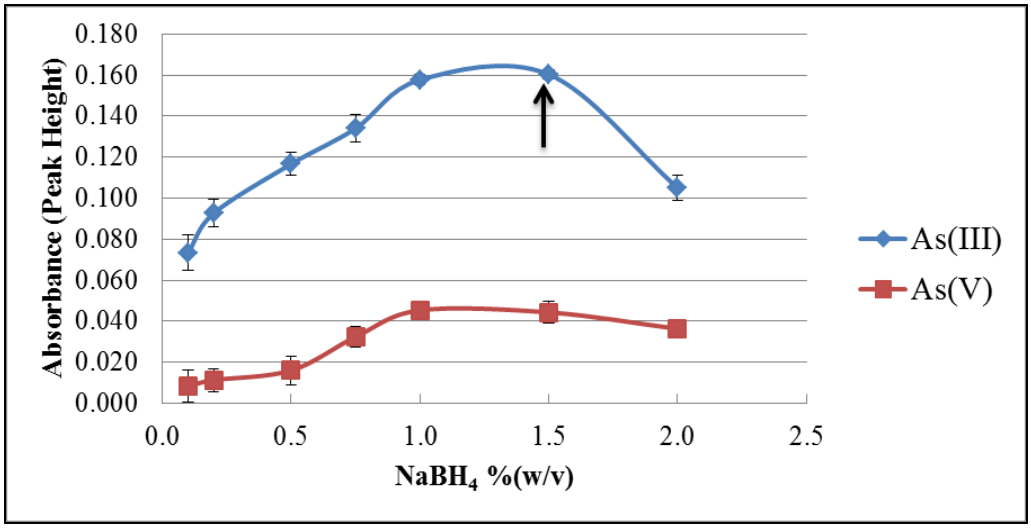


**Figure 3.22** Effect of $NaBH_4$ concentration on the signal of 1.0 ng/mL As(III) and 5.0 ng/mL As(V). $H_2$ and Ar gas flow were 73 and 75 mL/min respectively. 60 s trapping, flow rate of $NaBH_4$ was 2 mL/min and flow rate of HCl was 0.25 M and flow rate of 6.5 mL/min

### 3.3.2.7- The effect of HCl concentration on the pre-reduction reaction of thioglycolic acid and KI in Ascorbic acid on As(V) (CF-HG-WC-ETAAS)

By using the CF-HG-WC-ETA technique, the effect HCl concentration on the activities of the pre-reductant reagents of 1.0% (v/v) TGA and 0.5% (w/v) potassium iodide in 0.5% (w/v) L(+)ascorbic acid on 1.0 ng/mL As(V) were evaluated. In the study with TGA, the concentration of TGA was kept constant at 1.0% (v/v), and the concentration of HCl was varied from 0 to 1.0 mol/L. The result of the experiment is shown in Figure 3.23. The trapping time was 60 s. It was observed that, when there was even no HCl in the 1.0% (v/v) TGA solution of As(V), the signals were intense and they remain constant up to 0.02 mol/L HCl. However from 0.1 to 1.0 mol/L, the intensity of the signal started to drop and furthermore the formation of foams in the gas liquid separator at high HCl concentration was clearly observed.

The pH of the waste solutions was also simultaneously monitored during study when 1.0% (v/v) TGA without hydrochloric acid, 1.0% TGA with 0.002 and 0.005 mol/L HCl was used. The pH of the solutions was between 8.2 and 8.6; which is almost neutral.

To study effect of HCl concentration in the pre-reduction activity of KI in L(+)Ascorbic acid, the acid concentration was varied from 0 to 1.0 mol/L. The solutions were prepared by first adding the HCl at concentration to be studied and then 1.0 ng/mL of As(V) was added which was followed by adding 0.5% (w/v) KI in 0.5% (w/v) L(+) ascorbic acid. The solutions were allowed to stand for 30 min before analysis. By using trapping time of 60 s, the results shown in Figure 3.23 were obtained. It was observed that from 0 to 0.1 mol/L HCl, the intensity of the As(V) signals were less sensitive by 90%, but when the acid concentration was increased from 0.2 to 1.0 mol/L, the absorption signal started to increase. The result indicates that for As(V) to be reduced by KI in ascorbic acid, relatively high HCl concentration is required. Finally, thioglycolic acid was tested as the pre-reductant reagent for As(V), because it was fast, efficiency and needs low HCl concentration of 0.002 mol/L.

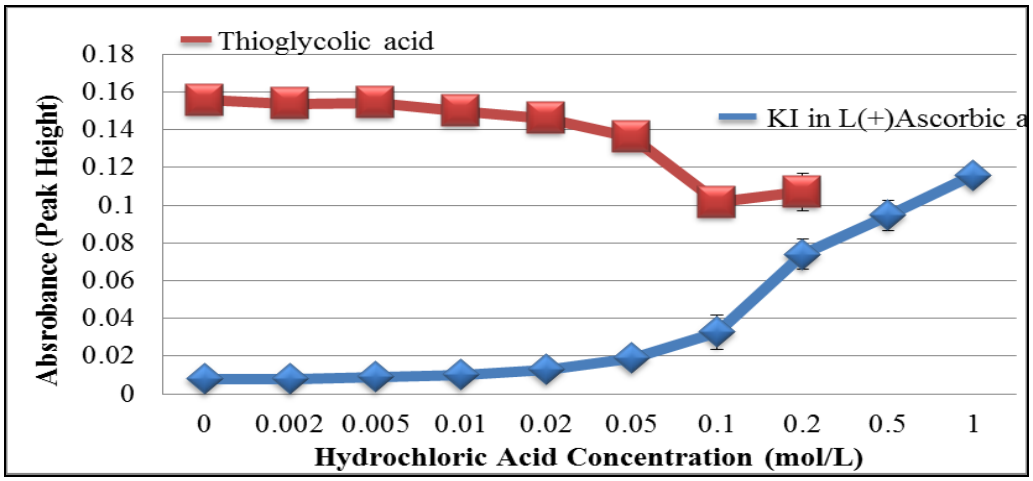


**Figure 3.23** The effect of HCl concentration in the reduction reaction of 1.0 ng/mL As(V), 1.0% (v/v) TGA and 0.5% (w/v) KI in 0.5% (w/v) L(+) ascorbic acid. Trapping period was 60 s, flow rate of $NaBH_4$ was 2.0 mL/min and flow rate of HCl was 6.5 mL/min.

### 3.3.2.8- Optimum concentration of thioglycolic acid using As(V) (CF-HG-WC-ETAAS)

The optimum concentration of TGA in the presences of 0.002 mol/L HCl was evaluated. The complete reduction of As(V) to As(III) was necessary to obtaine sensitive hydride formation from As(V). The concentrations of TGA was varied from 0.25 to 2.0% (v/v) in the solutions containing 0.002 mol/L HCl and 1.0 ng/mL As(V). In order to see the action of the TGA, separate studies of As(V) and As(III) were carried out using the same range of TGA.

For this study, 1.0 ng/mL As(III) and As(V) were used and the trapping time was 60 s. As shown in Figure 3.24, the optimum concentration for TGA was found to be 1.0% (v/v). The pH of the waste solutions was also monitored for each concentration of TGA. Since TGA has a p$K_1$ value of 3.6, by increasing its concentration from 0.25 to 2.0% (v/v) the pH of the waste solution was observed to decreases from 12.5, to 5.5. However at the optimum concentration of TGA (1.0%), the pH of the waste solution was 8.3.

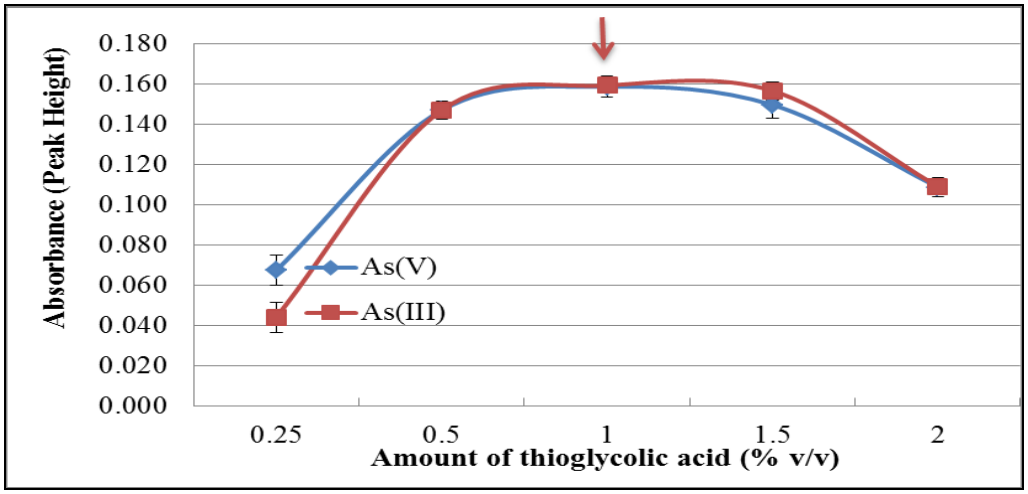


**Figure 3.24** The effect of TGA concentration on 1.0 ng/mL As(III) or As(V) in 0.002 mol/L HCl using CF-HG-WC-ETAAS optimum values, flow rate of $NaBH_4$ was 2 mL/min and flow rate of HCl was 6.5 mL/min.

### 3.3.2.9- Optimization of the trapping period using CF-HG-WC-ETAAS

The investigation on the relationship between the absorbance signal and the trapping period of 1.0 ng/mL As(III) and As(V) on the surface of the Ir-coated W-coil, was carried out by varying the trapping period from 30 to 240 s. The solutions were prepared in 0.002 mol/L HCl and 1.0% (v/v) TGA, and the flow of the analyte solution was 6.5 mL/min. By taking the product of flow rate with the trapping time (min), the volume of the solution introduced during trapping can be calculated for each trapping period. As can be seen from the results shown in Figure 3.25, a linear relationship between trapping period and absorbance signal was observed from 30 to 180 s studied period and when the time was increased to 240 s, the signal remains the same, thus deviating from linearity. The optimum trapping period selected for calibration and validation studies was then 180 s. The volume of solution consumed for this optimum trapping period is equal to 19.5 mL.

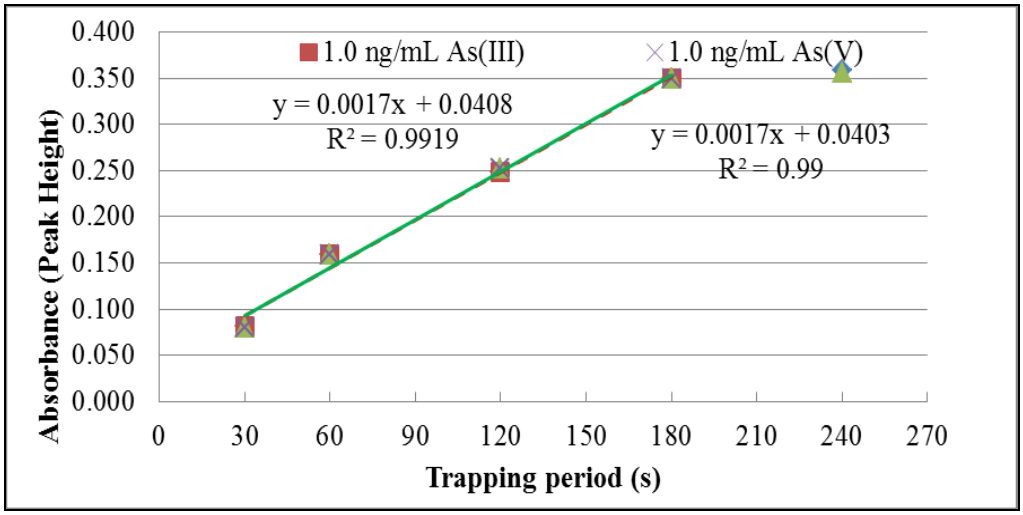


**Figure 3.25** The Analytical signal *versus* collection time for 1.0 ng/mL of As(III) and As(V) with 1.0 % TGA in 0.002 M HCl. The sampling volume was 6.5 mL/min. The parameters selected for CF-HG-WC-ETA given in Table 3.3 were used.

**Table 3.3** The optimized parameters for CF-HG-WC-ETAAS with As(III) and As(V)

| **Parameter** | **Optimum value** |
|---|---|
| Trapping temperature | 720 $^0$C |
| Atomization temperature | 1920 $^0$C |
| Trapping period | 180 s |
| Flow rate of $H_2$ | 73 mL/min |
| Flow rate of Ar | 75 mL/min |
| Flow rate of analyte solution | 6.5 mL/min |
| Flow rate $NaBH_4$ | 2.0 mL/min |
| Concentration of HCl without TGA | 0.2 mol/L |
| Concentration of HCl with TGA | 0.002 mol/L |
| Concentration of $NaBH_4$ | 1.5% (w/v) |
| Concentration of TGA | 1.0% (v/v) |

### 3.3.2.10- Analytical signals for As(III) and As(V) using CF-HG-WC-ETAAS

The analytical signals obtained by using 180 s trapping period for the analysis of 0.02 ng/mL As(V) and As(III) in 0.002 mol/L HCl and 1.0% (v/v) TGA are shown in Figure 3.26 and Figure 3.27, respectively. The repeatability of the measurements after 7 replicates ($N$ = 7) was less than 5% RSD. The transient signal have a half width < 0.5 s; therefore the absorbance signals were measured in peak height giving a better reproducibility at lower concentration than integrated peak area. As the atomization step was manually controlled by pushing the switch of the variable potential power supplier to the on position, the speed and precision with which it is operated affect the width and reproducibility of the analytical signal. Thus in order to obtain a sharp signal with half width less than 0.5 s, precise and reproducible fast switching of the power was necessary.

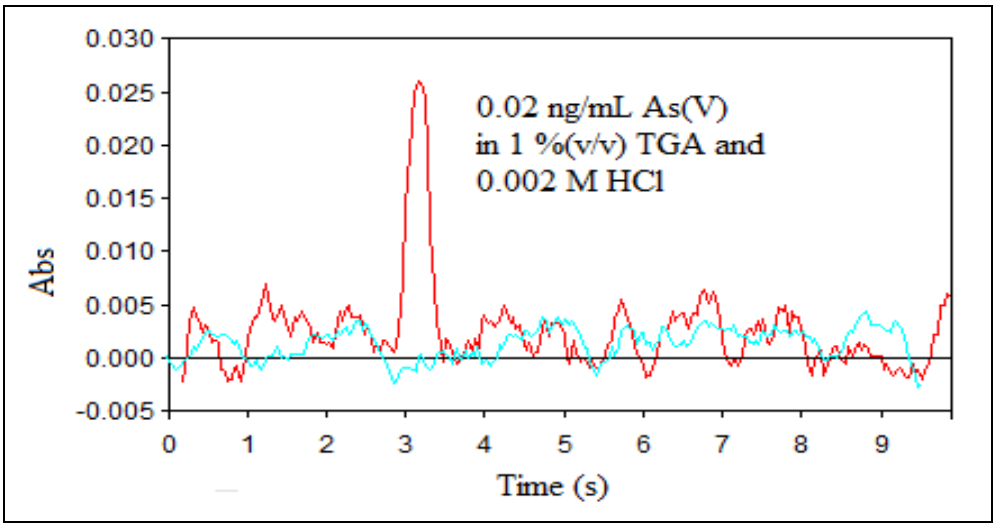


**Figure 3.26** The analytical signal of 0.02 ng/mL of As(V) in 1.0% (v/v) TGA and 0.002 mol/L HCl, obtained using the optimum parameters of CF-HG-WC-ETAAS given in Table 3.3

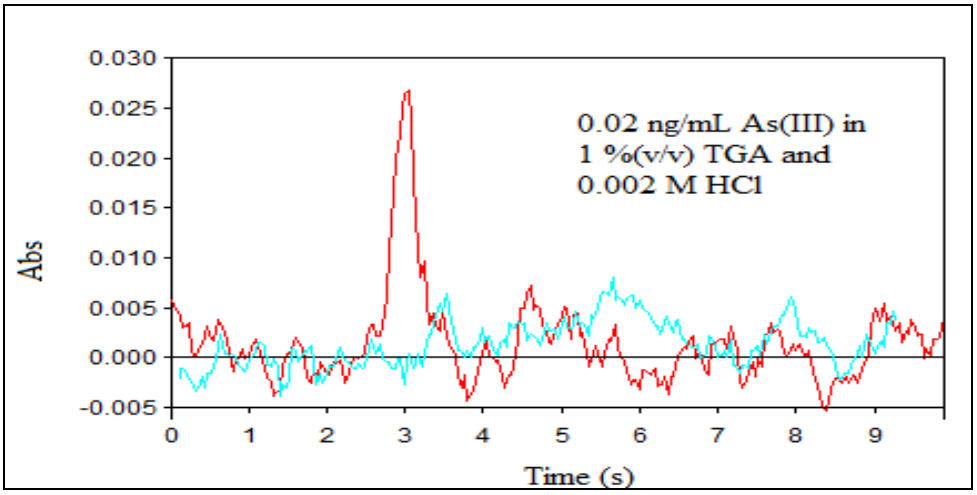


**Figure 3.27** The analytical signal of 0.02 ng/mL of As(III) in 1% (v/v) TGA and 0.002 mol/L HCl, obtained using the optimum parameters of CF-HG-WC- ETAAS given in Table 3.3.

The analytical signals obtained by using 180 s trapping period for the analysis of 1.0 ng/mL As(V) and As(III) in 0.002 mol/L HCl and 1.0% (v/v) TGA are also shown in Figure 3.28.

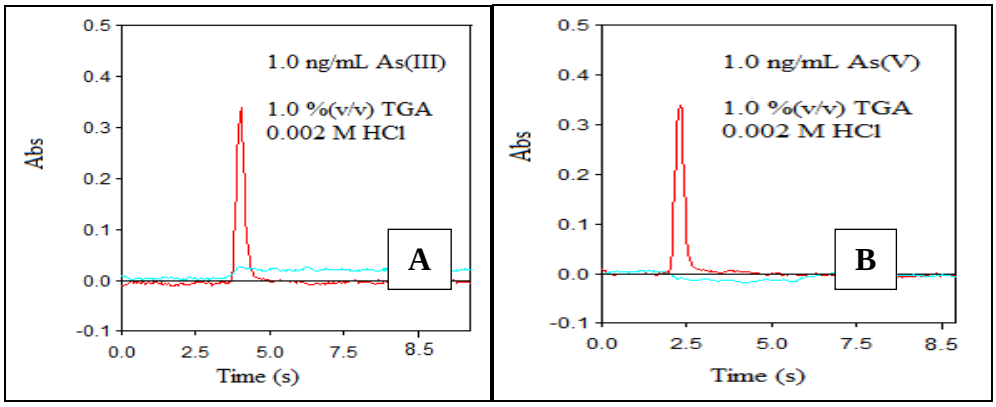


**Figure 3.28** The analytical signals of 1.0 ng/mL of **A-** As(III) and **B-** As(V) in 1.0% (v/v) TGA and 0.002 mol/L HCl, obtained using the optimum parameters of CF-HG-WC-ETAAS given in Table 3.3

### 3.3.2.11- Calibration plots of As(III) and As(V) in 0.2 mol/L HCl or 1.0% (v/v) TGA in 0.002 mol/L HCl using CF-HG-WC-ETAAS

The optimum parameters given in Table 3.3 were used to obtain the calibration plots of As(III) and As(V) in two different conditions. In the first set of conditions, As(III) and As(V) standard solutions were prepared using 1.0% (v/v) TGA and 0.002 mol/L HCl and in the second set of conditions, As(III) and As(V) standard solutions were prepared in 0.2 mol/L HCl. The linear dynamic range of both the inorganic arsenic species is from 0.02 to 1.0 ng/mL, and after 1.0 ng/mL a negative deviation was observed. For the calibration plot of As(V), the significant effect of the pre-reductant reagent was observed. As shown in Figure 3.29, the slope in plot **A** (with TGA) is 4 times the slope in plot **B** (with of 0.2 mol/L HCl). Hence As(V) became more sensitive in the presence of TGA as pre-reductant reagent. The slopes of the calibration plots of As(III) shown in Figure 3.30, are almost equal; thus indicating

that As(III) hydride formation is not affected whether the medium is TGA solution or 0.2 mol/L HCl solution.

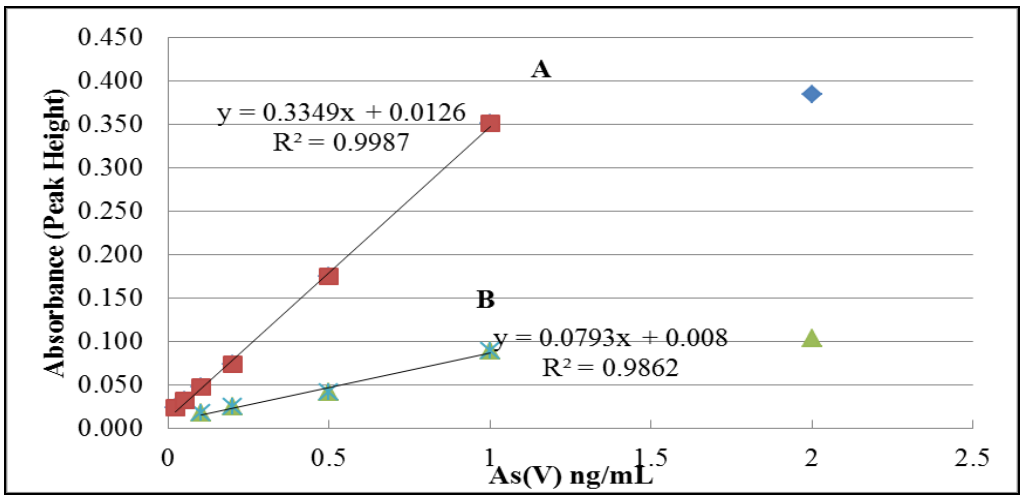


**Figure 3.29** The calibration of As(V): (**A**) in 1.0% (v/v) TGA in 0.002 mol/L HCl and (**B**) in 0.2 mol/L HCl, using the optimum parameters of CF-HG-WC-ETAAS in Table 3.3.

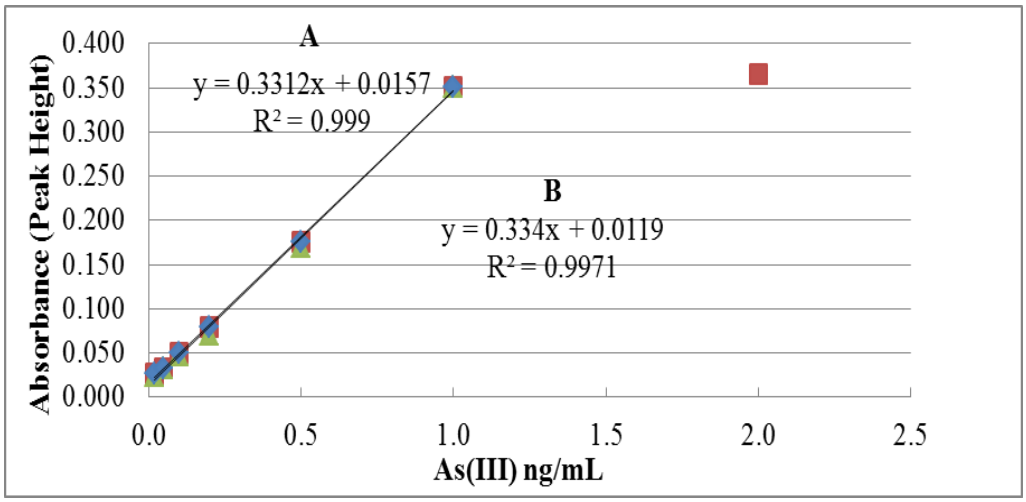


**Figure 3.30** The calibration of As(III): (**A**) in 1.0% (v/v) TGA in 0.002 mol/L HCl and (**B**) in 0.2 mol/L HCl, using the optimum parameters of CF-HG-WC-ETAAS given in Table 3.3.

### 3.3.2.12- Analytical figures of merit of CF-HG-WC-ETAAS system

The analytical figures of merit of the method are given in Table 3.4. The reproducibility of the measurements was <5% RSD for 7 replicates ($N$ = 7) using 0.02 ng/L As(III) and As(V) in 1.0% (v/v) TGA and 0.002 mol/L HCl solutions trapped for 3 min. The enhancement factor of CF-HG-WC-ETAAS over CF-HG-EHQTA is shown in Table 3.5.

In Table 3.6, the values of LOD and sample volume used in literature are compared with the developed method in this work. Ir-coated WC-ETAAS has the advantage of being simple and easily applicable to AAS or AFS instruments and the time required for the analysis depends on the collection time. The technique is a sensitive alternative for other relatively high cost systems such as ICP-MS and GFAAS.

**Table 3.4** The analytical figures of merit for CF-HG-WC-ETA using peak height for absorbance measurement

| **Figures of merit** | **Values** | | |
|---|---|---|---|
| | As(III) in 0.25 M HCl or in 1.0% (v/v) TGA and 0.002 mol/L HCl | As(V) in 0.2 mol/L HCl | As(V) in 1.0% (v/v) TGA and 0.002 mol/L HCl |
| LOD (ng/L) | 1.9 | 13 | 1.8 |
| LOQ (ng/L) | 6.3 | 45 | 6.0 |
| Linear Range (ng/mL) | 0.02 to 1.0 | 0.1 to 1.0 | 0.02 to 1.0 |
| $C_0$ (ng/L) | 12.5 | 51.9 | 12.4 |

**Table 3.5** The enhancement factors of CF-HG-WC-ETA over CF-HG-EHQTA calculated by comparison of characteristic concentration ($C_0$) using 1.0% (v/v) TGA in 0.002 mol/L HCl

| **Analyte** | | | | **$C_0$ (ng/mL)** | |
|---|---|---|---|---|---|
| | E | $E_t$ ($min^{-1}$) | $E_v$ ($mL^{-1}$) | CF-HG-EHQTA | CF-HG-WC-ETA |
| As(III) | 30.5 | 10.2 | 1.56 | 0.38 | 0.0125 |
| As(V) | 31.8 | 10.6 | 1.63 | 0.396 | 0.0125 |

**E** is the enhancement factor (ratio of $C_0$ for EQTA and W-coil ETA)

**$E_t$** is the E/min for sampling

**$E_v$** is the E/volume of sample in mL

**Table 3.6** The comparison of CF-HG-WC-ETAAS of limit of detection and sample volume with other the methods in literature for As determination

| **Values** | **LOD ($ngmL^{-1}$)** | | **Sample Volume (mL)** | **Reference** |
|---|---|---|---|---|
| | Total As | As(III) | | |
| Ir-coated W-trap HG-ETAAS | 0.0019 | 0.0019 | 19.5 | This work |
| Rh-coated W-trap HG-AFS | 0.0090 | 0.010 | 48 | [55] |
| Rh-coated W-trap HG-AAS | 0.11 | - | 1.5 | [116] |
| HG-CT-ICP-MS | 0.0034 | - | 0.5 | [120] |

### 3.3.3- Flow injection hydride generation electrically heated quartz tube atomizer atomic absorption spectrometry (FI-HG-EHQTA-AAS)

The parameters of the FI-HG manifold system shown in Figure 2.2 combined with EHQTA were optimized. By using 20.0 ng/mL of As(V), The parameters such as carrier solution and TGA flow rates; the concentration of HCl in the injected sample, the effect of TGA on As(V) and As(III) were optimized. Peak height was used for all absorbance evaluation except noted differently, and the reproducibility of the signals was measured for three replicates (N =3).

The studies in this part have been undertaken as a preparatory step for speciation studies involving HPLC.

#### 3.3.3.1- The effect of carrier solution and TGA flow rates using As(V) (FI-HG-EHQTA-AAS)

In this study, the carrier solution was made up of ammonium dihydrogen phosphate and phosphoric acid buffer solution; this carrier solution was chosen because it will be used also in chromatographic separation. The buffer solution had a pH of 5.8 and a concentration of 0.05 mol/L. Thioglycolic acid was used for online pre-reduction of As(V) to As(III).

The effect of the flow rate of TGA was first investigated and the optimum concentration 1% (v/v) in 0.002 mol/L HCl was used. In order to study the effect TGA flow rate, the flow rate was varied from 0.5 to 5.0 mL/min; the carrier solution flow rate was set at 3.5 mL/min and sodium tetrahydroborate flow rate was 2.0 mL/min. As shown in Figure 3.31, at the minimum flow rate of 0.5 mL/min, the repeatability of the peak was better than 5% RSD (N=3) and there was a drop in the sensitivity. But as the flow rate was increased to 1.0 and 1.5 mL/min, an increase in sensitivity of the signals were observed. However, the signals decrease when the

flow rate was 3.0 mL/min to 5.0 mL/min. The decreased in the sensitivity can be attributed to the incomplete pre-reduction of As(V) due to reduced time available. The optimum flow rate of 1.0 mL/min TGA was selected since stable and sensitive signals were obtained.

The carrier solution transports the analyte sample from the 0.5 mL sample loop to the pre-reduction loop to meet with TGA solution. The optimum flow rate of carrier solution was determined by varying its value from 1.0 to 6 mL/min. TGA solution flow was 1.0 mL/min and $NaBH_4$ flow was at 2.0 mL/min. The absorbance signal of As(V) steadily increases from 1.0 to 1.5 mL/min and then starts decreasing from 1.5 to 6.0 mL/min. The result of the study is shown in Figure 3.31. The selected flow rate for the buffer carrier solution was 1.5 mL/min.

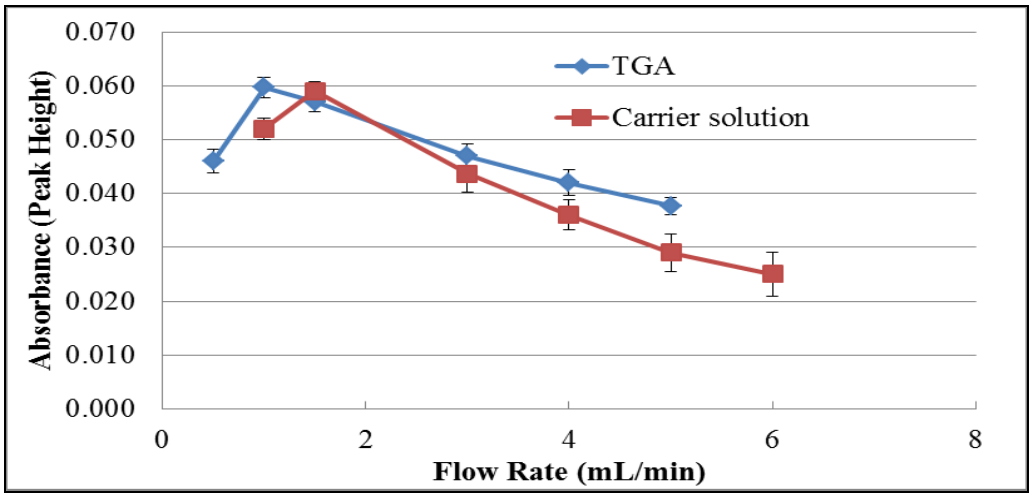


**Figure 3.31** The influence of carrier solution and TGA flow rates, using 20.0 ng/mL of As(V) in a sample loop of 0.5 mL and the volume of pre-reduction loop was 2.5 mL. The flow of argon gas was 200 mL/min. The concentration of TGA was 1.0% (v/v) in 0.002 mol/L HCl, and $NaBH_4$ was 1.5% (w/v) with 2.0 mL/min. The concentration of HCl in the sample was 0.2 mol/L. For TGA data, carrier flow rate was 3.5 mL/min and for carrier (buffer) data TGA flow rate was 1.0 mL/min.

### 3.3.3.2- Effect of sample loop volume using As(V) with TGA using FI-HG-EHQTA-AAS

The relationship between the volume of the sample loop and the absorbance signal of As(V) was examined using the optimized flow rate of the carrier solution of 1.5 mL/min and 1.0 mL/min of the TGA. The length of pre-reduction coil was 520 mm and 2.48 mm id. the volume of the sample loop was varied from 0.1 to 1.0 mL and as shown in Figure 3.32, a linear relationship between the absorbance signal and the volume of sample injected was observed with a correlation value of $R^2$ 0.9998. The volume of 1.0 mL was not selected due to the problem of blank at high volume of injection. Therefore, the volume of 0.5 mL was used for other optimization studies.

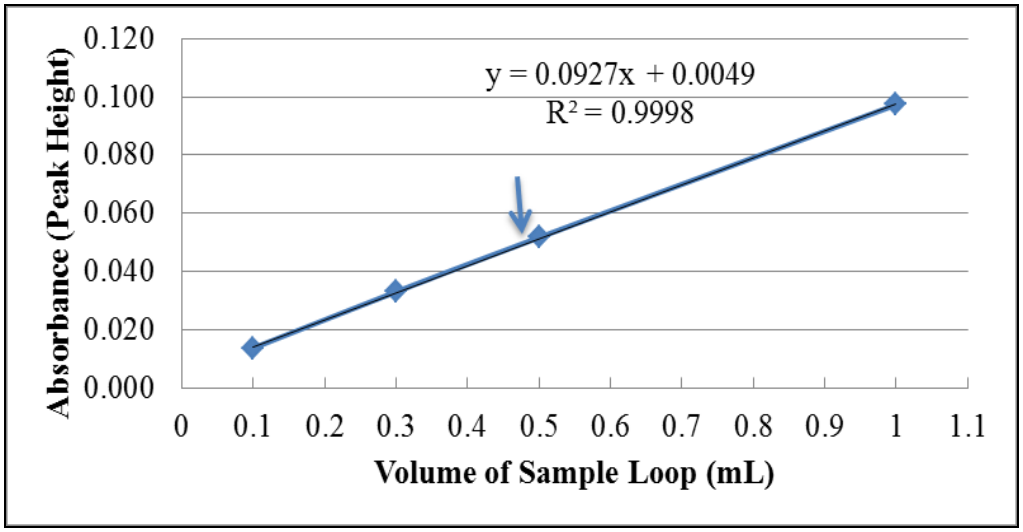


**Figure 3.32** The relationship between absorbance signal and sample loop volume. The concentration of TGA was 1.0% (v/v) in 0.002 mol/L HCl and the concentration of 20.0 ng/mL of As(V) was used.

### 3.3.3.3- Effect of TGA concentration on As(V) using FI-HG-EHQTA-AAS

A study on the effect of the concentration of TGA on As(V) signal using the FI-HG mode was again carried out. The lenght of the pre-reduction coil was 520 mm and 2.48 mm id and the volume of sample injected was 0.5 mL. The concentration of TGA was varied from 0.5 to 2.0% (v/v). The optimum value for the concentration was again found to be 1.0% (v/v) TGA. At 1.5 and 2.0% (v/v) TGA, a small decrease in the analytical signal was observed and the results are shown in Figure 3.33. The study indicates that concentration TGA in reacting with As(V) for complete reduction is little significant but the reaction time of TGA with As(V) is more important.

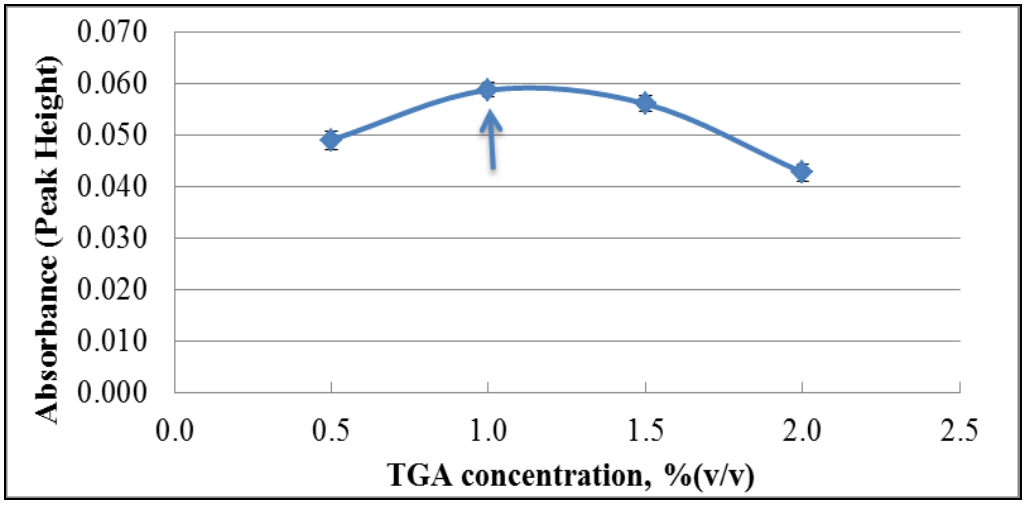


**Figure 3.33** The effect of TGA on 20.0 ng/mL As(V), FI-HG-EHQTA. Concentration of HCl in the TGA solution was 0.002 mol/L. flow of TGA was 1.0 mL/min and the flow of carrier solution was 1.5 mL/min.

### 3.3.3.4- Effect of TGA pre-reduction coil volume on As(V) using FI-HG-EHQTA-AAS

The pre-reduction of As(V) to As(III) by TGA is mainly taking place in the pre-reduction loop before reaching $NaBH_4$ flow. Therefore the optimum volume of pre-reduction coil is necessary to make sure that complete reduction of As(V) to As(III) is achieved. PTFE tubing with 1.3 mm internal diameter was used for the coil and by varying the lengths, the required volume was calculated using the equation $V = \pi r^2 h$. The volumes of 1.0, 2.0, 2.5 and 3.5 mL were investigated and the results are shown in Figure 3.34. The absorbance signals increase when the pre-reduction coil volume was increased from 1.0 to 2.5 mL and then remains constant between 2.5 and 3.5 mL. The coil volume of 2.5 mL was selected, because by using 3.5 mL, the analysis time was increased.

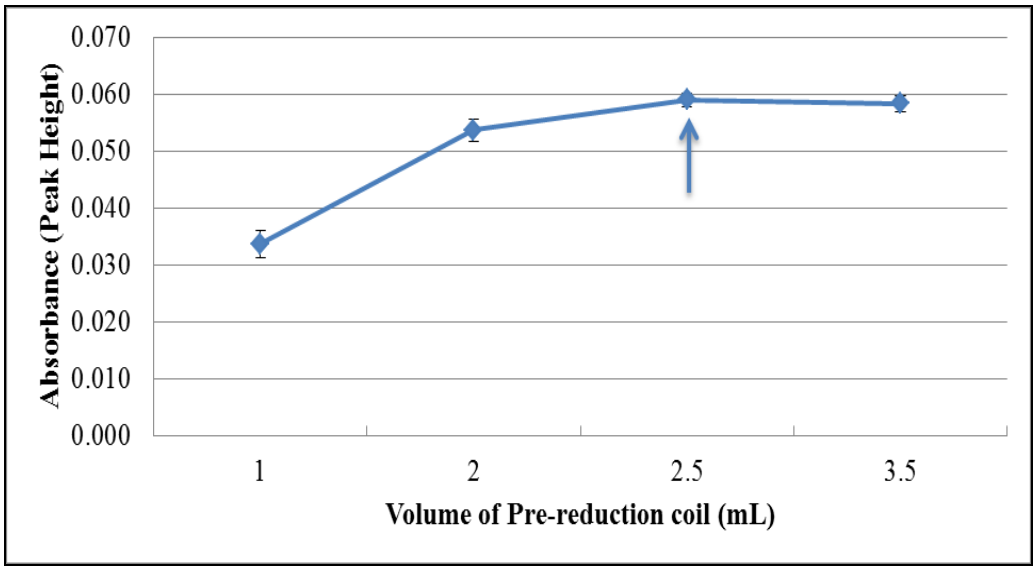


**Figure 3.34** The influence of the pre-reduction coil volume on the analytical signal of 20.0 ng/mL As(V), the concentration of TGA was 1.0% (v/v) in 0.002 mol/L HCl.

### 3.3.3.5- Effect of HCl concentration in the sample injected on As(V) using FI-HG-EHQTA-AAS

In the study of CF-HG-WC-ETAAS study, it was seen that, in the presence of TGA, increase in hydrochloric acid concentration was having a negative effect on the signal of As(V). Therefore it was also important to study the effect of the concentration of HCl in FI-HG-EHQTA system using a sample volume 0.5 mL. As shown in Figure 3.35, the absorption signal of As(V) slowly decrease when HCl concentration wa varied from 0.1 to 6.0 mol/L. considering the standard deviation of data, the signal is definitely decrease at high HCl concentration. Therefore the selected HCl concentration for dilution in the working standards was selected as 0.1 mol/L.

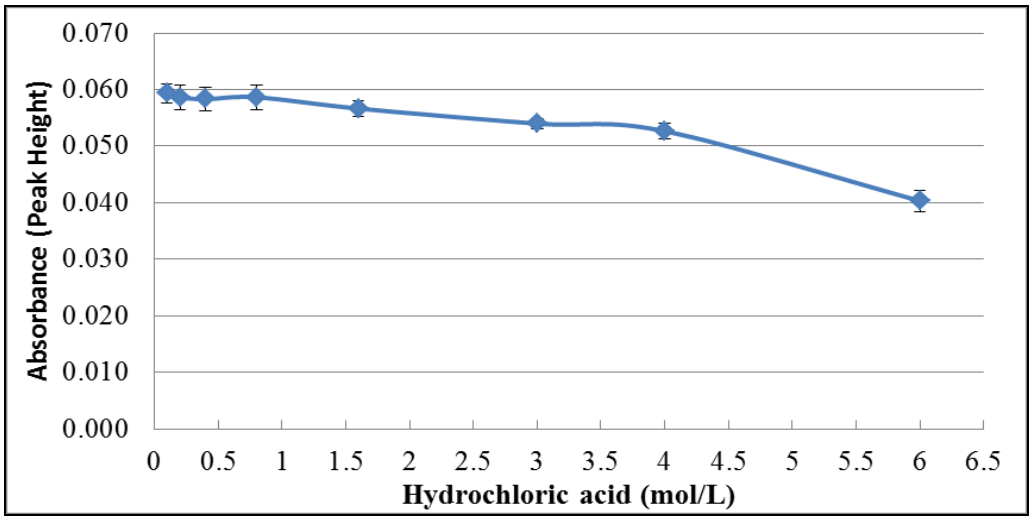


**Figure 3.35** The influence HCl concentration on 20.0 ng/mL As(V) with 0.5 mL sample loop and 1.0% (v/v) TGA in 2.5 mL pre-reduction loop and $NaBH_4$ was 1.5 % (w/v). The carrier solution and TGA flow rates were 1.5 and 1.0 mL/min respectively.

### 3.3.3.6- The effect of concentrations of sodium tetrahydroborate and sodium hydroxide on As(V) using FI-HG-EHQTA-AAS

The effect of the concentration of sodium tetrahydroborate and sodium hydroxide was evaluated in the presence of TGA for flow injection hydride generation. To study the influence of the concentration of $NaBH_4$ on the absorption signal of As(V), concentration of the reductant reagent was varied from 0.5 to 2.0% (w/v). The solutions were stabilized in 0.3% (w/v) NaOH and the flow rate was 2.0 mL/min. From Figure 3.36, it can be seen that as the concentration of sodium tetrahydroborate was increased from 0.5 to 1.5% (w/v), a gradual increase in the absorbance signal of As(V) was observed. However for 2.0% (w/v) $NaBH_4$, a decrease in absorbance signal was clearly noticed which indicated dilution from hydrogen gas produced during the acid hydrolysis of $NaBH_4$. The effect of $NaBH_4$ on the hydride generation efficiency remains the same as what was observed in CF-HG in Figure 3.6. The selected optimum concentration for $NaBH_4$ was again 1.5% (w/v).

Since efficiency of arsenic hydride formation also depends on the pH of the reaction medium, the concentration of sodium hydroxide used for stabilizing $NaBH_4$ was also investigated. The concentration of NaOH was varied from 0.01 to 1.0% (w/v). From the concentration of 0.01 to 0.3% (w/v), a linear relationship between absorbance and the concentration of NaOH was observed. A decrease in signal was seen 0.6 to 1.0% (w/v). The result of this study is also shown in Figure 3.36. The concentration of 0.3% (w/v) of NaOH was taken as the optimum value.

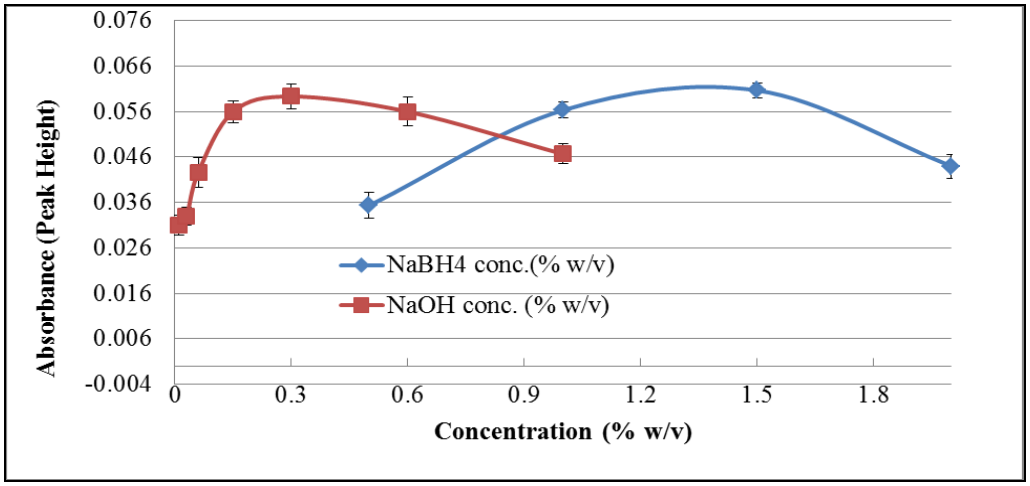


**Figure 3.36** The influence of $NaBH_4$ and NaOH concentration on the absorbance signal of 20.0 ng/mL As(V) using 0.5 mL sample loop and 1.0 %(v/v) TGA with flow rate of 1.0 mL/min. The flow of carrier solution was 1.5 mL/min.

### 3.3.3.7- Effect of TGA concentration on As(III) and As(V) signals using FI-HG-EHQTA-AAS

Following the optimization of the parameters of FI-HG-EHQTA using 20.0 ng/mL of As(V), the influence of TGA concentration on both As(III) and As(V) was also investigated. Even though the effect on the concentration of TGA produced little change on the As(V) signal with the CF-HG mode, it is important to repeat it with the FI-HG mode, because here a sample loop of 0.5 mL is used and furthermore the setup of FI-HG consists of a pre-reduction coil in which As(V) must be reduced to As(III) before reacting with sodium tetrahydroborate to form arsenic hydride. Thus the two limiting factors for complete pre-reduction of As(V) would be TGA concentration and its flow rate. As shown in Figure 3.37, when the concentration of TGA was 0.25% (v/v), the efficiency of arsine formation from As(V) was one quarter less than that of As(III); thus indicating that As(V) is not completely pre-reduced at this low concentration of TGA. However when TGA concentration was increased to 0.5% (v/v), the absorbance signal of As(V) sharply increases and then

levels off between 1.0 to 2.0% (v/v), then decreases when the concentration was increased to 3.0%.

Since the $pK_a$ value of $H_3AsO_3$ is 9.2; it displayed a wider range of pH condition upon which it gives arsenic hydride efficiently. Therefore when the concentration of TGA was varied from 0.25 to 2.0% (v/v), as shown in Figure 3.38, the absorbance signal of As(III) remains almost constant. The decrease in the absorbance signal was only observed when concentration of TGA was 3.0% (v/v). This decrease of signal is either due to dilution from hydrogen or high acidity of the system. It should be noted that the formation of foam in the gas liquid separator was also observed for both As(V) and As(III) when the concentration of TGA is 3.0% (v/v) or more.

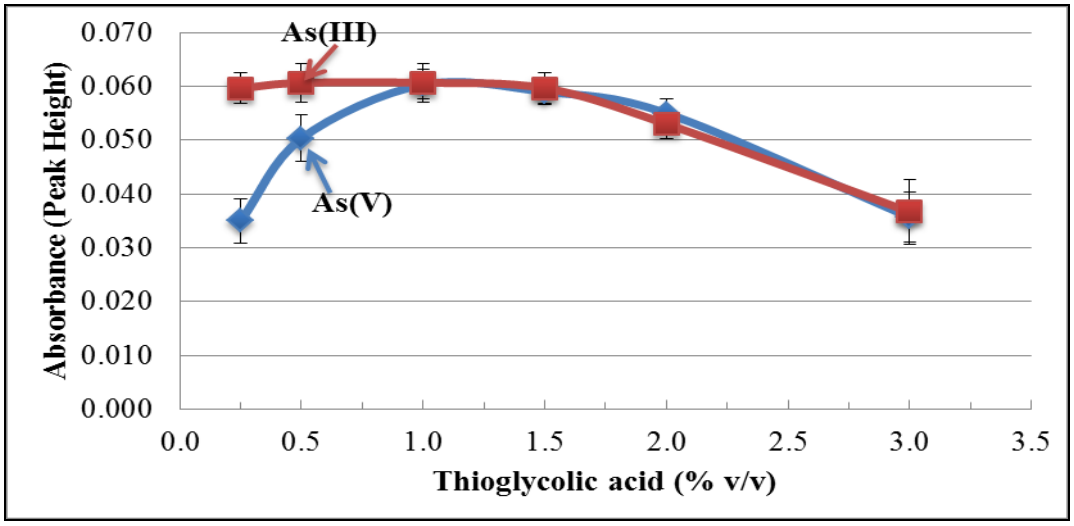


**Figure 3.37** Effect of TGA concentration on As(III) and As(V) signals. The optimum parameters of FI-HG-EHQTA shown in Table 3.7 were used

**Table 3.7** The optimum parameters for FI-HG-EHQTA using 20.0 ng/mL of As(V)

| **Parameters** | **Optimum value** |
|---|---|
| Flow rate of TGA | 1.0 mL/min |
| Flow rate of sample carrier solution | 1.5 mL/min |
| Trapping period | 120 s |
| Concentration of TGA | 1.0 %(v/v) |
| Volume of sample loop | 0.5 mL |
| Volume of pre-reduction coil | 2.5 mL |
| Flow rate of $NaBH_4$ | 2.0 mL/min |
| Concentration of $NaBH_4$ | 1.5% (w/v) |
| Concentration of NaOH | 0.3% (w/v) |

### 3.3.3.8- Calibration plot for As(III) and As(V) using FI-HG-EHQTA-AAS

By using the optimized parameters of the FI-HG-EHQTA shown in Table 3.7, the calibration plots of As(III) and As(V) were constructed. The calibration plot of As(III) is shown in Figure 3.38, and the calibration plot of As(V) is shown in Figure 3.39. Peak height was used for absorbance signal measurement. The linearity of the iAs species were found to be between 5.0 and 50.0 ng/mL and above the concentration of 50.0 ng/mL, a negative deviation from linearity was observed.

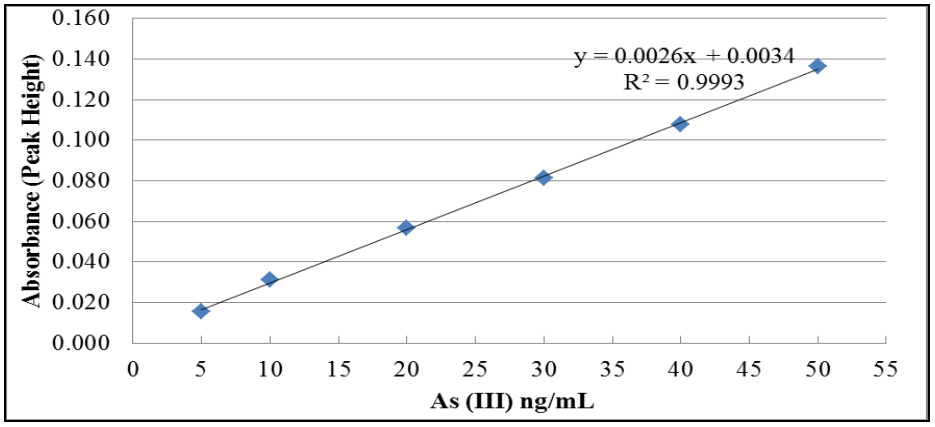


**Figure 3.38** The calibration of As(III) using the optimized parameters of FI-HG-EHQTA. Parameters are given in Table 3.7. (TGA 1.0 % v/v)

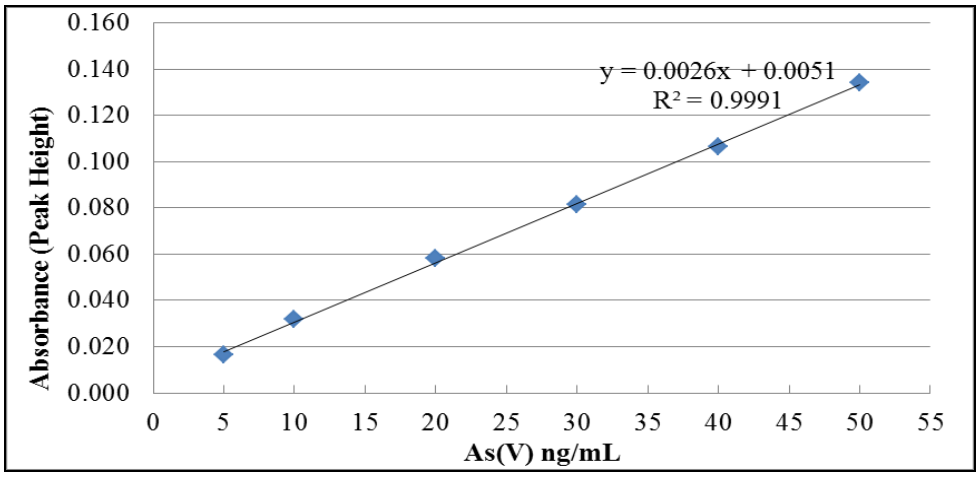


**Figure 3.39** The calibration of As(V) using the optimized parameters of FI-HG-EHQTA. Parameters are given in Table 3.7. (TGA 1.0 % v/v)

### 3.3.3.9- Analytical figures of merit of FI-HG-EHQTA-AAS system

The analytical signal of 5.0 ng/mL of As(III) and As(V) obtained by FI-HG-EHQTA system is shown in Figure 3.40. Peak height was used for absorbance measurement, and the reproducibility was 5.3% RSD for 10 replicates (N=10). The %RSD was better at higher concentrations.

The sensitivities of the FI-HG-EHQTA were calculated in terms of characteristic concentration ($C_0$) and limit of detection. The analytical figures merit are given in Table 3.8. The LOD was calculated from 3 times the standard deviation of the signal obtained by a standard at or slightly above the limit of quantitation.

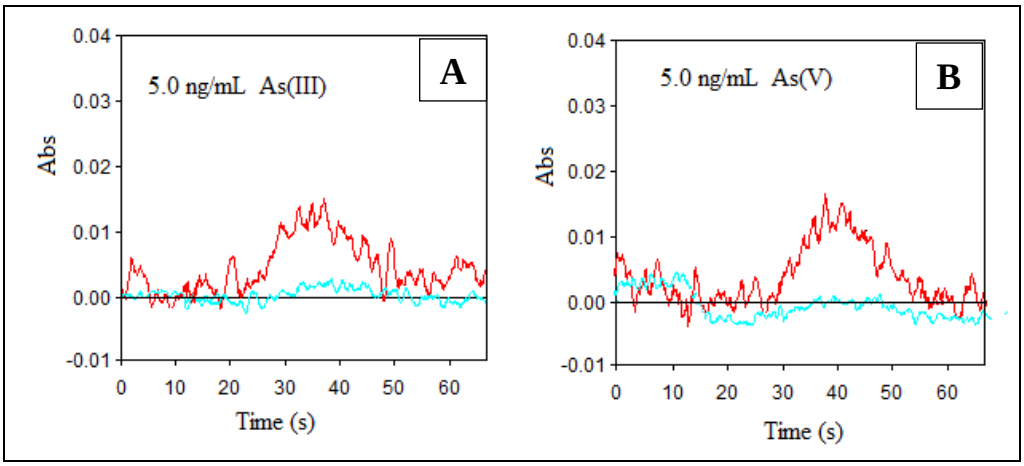


**Figure 3.40** The analytical signals of 5.0 ng/mL of **A-** As(III) and **B-** As(V), obtained using the optimized parameters given in Table 3.7.

**Table 3.8** The analytical figures of merit of FI-HG-EHQTA. Peak height was used for absorbance measurement with N=3

| **Figures of merit** | **Values** | |
|---|---|---|
| | As(III) | As(V) |
| LOD (ng/L) | 0.54 | 0.54 |
| LOQ (ng/L) | 1.8 | 1.8 |
| Linear Range (ng/mL) | 5 to 50 | 5 to 50 |
| $C_0$ (ng/L) | 1.60 | 1.56 |

### 3.3.4- Flow injection hydride generation W-coil trap electrothermal atomic absorption spectrometry (FI-HG-WC-ETAAS)

Because of the fact that the manifold of FI-HG-EHQTA and FI-HG-WC-ETAAS are the same; except the atomizer being different, the hydride generation efficiency was also the same. But nonetheless, an optimization study on the hydride generation parameters of FI-HG-WC-ETAAS method was carried since hydrogen gas is introduced in this system. However since atom trapping is performed with WC, a 10 fold increase in the absorbance signals were observed.

The effect of the carrier solution or TGA flow rate and the trapping period of 2.0 ng/mL As(V) were investigated in detail while the other optimized parameters of FI-HG-EHQTA shown in Table 3.7 were kept constant. The absorbance signals were measured using peak height and the reproducibility was measured using three replicates (N=3).

#### 3.3.4.1- Effect of TGA flow and trapping period using FI-HG-WC-ETAAS

The influence of TGA flow rate and trapping period in the sensitivity of 2.0 ng/mL As(V) was examined by keeping TGA flow rate at one constant value while the trapping period is varied. The flow rates of 0.5, 1.0, 1.5 and 2.0 mL/min of TGA were investigated, and the flow rate of the carrier solution was kept constant at 1.5 mL/min. when the flow rate of TGA was 0.5 mL/min the trapping period was varied from 60 to 180 s. As shown in Figure 3.41, the signal slowly increases with increasing of trapping period and then remains constant between 150 and 180 s. For the other flow rates of 1.0, 1.5 and 2.0 mL/min of TGA flows the same trend of increase in the analytical signal with the trapping period was also observed. However at the flow rate of 1.0 mL the signal was found to be better and more stable. Therefore 1.0 mL/min with trapping period of 120 s was selected as the optimum condition.

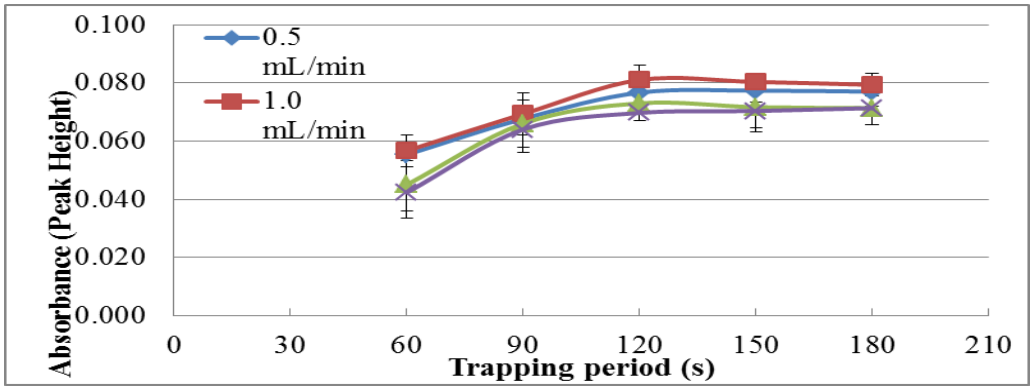


**Figure 3.41** The effect of TGA flow 2.0 ng/mL of As(V) absorbance signal when trapping period changes. The optimized parameters of FI-HG-EHQTA given Table 3.7 were used.

### 3.3.4.2- Effect of carrier solution flow rate and trapping period using FI-HG-WC-ETAAS

The flow rate of the carrier solution determines the analysis time, and also the time to start trapping of arsenic atoms on the Ir-coated tungsten coil in a flow system. Thus, a preliminary study to find the time at which the analyte solution reaches the pre-reduction coil and the reaction coil was carried out using the purple color of potassium permanganate ($KMnO_4$) solution injected into system and monitoring its position using a stopwatch. This preliminary study was conducted to have information about timing of trapping for different flow rates. The flow rate of TGA was kept constant at 1.0 mL/min and the carrier solution flow was varied from 0.5 to 2.0 mL/min. In order to obtain the optimum flow rate of the carrier solution, at each flow rate of carrier solution, the trapping period was varied from 60 to 180 s. As shown in Figure 3.42, at low and high flow rates, the signals were less sensitive; however from 1.0 to 1.5 mL/min, an increase in the analytical signal was observed as the trapping period increases from 60 to 120 s and then remains constant to 180 s. The flow rate of 1.5 mL/min with 120 s trapping period was therefore chosen as the optimum value for calibration studies.

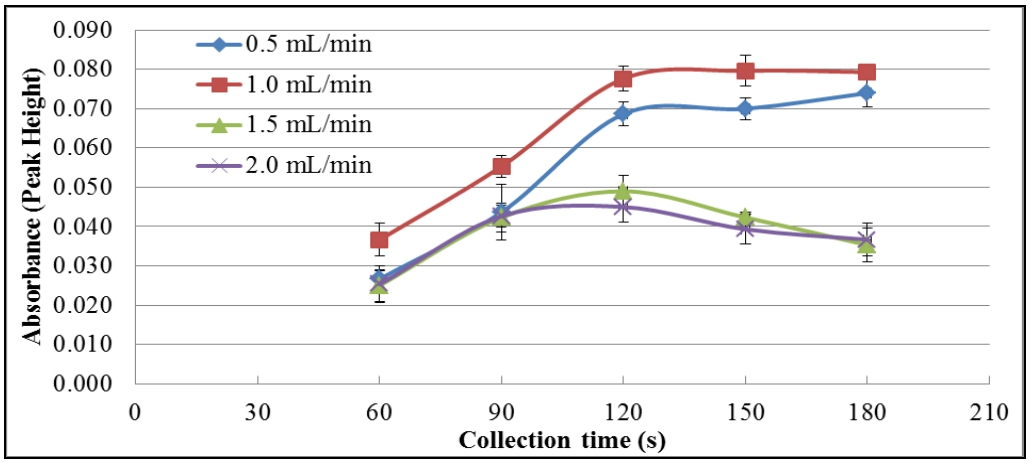


**Figure 3.42** The effect of carrier solution flow rate and trapping period using 2.0 ng/mL of As(V). The flow rate of TGA was 1.0 mL/min and the optimized parameters of FI-HG-EHQTA given in Table 3.7 were used.

**Table 3.9** The optimization parameters of FI-HG-WC-ETAAS. Parameters not included are those in Table 3.7.

| **Parameters** | **Values** |
|---|---|
| Carrier (buffer) solution | 0.05 M phosphate buffer pH 5.8 |
| Pre-reduction solution | 1.0% (v/v) TGA in 0.002 mol/L HCl |
| Flow rate of TGA solution | 1.0 mL/min |
| Flow rate of carrier solution | 1.0 mL/min |
| HCl in working standard | 0.1 mol/L |
| $NaBH_4$ concentration | 1.5% (w/v) |
| $NaBH_4$ flow rate | 2.0 mL/min |
| NaOH | 0.3% (w/v) |
| Volume of sample loop | 0.5 mL |
| Volume of pre-reduction coil | 2.5 mL |
| Length of reaction coil | 120 cm |
| Length of stripping coil | 10 cm |
| Trapping temperature | 720 $^0$C |
| Atomization temperature | 1920 $^0$C |
| Ar flow rate | 75 mL/min |
| $H_2$ flow rate | 73 mL/min |

### 3.3.4.3- Calibration plot of As(III) and As(V) using FI-HG-WC-ETAAS

By using the optimized parameters of FI-HG-WC-ETA shown in Table 3.9, the calibration plots of As(III) and As(V) were constructed. The calibration plot of As(III) is shown in Figure 3.43, and the calibration plot of As(V) is shown Figure 3.44. Peak height was used for absorbance measurements. The linearity of the iAs species were found to be between 0.25 and 20.0 ng/mL and at the concentration of 30.0 ng/mL, a negative deviation from linearity was observed in both cases.

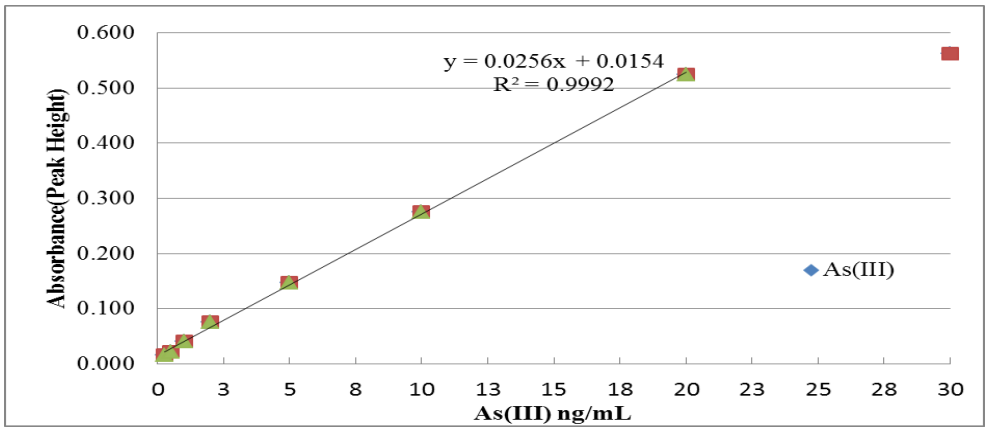


**Figure 3.43** Calibration plot of As(III) trapped in Ir-coated W-coil using FI-HG-WC-ETAAS. Parameters given in Table 3.9 were used.

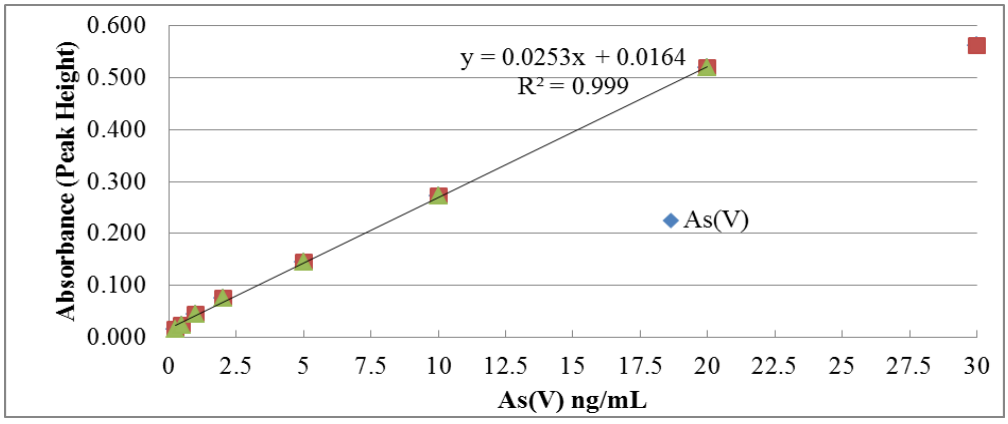


**Figure 3.44** Calibration plot of As(V) trapped in Ir-coated W-coil using FI-HG-WC-ETAAS. Parameters given in Table 3.9 were used.

### 3.3.4.4- Analytical figures of merit of FI-HG-WC-ETAAS system

The absorbance signals of 0.25 ng/mL As(III) and As(V), and 2.0 ng/mL As(III) and As(V) obtained by FI-HG-WC-ETAAS are shown Figure 3.45 and 3.46, respectively. The reproducibility of the absorbance signals were between 5.5 and 1.0% RSD for 7 replicates (N=7). The %RSD became even lower at higher concentrations. The sensitivities of the FI-HG-WC-ETA were calculated in terms of characteristic concentration ($C_0$) and LOD. The results of the analytical figures merit are given in Table 3.10. The LOD was calculated from 3 times the standard deviation of the signal obtained by a standard at or slightly above the limit of quantitation. The characteristic mass ($m_0$) of the flow injection method is also given in Table 3.10.
The enhancement factors of FI-HG-WC-ETAAS over FI-HG-EHQTA-AAS are shown in Table 3.11.

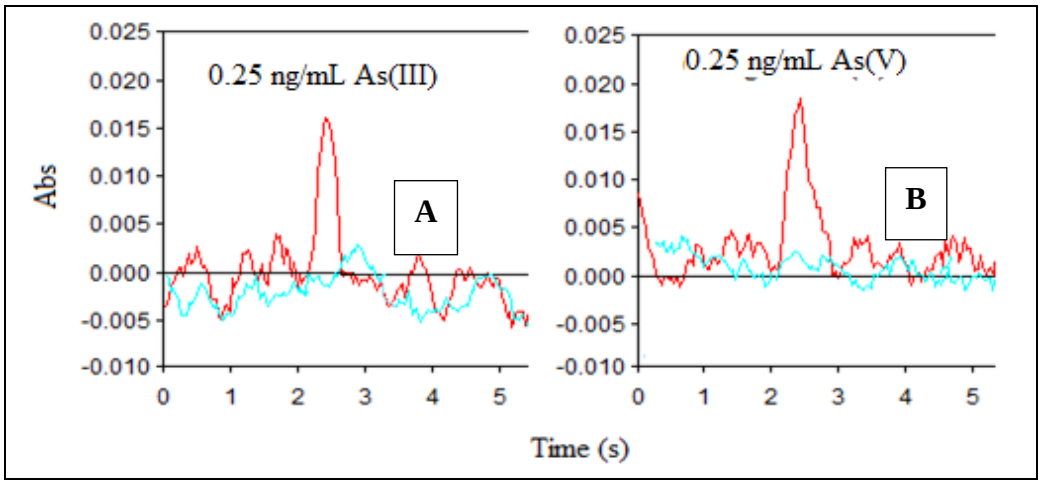


**Figure 3.45** The analytical signals of 0.25 ng/mL of **A-** As(III) and **B-** As(V), obtained using the optimized parameters of FI-HG-WC-ETAAS given in Table 3.9.

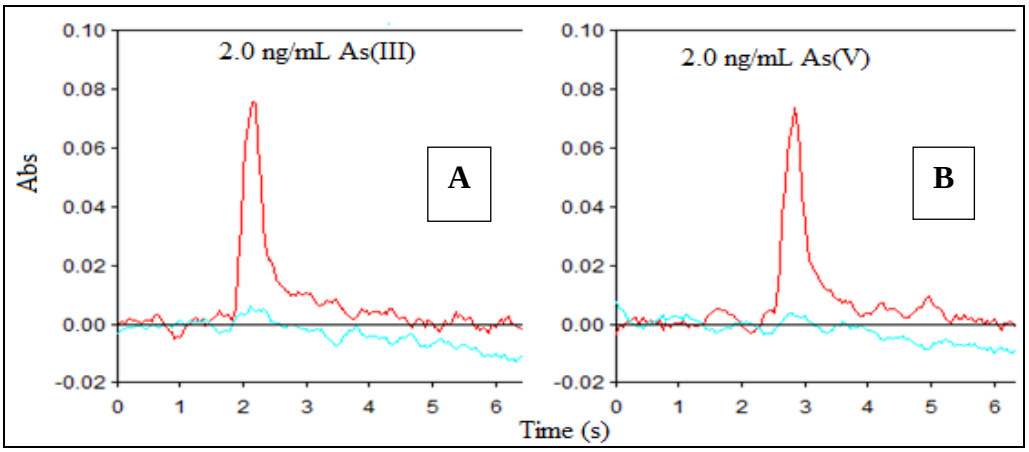


**Figure 3.46** The analytical signals of 2.0 ng/mL of **A-** As(III) and **B-** As(V), obtained using the optimized parameters of FI-HG-WC-ETAAS given in Table 3.9.

**Table 3.10** The analytical figures of merit for FI-HG-WC-ETAAS. Peak height was used for absorbance measurement with N=3

| **Figures of merit** | **Values** | |
|---|---|---|
| | As(III) | As(V) |
| LOD (ng/mL) | 0.047 | 0.050 |
| LOQ (ng/mL) | 0.16 | 0.17 |
| Linear Range (ng/mL) | 0.25 to 20.0 | 0.25 to 20.0 |
| $C_0$ (ng/L) | 0.116 | 0.116 |
| $m_0$ (ng) | 0.058 | 0.058 |

**Table 3.11** The enhancement factors of FI-HG-WC-ETAAS over FI-HG-EHQTA-AAS calculated by comparison of characteristic concentrations ($C_0$).

| **Analyte** | | | | **$C_0$ (ng/mL)** | |
|---|---|---|---|---|---|
| | E | $E_t$ ($min^{-1}$) | $E_v$ ($mL^{-1}$) | FI-HG-EHQTAAS | FI-HG-WC-ETAAS |
| As(III) | 13.8 | 6.91 | 27.6 | 1.60 | 0.116 |
| As(V) | 13.4 | 6.7 | 26.9 | 1.56 | 0.116 |

**E** is the enhancement factor (ratio of $C_0$ for EHQTA and WC-ETAAS)

$\mathbf{E_t}$ is the E/min for sampling

$\mathbf{E_v}$ is the E/volume of sample in mL

### 3.3.5- High performance liquid chromatography hydride generation (HPLC-HG-) studies without TGA

In the following sections, optimizations and measurements using HPLC for chromatographic speciation studies will be undertaken. In this part, the previous data using FI mode will be utilized.

#### 3.3.5.1- Using peak area or peak height for absorbance measurement

The absorbance signal of the chromatographic separation combined with hydride generation method was measured in both peak area and peak height for the two atomization methods: EHQTA and WC-ETA. In the EHQTA method, when measurement was based on peak area, the sensitivity is 3 times better when measurement is on peak height. However for the WC-ETA method, the peak height measurement gave 2 times more sensitive than peak area. But the sensitivity obtains using peak height measurement for WC-ETA is 4 times than the sensitivity obtained using peak area for EHQTA. All these sensitivities are calibration sensitivity or simply the slope of the calibration plot. In EHQTA, no trapping used and the signals are usual chromatography signals, reproducibility is affected by noise. But by using WC-ETA method, all atoms are collected and atomized to produce a sharp signal with half width < 0.5 s and repeatability with < 5%RSD for higher concentrations. Peak areas were calculated using the OriginPro.8.5 software.

### 3.3.5.2- Determination of appearance periods of As(III) and As(V)

In the preliminary study using HPLC-HG, the determination of the retention times for As(III) and As(V) were investigated using the mobile phase ammonium dihydrogen phosphate and phosphoric acid buffer solution ($NH_4H_2PO_4/H_2PO_4$) at pH 5.8 used by Julian F. Tyson *et al* [121] and the concentration of 0.05 mol/L, was selected. The mobile phase flow rate was 1.0 mL/min with isocratic elution. The flow rate of sodium tetrahydroborate was 2.0 mL/min. Standard concentrations of individual arsenic species of As(III) or As(V) or their mixtures were prepared in deionized water. The injecting volume was 0.16 mL, and 0.2 mol/L HCl was used in flow system downstream HPLC column to react with the $NaBH_4$ solution; this solution was placed instead of the TGA solution in Figure 2.3. The setup of the HPLC-HG shown in Figure 2.3 was used to determine the retention time of the arsenic species combined with the EHQTA atomizer.

### 3.3.5.3- HPLC-HG-EHQTA-AAS system using 0.2 mol/L HCl without TGA to determine the appearance period of As(III) and As(V)

Since the electrically heated quartz tube atomizer (EHQTA) directly atomized the arsenic hydrides, it was used for online atomization of the inorganic arsenic species so that their retention time can be directly determined. During this study, 0.2 mol/L HCl was used, and no TGA was introduced into the hydride generation system. The atomic absorption spectrometer software can only read from 0 to 100 s on the time axis in a single run. Therefore due to this limitation, 9 consecutive runs of 100 s program were utilized in order to cover 15 min corresponding to the highest retention time. For this study, peak height was used for absorbance measurements and the parameters used are given in Table 3.12.

In the first run, only 80 ng/mL of As(III) was loaded into the 0.16 mL sample loop and as soon as the sample was injected, a stopwatch timer was simultaneously

initiated so that the time of elution of the signal is monitored. In Figure 3.47, the signal for 80 ng/mL of As(III) is shown. The injection time is indicated by zero second and the time taken for the chromatographic signal to show up was between 120. The experiment was repeated for 5 replicates (N=5) with < 5% RSD. In the case of As(V), the same timing process was also followed. However because no pre-reduction reagent was used, the sensitivity As(V) 18 times less than that of As(III). Therefore the signal was observed using 500 ng/mL As(V) and the appearance time was 345 s. The signal is shown in Figure 3.48; the repeatability of the signals was ≤ 5% RSD.

Following the individual analysis of arsenite and arsenate, a mixture of As(III) and As(V) containing 80 ng/mL As(III) and 1000 ng/mL As(V) in 50 mL volumetric flask was prepared. By using again the 0.16 mL of the injection loop, the mixture was injected and run for analysis. The two arsenic species were clearly separated in one isocratic elution. The signal of the two species is shown in Figure 3.49.

**Table 3.12** The optimized parameters of HPLC-HG-EHQTA-AAS for As(III) and As(V) determination

| **Parameters** | **Conditions** |
|---|---|
| HPLC sample loop | 0.16 mL |
| Mobile phase (carrier solution) | 0.05 M phosphate buffer pH 5.8 |
| Flow rate of mobile phase | 1.0 mL/min |
| Flow rate of HCl | 1.5 mL/min |
| Concentration of HCl | 0.2 mol/L |
| Flow rate of $NaBH_4$ | 2.0 mL/min |
| Concentration of $NaBH_4$ | 1.5% (w/v) |
| Concentration of NaOH | 0.3% (w/v) |
| Length of reaction coil (RC) | 120 cm |
| Length of stripping coil | 10 cm |
| Ar gas flow | 200 mL/min |

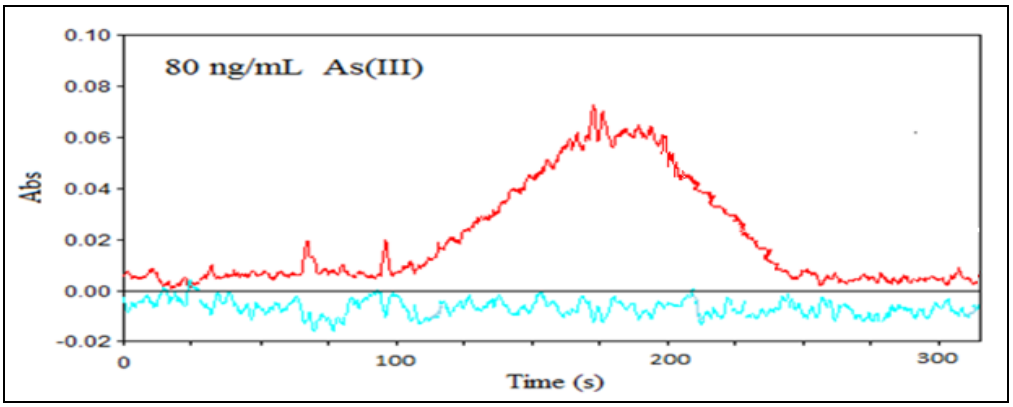


**Figure 3.47** Chromatographic signal of 80 ng/mL As(III) obtained by EHQTA using the parameters given in Table 3.12.

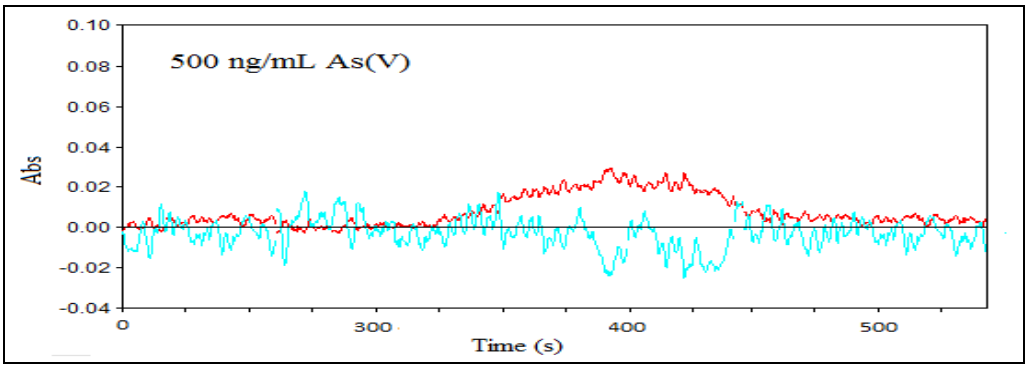


**Figure 3.48** The chromatographic signal of 500 ng/mL As(V) obtained by EHQTA using the parameters given in Table 3.12.

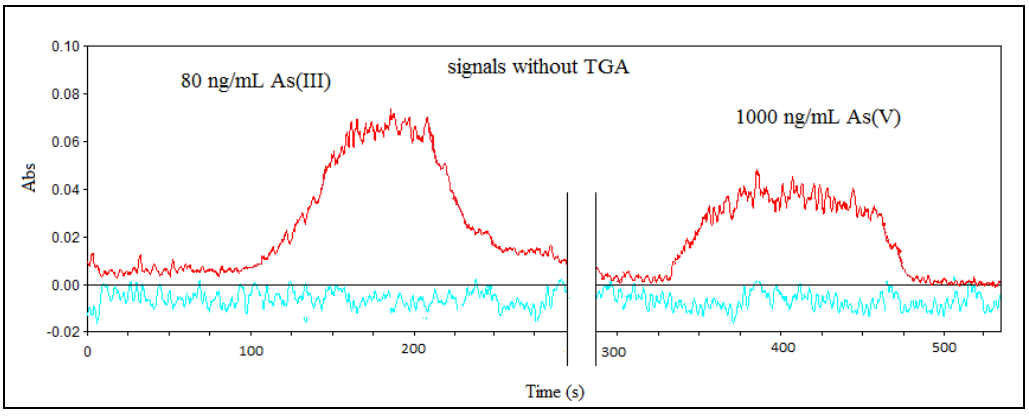


**Figure 3.49** The separated chromatographic signals of As(III) and As(V) mixture using EHQTA using the parameters given in Table 3.12.

### 3.3.5.4- HPLC-HG-WC-ETAAS system using 0.2 mol/L HCl without TGA for As(III) and As(V)

Following the study of the HPLC-HG-EHQTA, a clear understanding of the elution times of the inorganic arsenic species was acquired. Therefore during the study with HPLC-HG-WC-ETAAS, a stopwatch was utilized to monitor the times such as the elution time, time to start trapping and the time to end trapping. The time between sample injection and the start of trapping was referred to as the waiting period. Individual concentration of As(III) and As(V) were first determined and then a mixture of the iAs species. 0.2 mol/L of hydrochloric acid was used without TGA.

The principle of operation of the HPLC-HG-WC-ETAAS technique for the determination of the iAs species was as following: In the *load* position of the HPLC injection port, 80 ng/mL of As(III) was loaded into the 0.16 mL sample loop, and as soon as injection was made, the stopwatch was simultaneously started. The waiting period for As(III) was 120 s, so during this time the tungsten coil was off and no trapping was performed. The significance of the waiting period was to avoid blank problem. When the time reaches to 120 s, trapping was initiated and the stopwatch kept running. When the time reaches 250 s, making a trapping period of 120 s, the trapping was stopped by turning off the tungsten coil. The voltage was then rapidly adjusted to atomization temperature (1920 $^{\circ}$C) while the W-coil is off, and then rapidly turned on again to atomize the trapped arsenic atoms. At atomization step, the tungsten coil was kept on for approximately 5 s before turning it off again. This step of leaving the lamp on for 5 s was important so that all trapped species are atomized and the memory effect was eliminated. Hence no signal was observed when momentary second atomization was carried out. The whole process of trapping As(III) atoms and releasing starting from the waiting period to the atomization stage lasted for 250 s. It was observed that the analytical and background signals were not affected when the pumps were left running during atomization, and therefore it was not necessary to turn them off. The study was repeated for 5 replicates (N=5). The repeatability was $\leq$ 5% RSD. The signal of 80 ng/mL of As(III) is shown in Figure 3.50.

Following the study of As(III), 400 ng/mL of As(V) was also individually run into the HPLC anion exchanged column and after hydride generation it was trapped on the Ir-coated tungsten. In this study 0.16 mL of As(V) was also loaded to the sample loop, and as soon as the sample was run, the stopwatch was simultaneously started. However, the waiting period for As(V) was 355 s, therefore until this time, trapping was not commenced. When the time reaches to 355 s, trapping is started and it lasts for 120 s when the time will read 475 s from the stopwatch, then trapping is stopped. The process of trapping and atomization described for As(III) was the same for As(V). The details of the waiting period, trapping and atomization stages for As(V) is shown in Figure 3.51.

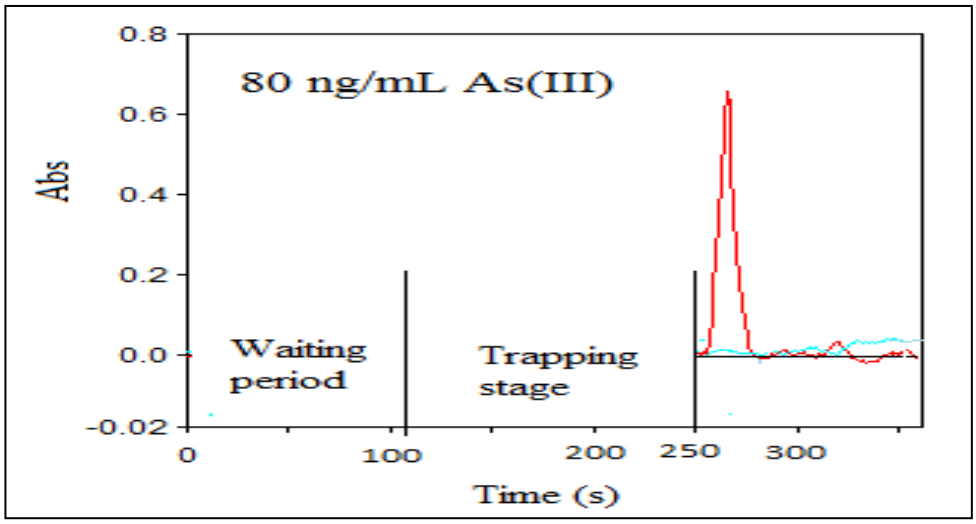


**Figure 3.50** The signal for 80 ng/mL As(III) using HPLC-HG-WC-ETAAS without TGA. Parameters given in Table 3.12 were used.

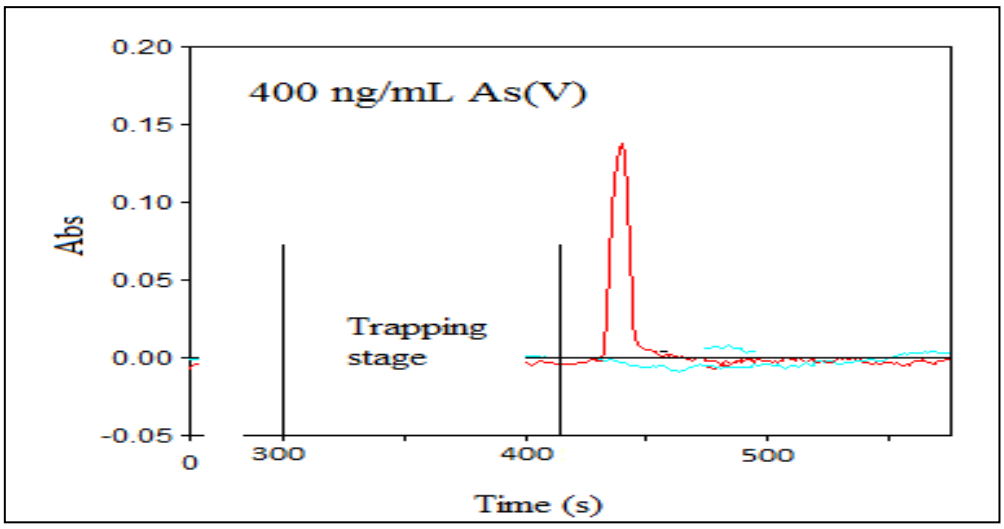


**Figure 3.51** The signal for 400 ng/mL As(V) using HPLC-HG-WC-ETAAS without TGA. Parameters given in Table 3.12 were used.

### 3.3.5.5- Determination of As(III) and As(V) mixture by HPLC-HG-WC-ETAAS

A mixture of the inorganic arsenic species containing 80 ng/mL As(III) and 400 ng/mL As(V) was prepared in a 50 mL volumetric flask from the individual stock solutions. The trapping and atomization process was carried as follows: after the waiting period of As(III) was completed at 120 s, it was trapped on the Ir-coated tungsten for 120 s. When trapping was completed after 250 s, the variac was quickly turned off and adjusted to atomization voltage and the As(III) atoms are rapidly atomized. The variac is then turned off again and the pointer was return to trapping voltage to trap As(V) atoms for another 120 s. The whole analysis time last for 450 s and the trapped signals of As(III) and As(V) are shown in Figure 3.52.

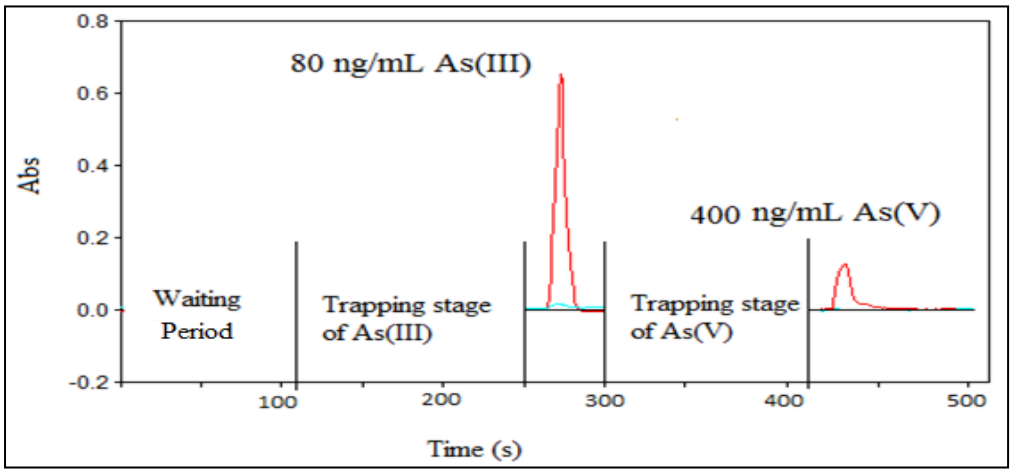


**Figure 3.52** The signals for 80 ng/mL As(III) and 400 ng/mL As(V) using HPLC-HG-WC-ETAAS without TGA. Parameters given in Table 3.12 were used.

### 3.3.5.6- Separation of As(III), DMA, MMA and As(V) using HPLC-UV-VIS

The anion exchange column used in this experiment was mounted in a HPLC-UV-VIS instrument and the same conditions were applied. These conditions are 1.0 mL/min mobile phase flow rate that is composed of 0.05 M $NH_4H_2PO_4/H_3PO_4$ buffer solution with pH 5.8. The mobile phase was first run without injecting the analyte so that a clear background is obtained. When the analyte mixture with concentration of 100 mg/L As for each species was injected into the instrument, the chromatogram shown in Figure 3.53 was obtained.

As seen in the chromatogram, DMA and MMA appeared between As(III) and As(V) and because of waiting period between the trappings of As(III) and As(V), the DMA and MMA peaks were not trapped. Moreover since inorganic arsenic species As(III) and As(V) are more toxic than the organic forms DMA and MMA [59, 60, 78] the emphasis in this study has been only on the inorganic arsenic species.

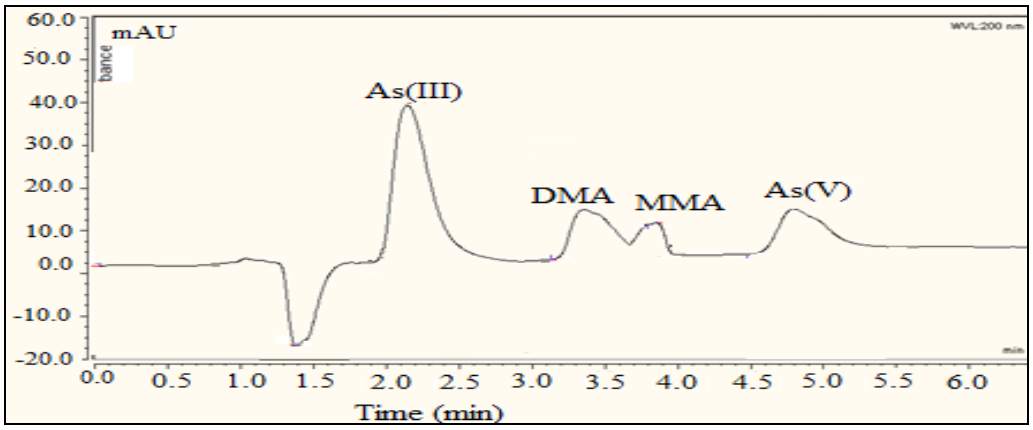


**Figure 3.53** The chromatogram of the As compounds obtained using the anion exchange column fixed to the HPLC-UV-VIS.

### 3.3.5.7- The effect of mobile phase pH on the retention time of the arsenic species using HPLC-HG-EHQTA-AAS

Even though a separation of the inorganic arsenic species was achieved with the mobile phase used, a study in the effect of pH on the retention time of species was carried out. During this study, the concentration of the mobile phase, phosphate buffer was kept constant at 0.05 mol/L, and the pH was varied from 3.14, 4.0, 5.12, 6.14, to 7.1. As shown in Figure 3.54, when pH was increased from 3.14 to 7.1, As(III) retention time increases almost linearly. However for As(V) signal, the retention time increases also almost linearly between 3.14 to 6.1 and at pH 7.1, there is a larger increase in retention time. The trend of this increase in pH can explain as follows:

For As(III), as pH increases, the removal of hydrogen atom from the molecule $H_3AsO_3$, cannot be achieved until at pH 10 when $H_2AsO_3^-$ will be formed and at pH 12, $HAsO_3^{2-}$ will start forming. Therefore, within the pH range of 2.14-7.1, the As(III) species should have no charge and are not expected to be retained by the column. However, the role of the mobile phase should also be taken into consideration. The solution of the problem requires further and deeper investigation, taking into account also the surface charges of $H_3AsO_3$ which may become more

negative with the increase in pH, explaining the longer retention times. As a result, the experiments show that the retention of the As(III) species on the anion exchange column increases as the pH of the mobile phase increases.

For As(V), the removal of hydrogen atom from molecule $H_3AsO_4$, is appreciable in the given pH range. Thus at pH 2, $H_3AsO_4$ is more abundant in the solution and as the pH increases the molecule changes from $H_2AsO_4^-$, $HAsO_4^{2-}$, to $AsO_4^{3-}$ with the removal of hydrogen atom for every increase by two. That is why As(V), is retained more in the anion exchange column. In the Eh-pH diagram shown in Figure 3.55 it is clearly seen how the different arsenic species are deprotonated as pH increases [122].

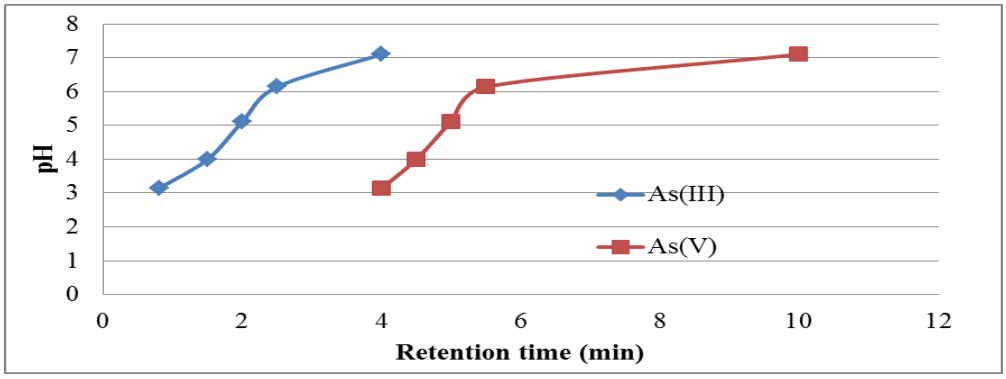


**Figure 3.54** The effect of pH of the mobile phase on the retention times of As(III) and As(V), using HPLC-HG-EHQTA-AAS without TGA. Parameters given in Table 3.12 were used.

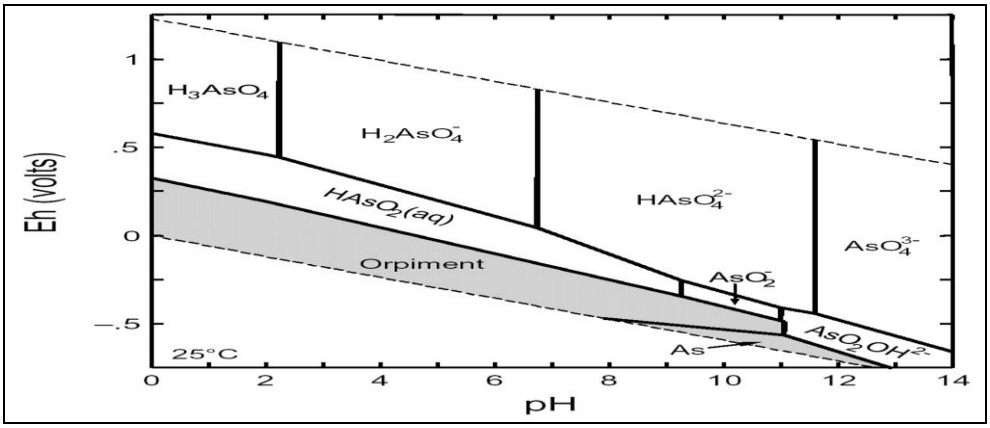


**Figure 3.55** The Eh-pH diagram for arsenic As(III) and As(V) compounds [122]

### 3.3.5.8- Calibration plot using HPLC-HG-EHQTA and 0.2 M HCl without TGA

The calibration plots of As(III) and As(V) using HPLC-HG-EHQTA without using TGA, were drawn by using both peak height and peak area. The sample volume was 0.16 mL and the result of the calibration studies are shown in Figure 3.56 for As(III) and Figure 3.57 for As(V). It was found that the plot of As(III) was linear between 5.0 and 100.0 ng/mL in both peak area and peak height. However, for the calibration plot of As(V), the peak height has a linearity between 0.5 to 10.0 µg/mL, but the peak area has a linearity between 0.5 to 4.0 µg/mL. Above this concentration, a deviation from the linearity was observed. The measurement of absorbance using peak area show a poor precision with %RSD of >5. In the Figures 3.56 the peak height plot is less sensitive than the peak area plot of Figure 3.57, this actually due to the different atomizer used EHQTA and WC-ETA have different dimension and operational process and the efficiency of trapping for WC-ETA is not 100 %, thus not all the arsenic atoms are trapped.

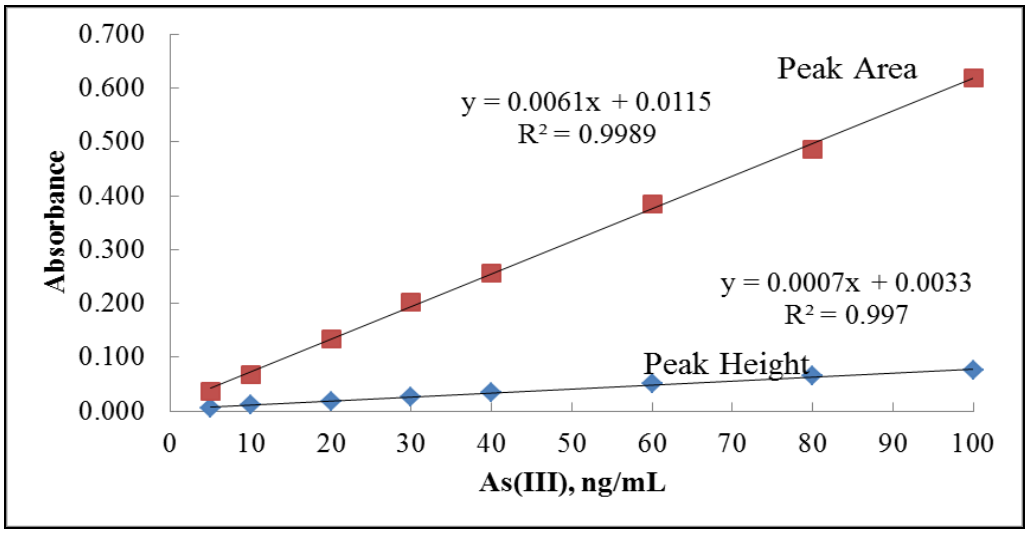


**Figure 3.56** Calibration plot for As(III) using both peak area and peak height and HPLC-HG-EHQTA-AAS without TGA. Parameters given in Table 3.12 were used.

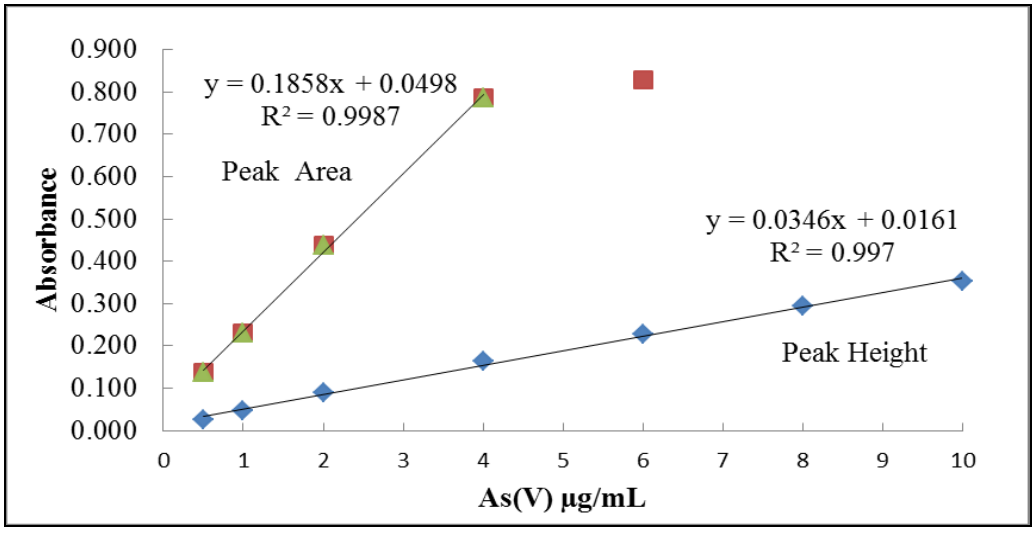


**Figure 3.57** Calibration plot for As(V) using both peak area and peak height and HPLC-HG-EHQTA-AAS without TGA. Parameters given in Table 3.12 were used.

### 3.3.5.9- Calibration plot using HPLC-HG-WC-ETAAS and 0.2 M HCl without TGA

The calibration plots of As(III) and As(V) obtained using HPLC-HG-WC-ETAAS without using TGA are shown are shown in Figure 3.58 and 3.59. Both peak area and peak height were used for the absorbance measurement of the analytical signal. In this system, peak height results were 2 times more sensitive than peak area. The linear dynamic range for As(III) was between 5.0 and 80.0 ng/mL with both peak height and peak area and for As(V) the linearity was 50 to 1000 ng/mL.

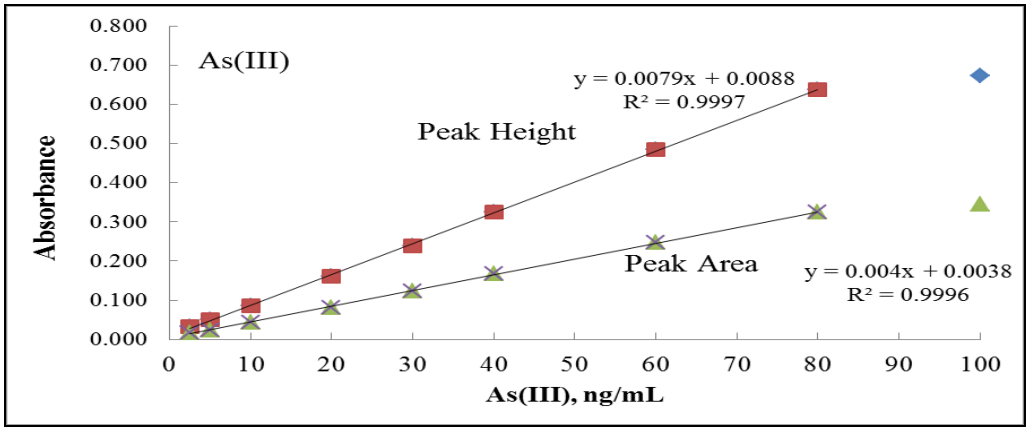


**Figure 3.58** Calibration plots for As(III) with both peak height and peak area, using HPLC-HG-WC-ETAAS. The parameters given in Table 3.12 were used.

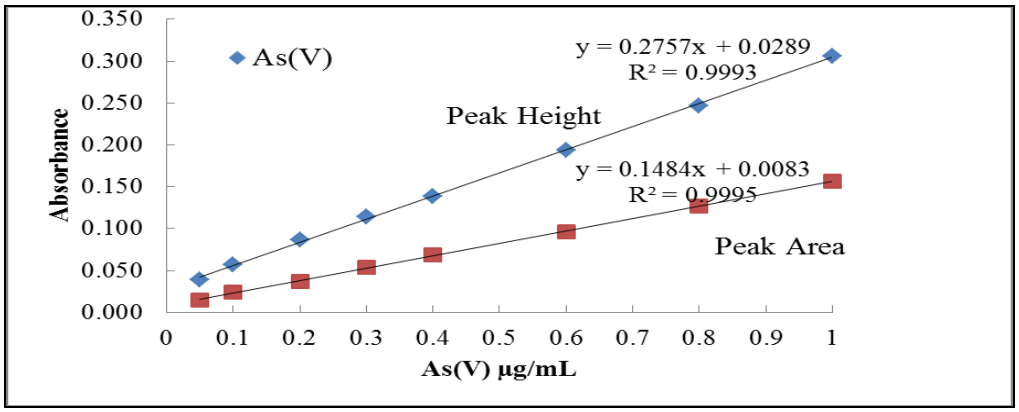


**Figure 3.59** Calibration plots for As(V) with both peak height and peak area, using HPLC-HG-WC-ETAAS. The parameters given in Table 3.12 were used

### 3.3.5.10- Analytical figures of merit of HPLC-HG-EHQTA and HPLC-HG-WC-ETAAS systems without TGA

The operational efficiency of trapping by Ir-coated W-coil was estimated by comparing the limit of detection (LOD) and characteristic concentration ($C_0$) of WC-ETA with EHQTA atomizers using both peak height and peak areas. The results of the calculations are given in Table 3.13 for peak height and Table 3.14 for peak area. The enhancement factor of the atom trapping over the EHQTA for both As(III) and

As(V) also calculated in peak height for the two atomizers and the results are given in Table 3.15. Obviously for the peak area measurements, EHQTA was more sensitive. The low enhancement observed for As(V) with the WC-ETAAS atom trapping method can be attributed to poor trapping of $As_2H_4$ volatile compound produced in a non-analytical manner during arsenic chemical hydride generation [21]. The enhancement factor was calculated by taking the ratio of characteristic concentration ($C_0$) of normal hydride signal using HPLC-HG-EHQTA to the $C_0$ of the trapped signal using HPLC-HG-WC ETAAS. The repeatability of the absorbance signals in peak height were better than or equal to 5% RSD.

**Table 3.13** Comparison of the analytical figures of merit of EHQTA and WC-ETA atomizers using **peak height** without the use of TGA (N=7)

| **Figure of Merit** | **HPLC-HG-EHQTA-AAS** | | **HPLC-HG-WC-ETAAS** | |
|---|---|---|---|---|
| | As(III) | As(V) | As(III) | As(V) |
| LOD (ng/mL) | 2.5 | 60 | 0.22 | 5.9 |
| LOQ (ng/mL) | 8.3 | 200 | 0.74 | 21 |
| $C_0$ ng/mL | 5.74 | 115 | 0.54 | 13.1 |
| Range (ng/mL) | 5 to 80 | 500 to 10,000 | 2.5 to 80 | 50 to 1000 |

**Table 3.14** Comparison of the analytical figures of merit of EHQTA and WC-ETA atomizers using **peak area** without the use of TGA (N=7)

| **Figure of Merit** | **HPLC-HG-EHQTA-AAS** | | **HPLC-HG-WC-ETAAS** | |
|---|---|---|---|---|
| | As(III) | As(V) | A(III) | As(V) |
| LOD (ng/mL) | 0.42 | 11 | 0.82 | 21 |
| LOQ (ng/mL) | 1.1 | 41 | 2.7 | 70 |
| $C_0$ ng/mL | 0.69 | 20.7 | 1.07 | 26.0 |
| Range (ng/mL) | 5 to 80 | 500 to 10,000 | 2.5 to 80 | 50 to 1000 |

**Table 3.15** Enhancement factors of As(III) and As(V) with EHQTA and W-coil ETA using **peak height** without using TGA (N=7)

| Analyte | | | | $C_0$ (ng/mL) | |
|---|---|---|---|---|---|
| | **E** | $E_t$ ($min^{-1}$) | $E_v$ ($mL^{-1}$) | HPLC-HG-EHQTA-AAS | HPLC-HG-WC-ETAAS |
| As(III) | 9.6 | 4.8 | 60 | 5.74 | 0.54 |
| As(V) | 5.2 | 2.6 | 33 | 115 | 13.1 |

**E** is the enhancement factor (ratio of $C_0$ for EQTA and W-coil ETA)

**$E_t$** is the E/min for sampling,

**$E_v$** is the E/volume of sample in mL

### 3.3.6- Optimization studies on high performance liquid chromatography hydride generation W-coil (HPLC-HG-WC) with TGA

Optimization studies were again carried out on the interacting parameters for HPLC-HG-WC in the presence of TGA using 10.0 ng/mL of As(V) for online pre-reduction. Peak height and peak area were used for absorbance measurement. The optimized trapping and atomization temperature 720 °C and 1920 °C respectively for the Ir-coated tungsten coil remains the same.

#### 3.3.6.1- The effect of mobile phase flow rate on the trapping period in HPLC-HG-WC-ETAAS with TGA using As(V)

It should be mentioned that the flow rate of the mobile phase significantly affect the retention time of As(V) used for the optimization study. Therefore the retention times were first examined using the EHQTA atomizer. The flow rate of the mobile phase was varied from 0.5 to 2.0 mL/min. It was observed that, for 0.5 mL/min, the retention time was 10 min and the peaks were broadened. However, as the flow rate

was increased to 1.0, 1.5 and 2.0 mL/min the retention time naturally decreased to 5, 3 and 2 min respectively.

Following this study, the effect of the mobile phase flow rate on trapping period was then investigated. The trapping period was varied between 60 and 180 s while the flow rate of the mobile phase was varied from 0.5 to 2.0 mL/min. As shown in Figure 3.60, by keeping the flow rate at one constant value, the trapping time was varied from 60 to 180 s, and a linear relationship between the trapping time and absorbance signal was observed for flow rates of 0.5 and 1.0 mL/min. However, for the flow of 1.0 mL/min, produced stable signals were with % RSD < 5 at 120 s trapping period. For the flow rate of 1.5 and 2.0 mL/min, the sensitivity of the signals decrease and the reproducibility were poorer than 5% RSD. Therefore, the flow rate of 1.0 mL/min with trapping period of 120 s was selected for the mobile phase.

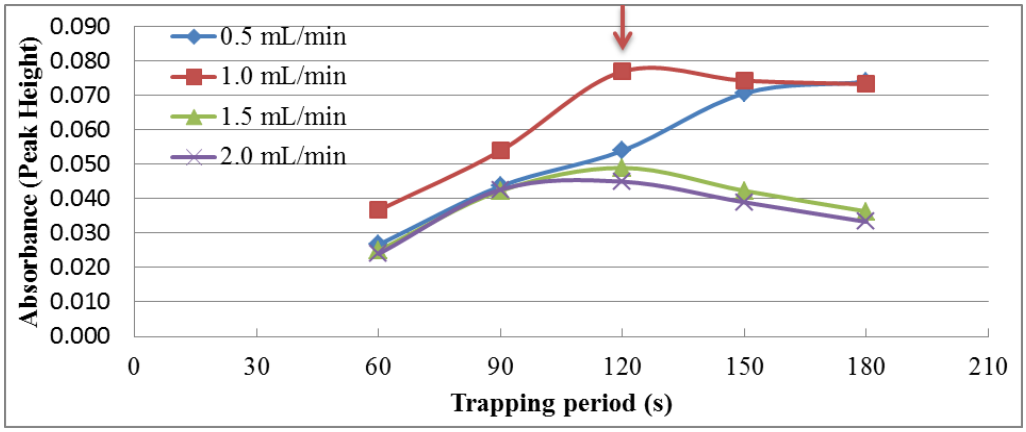


**Figure 3.60** The effect of the mobile phase flow rate with respect to trapping time using HPLC-HG-WC-ETAAS with TGA. The concentration of TGA was 1.0 % (v/v) and HCl was 0.002 mol/L, The other parameters were same as those in Table 3.3.

### 3.3.6.2- Effect of TGA solution flow rate on trapping period in HPLC-HG-WC-ETAAS using As(V)

The flow rate of TGA solution does not affect the retention time of the arsenic species, however since it was used for online pre-reduction of As(V) to As(III), its flow rate directly effects the sensitivity for As(V). In order to determine its optimum flow rate, it was varied from 0.5 to 2.0 mL/min, and by keeping one flow rate value constant the trapping period was varied between 60 and 180 s. The volume of the pre-reduction coil was 2.5 mL.

The reaction time of TGA with As(V) sample was calculated by dividing the coil volume by TGA flow rate in mL/min. Thus at flow of 0.5 mL/min, the reaction time is 5 min. Therefore at the lowest flow rate, the reaction time is 5 min and at the highest flow rate the reaction time is 1.25 min. In Figure 3.1, it was seen that TGA has a maximum pre-reduction reaction time of 50 s, which renders it compatible for online pre-derivatization of As(V). So even though it has a foul smell, it was preferred to cysteine or KI in ascorbic acid or thiourea in ascorbic acid.

In the first study, the flow rate of thioglycolic was set at 0.5 mL/min, and trapping time was varied from 60 to 180 s, and as shown in Figure 3.61, the sensitivity of As(V) signal increases with increase in trapping period up to 120 s and then remains constant until 180 s. The same trend was observed for the other flow rates as the trapping period was increased from 60 to 180 s. The flow rate of 1.0 mL/min with the trapping period of 120 s was selected as the optimum values.

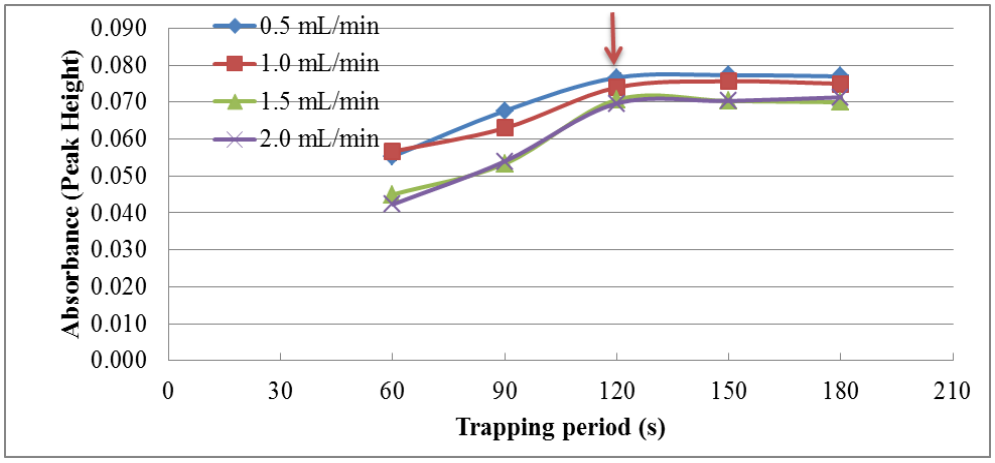


**Figure 3.61** The effect of TGA solution flow with respect to trapping time of As(V) atoms for HPLC-HG-WC-ETAAS studies with TGA. As analyte, 10.0 ng/mL As(V) was used. Other parameters were as those in Table 3.16.

### 3.3.6.3- Effect of HCl concentration in TGA solution in HPLC-HG-WC-ETAAS using As(V)

From the optimization study of CF-HG-WC-ETAAS, it was observed that high concentration of hydrochloric acid in TGA solution reduces absorbance signal of As(V). Therefore the effect of HCl concentration in TGA solution was again investigated using the HPLC-HG-WC-ETAAS. In the initial study, the HCl and TGA solutions were placed in separate volumetric flasks; however this was creating further dilution of the sample. Then in the second setup, the HCl and TGA were mixed in the same flask. The results for the effect of HCl concentration is shown in Figure 3.62. It was found that as the concentration of HCl increases from 0.0 to 0.1 mol/L the pre-reduction of As(V) was less affected and the sensitivity of signal decreases at higher HCl concentration. The effect of the acid on the system was apparently seen, because as acidity increases, foams were forming in the first GLS, this was caused by too much of $H_2$ gas being produced in the reaction, therefore the low signal can be attributed partly to hydrogen dilution effect. The optimum value of HCl concentration in the TGA solution was chosen as 0.002 mol/L.

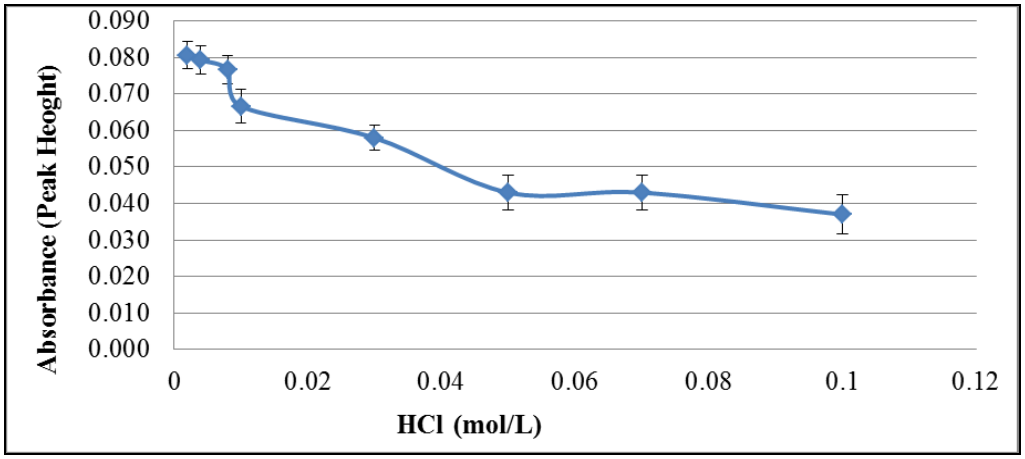


**Figure 3.62** The effect of HCl concentration added in 1.0% (v/v) TGA using HPLC-HG-WC-ETAAS. 10.0 ng/mL As(V) was used. Other parameters were as those in Table 3.16.

### 3.3.6.4- Effect of TGA concentration in HPLC-HG-WC-ETAAS using As(V)

The concentration of TGA that will sufficiently pre-reduce As(V) was again investigated for the HPLC-HG-WC-ETAAS system. From the results shown in Figure 3.63, it can be seen that when the concentration of TGA was varied from 0.25 to 3.0% (v/v), the absorbance signal in peak height remains constant between 0.5 to 3.0%. In the study of Tomáš Matoušek *et al.* [104] the optimum concentration of TGA was also found to be 1.0% (w/v). In this study also 1.0% (v/v) was found to be the optimum value for complete pre-reduction of As(V) and hence was used for further optimization studies.

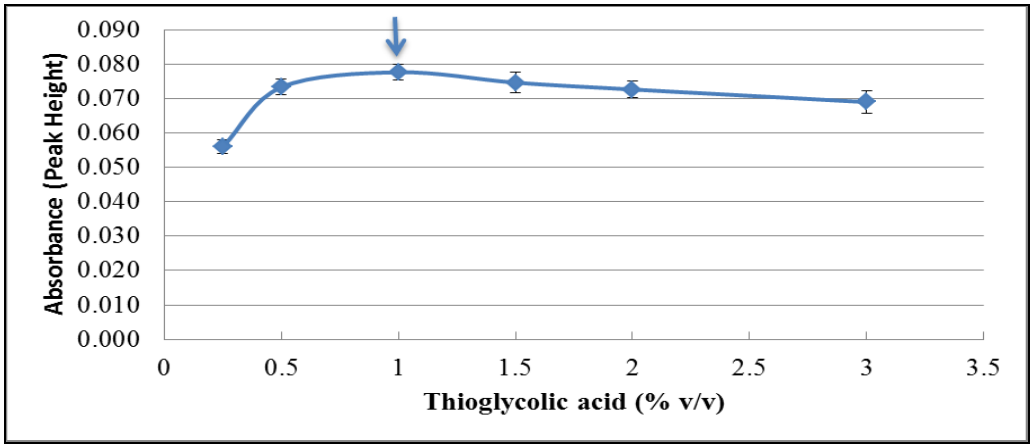


**Figure 3.63** The effect of TGA concentration on the absorbance signals of 10.0 ng/mL As(V). Other parameters were as those in Table 3.16.

### 3.3.6.5- The effect of sodium tetrahydroborate concentration in HPLC-HG-WC-ETAAS using As(V)

To examine the influence of the concentration of $NaBH_4$, on the HPLC-HG-WC-ETAAS system for arsenic hydride generation from As(V), this value was varied from 0.5 to 2% (w/v), and all the solutions of $NaBH_4$ were stabilized in 0.3% (w/v) NaOH.

As shown in Figure 3.64, from 0.5 to 1.5%, the absorbance signal of As(V) was constant. However when the concentration of $NaBH_4$ was increased to 2.0%, the signal drops significantly, and this was obviously due to the hydrogen dilution factor produced from the reaction. The optimum concentration of $NaBH_4$ was also found to be 1.5% (w/v).

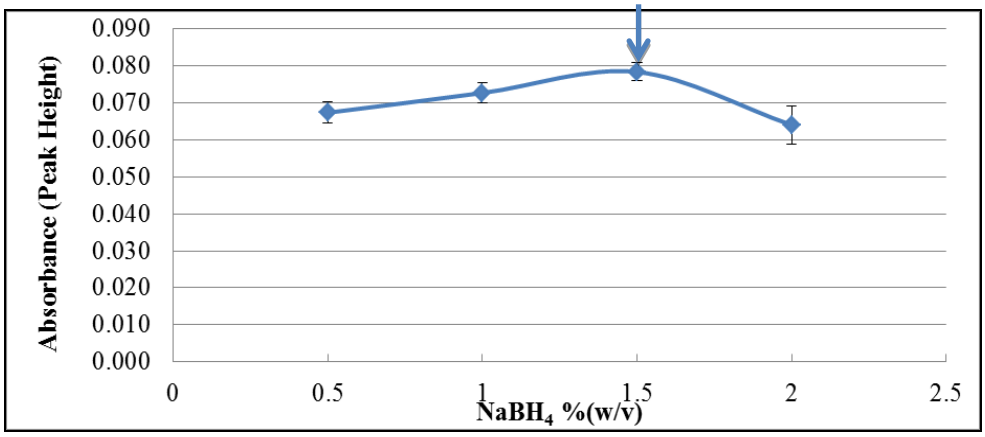


**Figure 3.64** The effect of the concentration of $NaBH_4$ (%w/v) on the absorbance signals of 10.0 ng/mL As(V). Other parameters were as those in Table 3.16.

### 3.3.6.6- The effect of sodium tetrahydroborate flow rate in HPLC-HG-WC-ETAAS using As(V)

The effect of sodium tetrahydroborate flow rate was also studied when its concentration was 1.5% (w/v). The flow rate was varied from 0.5 to 4.0 mL/min. It was found out that from the flow rate of 0.5 to 1.5 mL/min the absorbance signal also increases and from 1.5 to 4.0 mL/min, the signal levels off and decreases slowly at higher flow rates. The result of the study is shown in Figure 3.65. The optimum flow rate found to produce stable signals was 1.5 mL/min and this value was selected.

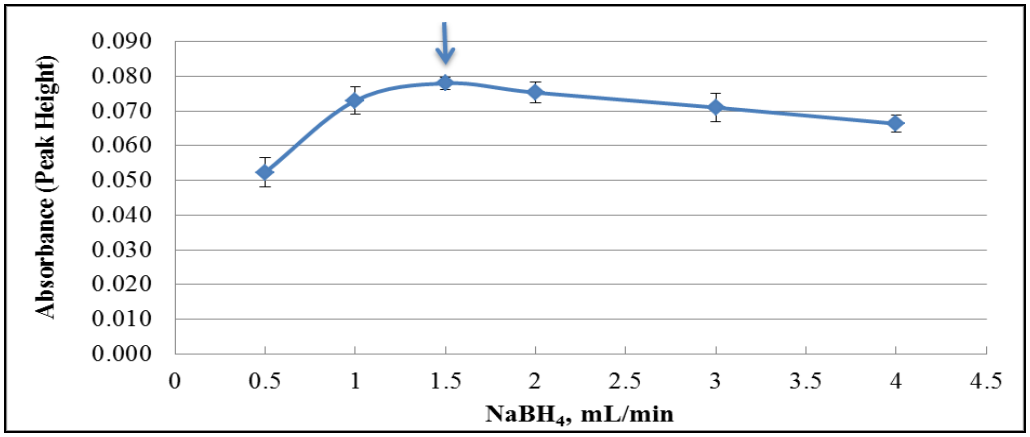


**Figure 3.65** The effect of $NaBH_4$ flow rate on the absorbance signals of 10 ng/mL As(V). Other parameters were as those in Table 3.16.

**Table 3.16** The values of the optimum parameters of HPLC-HG-WC-ETAAS

| **Parameters** | **Values** |
|---|---|
| Mobile phase | 0.05 mol/L phosphate buffer, ph 5.8 |
| Mobile phase flow rate | 1.0 mL/min |
| Sample loop volume | 0.16 mL |
| TGA flow rate | 1.0 mL/min |
| TGA concentration | 1.0% (v/v) |
| HCl concentration in TGA | 0.002 mol/L |
| $NaBH_4$ flow rate | 1.5 mL/min |
| $NaBH_4$ concentration | 1.5% (w/v) |
| NaOH concentration | 0.3% (w/v) |
| Ar flow rate | 75 mL/min |
| $H_2$ flow rate | 73 mL/min |
| Trapping period | 120 s |
| Trapping temperature | 720 $^0$C |
| Atomization temperature | 1920 $^0$C |
| Prereduction coil volume | 2.5 mL |
| Reaction coil length | 120 cm |
| Stripping coil length | 10 cm |

### 3.3.6.7- Calibration plots of As(III) and As(V) using HPLC-HG-EHQTA-AAS with TGA

The calibration plots of As(III) and As(V) obtained using HPLC-HG-EHQTA-AAS in the presence of TGA are shown in Figure 3.66 and 3.67, respectively. Both peak area and peak height values were used for the absorbance measurement of the analytical signal. However peak area measurements in EHQTA were 10 times more sensitive and more reproducible than measurement using peak height, when slope

sensitivities are used. By using a sample volume of 0.16 mL, the linear dynamic range obtained for As(III) and As(V) was between 5.0 and 80.0 with both peak height and peak area.

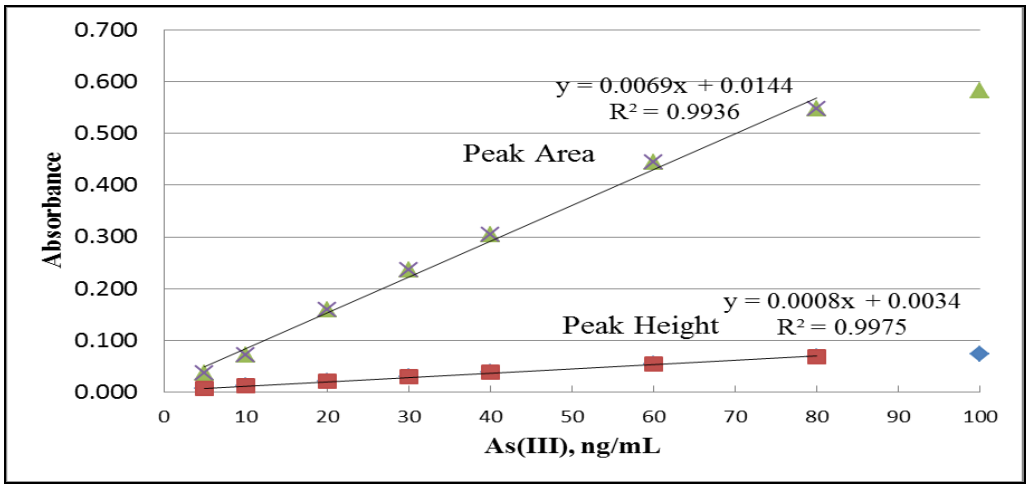


**Figure 3.66** The calibration curve for As(III) using HPLC-HG-EHQTA-AAS. The sample volume was 0.16 mL and 1.0% (v/v) TGA in 0.002 mol/L HCl was used in the system for online pre-reduction, and the other parameters were as those in Table 3.16.

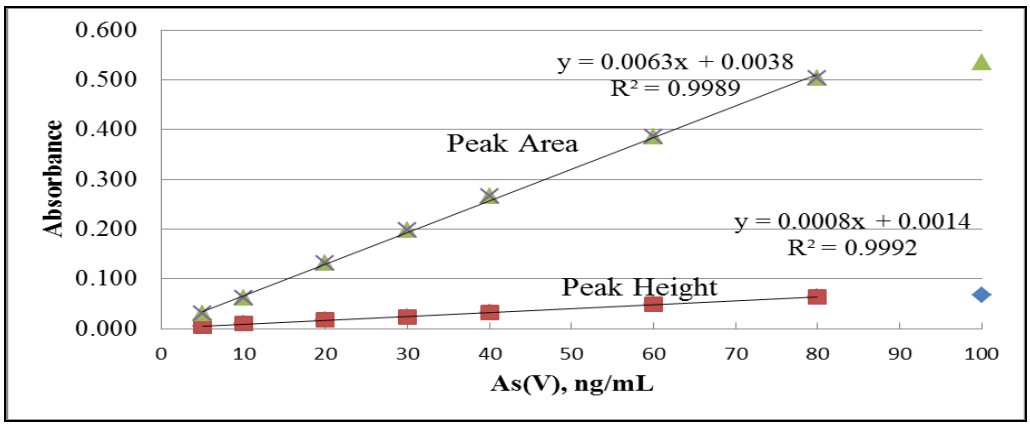


**Figure 3.67** The calibration curves for As(V) using HPLC-HG-EHQTA-AAS. The sample volume was 0.16 mL and 1.0% (v/v) TGA in 0.002 mol/L HCl was used in the system for online pre-reduction and the other parameters were as those in Table 3.12.

### 3.3.6.8- Analytical signals for As(III) and As(V) using HPLC-HG-EHQTA with TGA

The signals of As(III) and As(V) from 10.0 to 80.0 ng/mL are shown in Figure 3.68. The parameters for HPLC and other relevant parameters were as those in Table 3.12. The repeatability of the signals ranges from 6 to 1.7% RSD. The peak area measurement of the signals was 10 times more sensitive than peak height measurement.

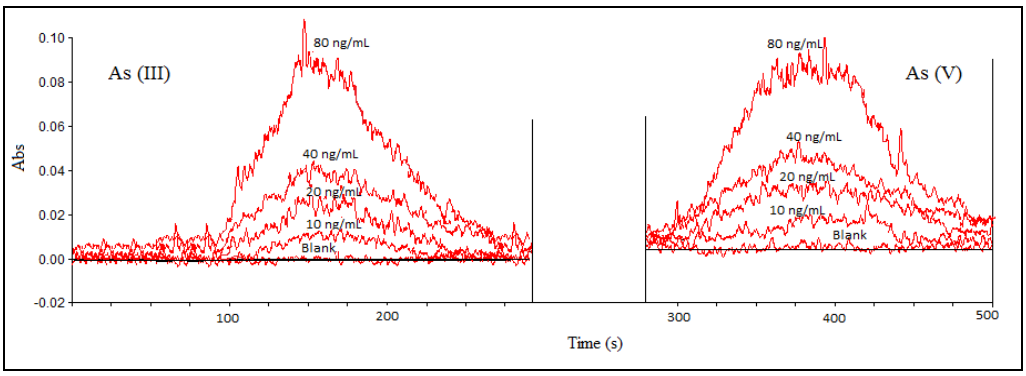


**Figure 3.68** The signals for As(III) and As(V) using HPLC-HG-EHQTA, the parameters in Table 3.12 were used.

### 3.3.6.9- Calibration plots for As(III) and As(V) using HPLC-HG-WC-ETAAS with TGA

The calibration plots for As(III) and As(V) obtained using HPLC-HG-WC-ETAAS with TGA are shown in Figures 3.69 and 3.70 respectively. The parameters in Table 3.16 were used. The plots were drawn using both peak area and peak height and the linear dynamic range was found to be between the concentrations of 2.50 and 80.0 ng/mL, above this concentration a negative deviation from the linearity was observed. When slope sensitivities are used, the measurement of the analytical signal using peak height was more than the double of that was obtained from peak area, with a repeatability of < 5.9% RSD and % RSD value became smaller at higher

concentrations. The half width of the trapped signals was < 0.5 s therefore the peak area measurement was less sensitive.

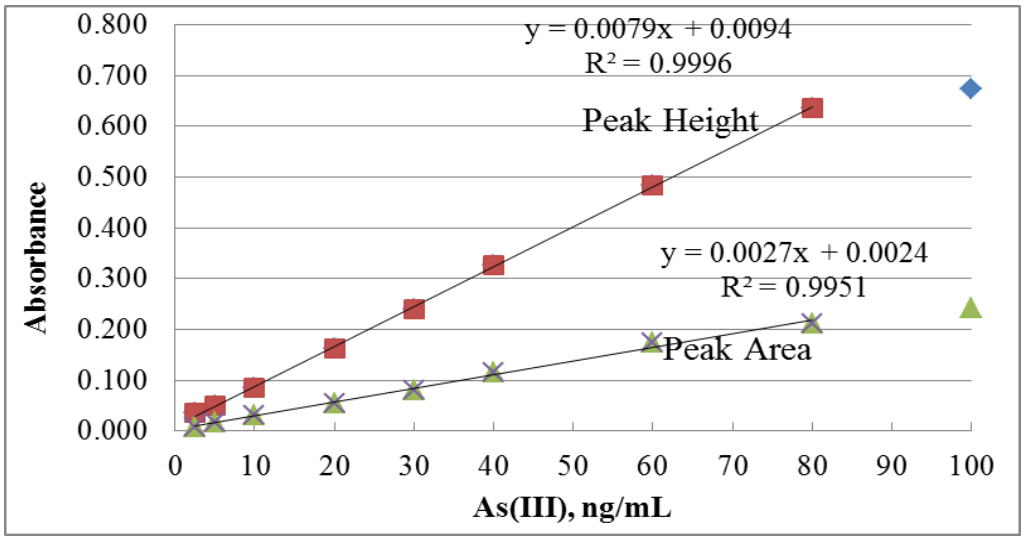


**Figure 3.69** The calibration plot of As(III) using HPLC-HG-WC-ETAAS. The parameters in Table 3.16 were used.

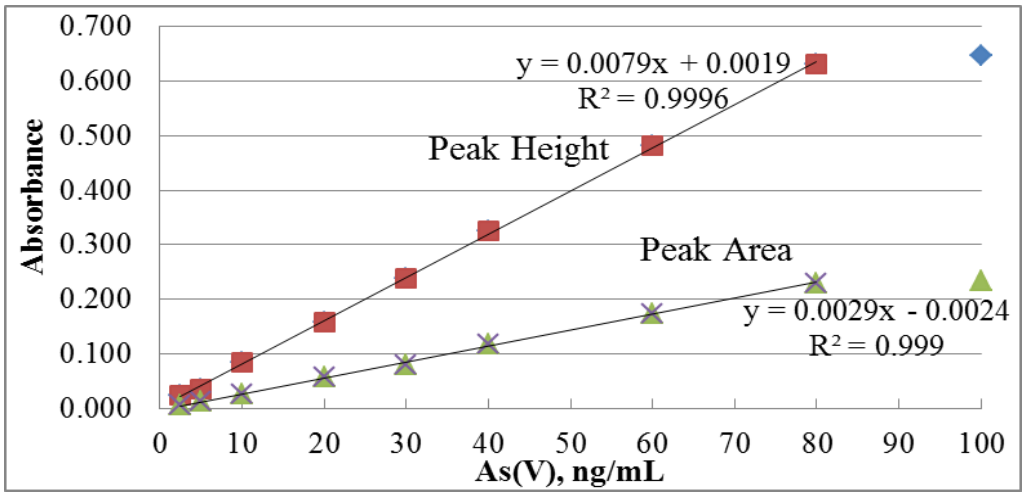


**Figure 3.70** The calibration plot for As(V) using HPLC-HG-WC-ETAAS. The parameters in Table 3.16 were used.

### 3.3.6.10- Signals of As(III) and As(V) using HPLC-HG-WC-ETAAS with TGA

Analytical signals using HPLC-HG-WC-ETAAS are shown in Figure 3.71. The parameters in Table 3.16 were used. The repeatability of the signals was < 6% RSD for 3 replicates (n= 3) and repeatability becomes better at higher concentrations. Peak height was used was used for absorbance measurements.

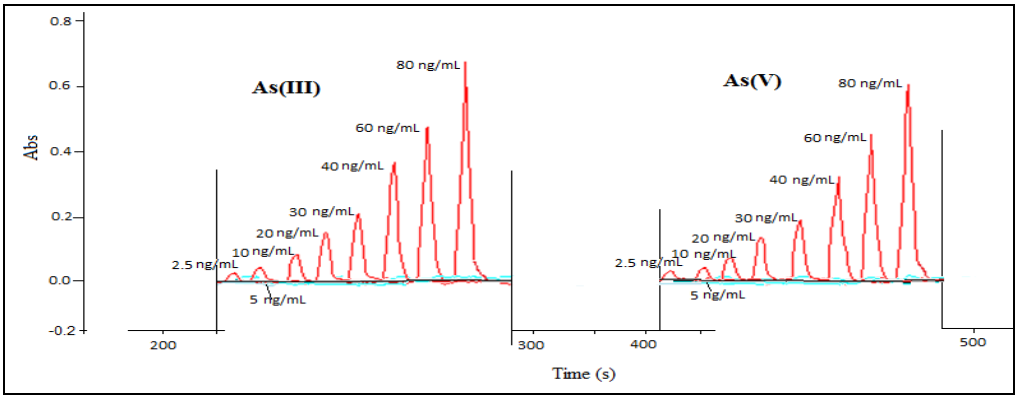


**Figure 3.71** Signals for 2.5 to 80.0 ng/mL of As(III) and As(V) using HPLC-HG-WC-ETAAS method. The parameters in Table 3.16 were used.

### 3.3.6.11- Analytical figures of merit for HPLC-HG-WC-ETAAS and HPLC-HG-EHQTA-AAS

The analytical figures of merit of HPLC-HG-WC-ETAAS and HPLC-HG-EHQTA-AAS methods were calculated in both peak height and peak area. In Table 3.17, the values were calculated using peak height and in Table 3.18, the values were calculated using peak area. As it is clearly shown from the tables, by using peak height, WC-ETA is 10 times more sensitive than EHQTA, and by peak area, EHQTA is just 4 times more sensitive than WC-ETAAS. With the use of peak height values, the repeatability of the absorbance signals of WC-ETAAS were <5% RSD and by using peak area, the repeatability of EHQTA, was < 10% RSD and only decreases at high concentrations. The high value of the % RSD for EHQTA was due

to the noise coming from the lamp and the several atom decaying processes in the absorption zone of the QTA [12]. However, with atom trap, a sharp and transient signal is generated during atomization temperature, thus having the advantage of not being affected by either the noise of the lamp or the decaying processes in the absorption volume. The comparison of enhancement of HPLC-HG-WC-ETAAS and HPLC-HG-EHQTA-AAS in peak height is given in Table 3.19. The enhancement was calculated by taking the ratio of the characteristic concentrations of EHQTA to WC-ETA.

**Table 3.17** Comparison of the analytical figures of merit for EHQTA and WC-ETA atomizers using **peak height** with TGA (N=7)

| **Figures of merit** | **HPLC-HG-EHQTA-AAS** | | **HPLC-HG-WC-ETAAS** | |
|---|---|---|---|---|
| | As(III) | As(V) | As(III) | As(V) |
| LOD, ng/mL | 2.5 | 3.0 | 0.25 | 0.30 |
| LOQ, ng/mL | 8.3 | 10 | 0.74 | 0.78 |
| $C_0$, ng/mL | 5.45 | 5.45 | 0.54 | 0.55 |
| Range, ng/mL | 5 to 80.0 | 5 to 80 | 2.5 to 80 | 2.5 to 80 |

**Table 3.18** Comparison of the analytical figures of merit of EHQTA and WC-ETA atomizers using **peak area** with TGA (N=7)

| **Figure of Merit** | **HPLC-HG-EHQTA-AAS** | | **HPLC-HG-WC-ETAAS** | |
|---|---|---|---|---|
| | As(III) | As(V) | A(III) | As(V) |
| LOD, ng/mL | 0.42 | 0.48 | 1.6 | 1.7 |
| LOQ, ng/mL | 1.4 | 1.6 | 2.1 | 5.5 |
| $C_0$, ng/mL | 0.600 | 0.682 | 1.58 | 1.54 |
| Range, ng/mL | 5 to 80 | 5 to 80 | 2.5 to 80 | 2.5 to 80 |

**Table 3.19** Enhancement factors of As(III) and As(V) with EHQTA and WC-ETA using **peak height** with TGA (N=7)

| **Element** | | | | **$C_0$ (ng/mL)** | |
|---|---|---|---|---|---|
| | **E** | $E_t$ ($min^{-1}$) | $E_v$ ($mL^{-1}$) | **HPLC-HG-EHQTA** | **HPLC-HG-WC-ETA** |
| As(III) | 10.1 | 5.05 | 63.13 | 5.45 | 0.54 |
| As(V) | 9.91 | 4.96 | 61.94 | 5.45 | 0.55 |

**E** is the enhancement factor (ratio of $C_0$ for EQTA and W-coil ETA)

**$E_t$** is the E/min for sampling,

**$E_v$** is the E/volume of sample in mL

### 3.3.7- Validation of developed methods

In order to evaluate the accuracy of the developed methods, experiments were performed using two certified reference material of water samples: CRM EU-L-2 waste water and CRM 1643e trace elements in water. In addition, CRM 1570a Trace Elements in Spinach Leaves and CRM BCR 627 of Tuna Fish Tissue were also used. Total arsenic determination was performed in the water CRMs. However for the 1570a both total As and speciation analysis was performed.

#### 3.3.7.1- Total arsenic determination in water CRMs

Total arsenic standards containing both As(III) and As(V) in 1 to 1 ratio were prepared in 1.0% (v/v) TGA and 0.002 mol/L HCl and measured using CF-HG-WC-ETAAS. A direct calibration study was performed with the standard solution. A concentration of 0.5 ng/mL was prepared from each of the water CRMs by using the appropriate dilution methods. The standard solutions were measured in 5 replicates (N=5) and the blank was measured in 10 replicates (N=10). The repeatability of the absorbance signal was < 5% RSD and the equation y= 0.3349x + 0.0126 was

obtained from the line of best fit. This equation was used to determine the concentration of total arsenic in the certified water materials. The values of the certified reference materials and values found are given in Table 3.20.

**Table 3.20** Results of the analysis of water certified reference materials and their certified values (N=10)

| **CRM** | **Found value** | **Certified value** |
|---|---|---|
| 1643e[a] /ngmL$^{-1}$ | 61.06 ± 0.01 | 60.45 ± 0.72 |
| EU-L-2[b]/ ngmL$^{-1}$ | 80.45 ± 0.009 | (80.00 ± 0.002)[c] |

[a] Sample solution was diluted in 120 folds

[b] Sample solution was obtained by 1:100 dilution and from this stock 160 folds dilution was performed. The aqueous solutions were all in 1.0% (v/v) TGA with 0.002 mol/L HCl.

[c] This value was obtained after1:100 dilution with water.

### 3.3.7.2- Non-chromatographic speciation of inorganic arsenic in water CRM

By using the optimized parameters of CF-HG-WC-ETAAS, a non-chromatographic speciation of inorganic arsenic species study was carried out by one to one mixing of As(III) and As(V) to make a total concentration of 1.0 ng/mL of inorganic arsenic. The standard solutions of the arsenic species were prepared as given in Table 3.21. The analytical signals of all solutions have the same absorbance value for total As using CF-HG-ETAAS with TGA procedure. A separate set of solutions containing only As(III) corresponding to the same values in mixtures are also analyzed by the same method to find As(III) signals alone. The absorption values of As(V) were obtained by subtracting As(III) absorbance signal from the total signal. The calibration plot is shown in Figure 3.72.

**Table 3.21** Preparation of the standard solution of As(III) and As(V) solution mixture for non-chromatographic speciation

| **Analyte concentration ng/mL** | | |
|---|---|---|
| As(III) | As(V) | Total As |
| 1.0 | 0.0 | 1.0 |
| 0.8 | 0.2 | 1.0 |
| 0.5 | 0.5 | 1.0 |
| 0.2 | 0.8 | 1.0 |
| 0.0 | 1.0 | 1.0 |

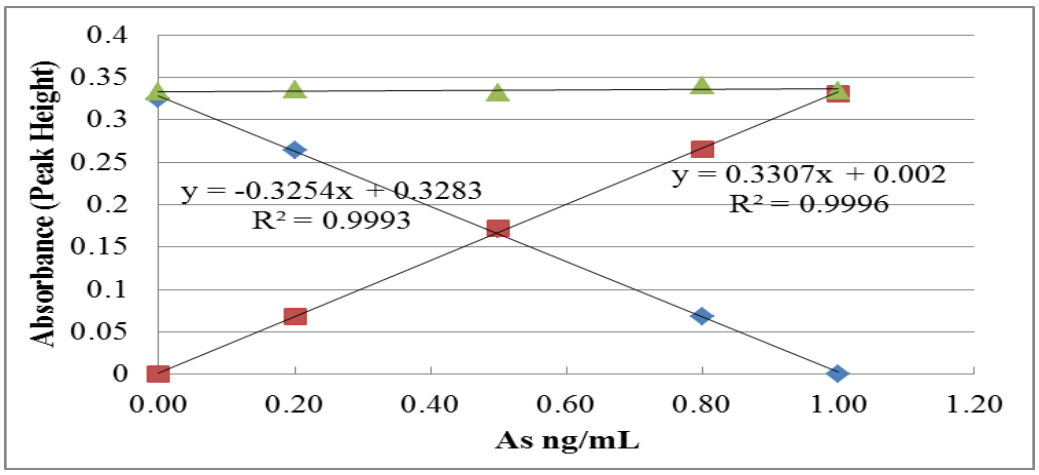


**Figure 3.72** The calibration plot of the total inorganic arsenic species in working standard. The parameters of CF-HG-WC-ETAAS with TGA are given in Table 3.3.

### 3.3.7.3- Total arsenic determination in 1570a and BCR 627 CRMs

For total arsenic determination in 1570a Trace Elements in Spinach Leaves, acid digestion of the sample was performed. As explained in Section 2.3.2, two parallel samples of 0.1 g of the CRM were digested in 4.0 mL solution containing 3.0 mL of 25% $HNO_3$ and 1.0 mL of 30% $H_2O_2$. Two blank solutions were also digested.

The digested CRM solutions and the blank solutions were then adjusted to weight of 30.0 g using deionized water and then the resulting solutions were measured with CF-HG-WC-ETAAS. An external calibration was curve was prepared from freshly prepared As(III) standard solution using this system and this linear equation y= 0.3349x + 0.0126 was obtained. After analyzing the digested blank of $HNO_3$ and $H_2O_2$ the concentration of total inorganic arsenic in the 1570a Trace Elements in Spinach Leave CRM was determine. The repeatability of the signals in peak height was <5% RSD and the absorbance of the blank was 0.005 Abs Unit. The certified and the found values of this study are given in Table 3.22.

Total arsenic determination was also carried out in Tuna Fish Tissue CRM (BCR 627). The procedure of the experiment was explained in section 2.7. Two parallel samples of the CRM and two blank solutions were all digested together. Double microwave cycles digestions were performed and the solutions were adjusted with 30.0 g using water and then measured with FI-HG-EHQTA-AAS. An external calibration was curve was prepared from freshly prepared As(III) standard solution using this system and this linear equation y= 0.0026x + 0.0034 was obtained. After analyzing the digested blank of $HNO_3$ and $H_2O_2$ the concentration of total inorganic arsenic in BCR 627 CRM was then analysed. The repeatability of the signals in peak height was <5% RSD and the absorbance of the blank was 0.003 Abs Unit. The certified and the found values of this study are given in Table 3.22.

**Table 3.22** The experimental values and certified values of the solid CRMs, mg/kg

| **CRM** | **Found value** | **Certified value** |
|---|---|---|
| 1570a | 0.0684 ± 0.0022 | 0.068 ± 0.012 |
| BCR 627 | 4.75± 0.01 | 4.8 ± 0.3 |

### 3.3.7.4- Extraction of arsenic compounds in 1570a CRM spinach leaves

Two extraction solvents were tested for efficient extraction of inorganic arsenic in 1570a Trace Elements in Spinach Leaves CRM. The first solvent used was 0.1 mol/L NaOH in 1/3 Methanol and water. The procedure of the extraction is explained in Section 2.5. The second solvent was 1.0% (v/v) trifluoroacetic acid and extraction procedure is explained in Section 2.6. After extraction, 4.0 mL of the extract was used for acid digestion and the remaining extract was used for chromatographic speciation. The total concentration of arsenic extracted from the spinach leaves was calculated using the equation $y = 0.3349x + 0.0126$ and the value for the two solvents are given in Table 3.23.

### 3.3.7.5- Extraction efficiency of solvents to arsenic compounds in 1570a CRM

To evaluate the extraction efficiency of the two solvents used for extraction of total arsenic from spinach leave CRM, extraction efficiencies were calculated as the ratio of total As in the extract to total As in the sample. The values of the extraction efficiency of the two solvents are given in Table 3.23 and extraction efficiency appeared to be highly variable, depending on the extraction solvent.

### 3.3.7.6- Chromatographic speciation of inorganic arsenic in 1570a CRM

The remaining of the extracted solution using trifluoroacetic acid solvent was used for chromatographic speciation of inorganic arsenic species. Since the electrically heated quartz tube atomizer was not sensitive enough for the concentration of the arsenic species in the extract, the tungsten coil electrothermal atomization was used. By using of 0.16 mL sample volume, and the optimized parameters of HPLC-HG-WC-ETAAS, the two inorganic arsenic species were separated in the extract and analyzed. Results are given in Table 3.23.

**Table 3.23** Comparison of two solvent used for extraction of arsenic from Trace Elements in Spinach Leaves 1570a CRM.

| **Extraction solvent** | Total As, mg/kg | Total extracted As, mg/kg | iAs, mg/kg (by HPLC-HG-WC-ETAAS) | Extraction efficiency (%) |
|---|---|---|---|---|
| 1/3 MeOH/$H_2O$ and 0.1 mol/L NaOH | 0.0684 ±0.002 | 0.0585±0.007 | 0.0429 ± 0.004 | 85.5 |
| 1.0% (v/v) trifluoroacetic acid | 0.0684 ±0.002 | 0.0675±0.002 | 0.052 ± 0.004 | 98.7 |

### 3.3.8- Real sample analysis

#### 3.3.8.1- Microwave acid digestion for total arsenic determination vegetable samples from Beypazarı

Vegetable samples from Beypazarı Ankara, Turkey were used for real sample analysis with the methods developed in this study. The samples were subjected to dry freezing and then analysed for total arsenic after microwave acid digestion. An amount of 0.100 g of each of the sample was accurately weighed and transferred to the microwave digestion vessel and then 3.0 mL of 25% $HNO_3$ and 1.0 mL of 30% $H_2O_2$ were added to sample. A blank solution containing only nitric acid and hydrogen peroxide was also digested. Before sample digestion, a calibration of total inorganic arsenic was first carried out using the CF-HG-WC-ETAAS. The equation of the line of best y=0.1536x + 0.0276, was used to calculate the total concentration of As in each of the samples. The calculation was based on dry mass. The results of the total As and the percentage of water content of the vegetable are given in Table 3.24.

Among the vegetables, only Dill samples contained significant concentration of total arsenic therefore the extraction of total inorganic arsenic was further carried out using Dill vegetable for chromatographic speciation.

The percentage of moisture content was calculated using this equation

$P = [(m_{wet} – m_{dry}) / m_{wet} ] \times 100\%$

Where P is percent moisture content, $m_{wet}$ is mass of wet sample and $m_{dry}$ is the mass of dry sample.

**Table 3.24** The results for the vegetable samples obtained from Beypazarı using CF-HG-WC-ETAAS

| **Sample** | **Total As (µg/g)** | **Percent moisture content (%)** |
|---|---|---|
| Lettuce-1 | Not detected | 94.8 |
| Lettuce-2 | Not detected | 94.8 |
| Spinach-1 | Not detected | 89.7 |
| Spinach-2 | Not detected | 90.1 |
| Parsley-1 | Not detected | 88.5 |
| Parsley-2 | Not detected | 88.7 |
| Garden rocket-1 | Not detected | 93.5 |
| Garden rocket-2 | Not detected | 92.9 |
| Dill-1 | 0.414 ± 0.004 | 90.1 |
| Dill-2 | 0.429 ± 0.002 | 88.9 |

### 3.3.8.2- Extraction of arsenic compounds in dill plant sample for HPLC-HG-WC-ETAAS

The Dill plant was cut in the middle to make two portions and the upper part was label as dill 1 and the lower part was label as dill 2. This was made to compare the distribution of arsenic at the part near the roots and near the leaves. The labeling of the plant is shown in Figure 3.73.

Each part of the dill plant was separately subjected to inorganic arsenic extraction by using 1.0 %(v/v) of trifluoroacetic acid as the extracting solvent. 10.0 mL of the solvent was poured onto 0.20 g of the freeze dried Dill-1 and Dill-2 samples placed in a separated plastic container. The sample solutions were shaken for 12 hours, and further shaken with vortex shaker before placing them into sonication bath for 20 min and finally centrifuged for 15 min with 5000 rpm. The liquid part was filtrated through 0.45 μm membrane filter paper. An amount of 4.0 mL of the filtrate was used for extracted total As determination by using the microwave digestion and analyzed with the CF-HG-WC-ETAAS. By using the results for total As and extracted total arsenic, % extraction efficiency is calculated. The rest of the filtrate was subjected to chromatographic separation for the speciation analysis of the inorganic arsenic species using the HPLC-HG-WC-ETAAS. The results found for As(III) and As(V) were corrected by using % extraction efficiency. The results of the experiment are given in Table 3.25.

The total inorganic arsenic was calculated for the sample and Dill-1 was found to contain 0.338 ± 0.005 μg/g inorganic arsenic by dry mass. In Dill-2 the total inorganic arsenic content was 0.372 ± 0.011 μg/g. From this result it can be inferred that Dill-2, which represents the lower part of the Dill plant that is nearer to the root area contain higher inorganic arsenic species than the upper part of the plant. It should be noted that at 95% confidence level, according to t-test, there is no significant difference between these two values.

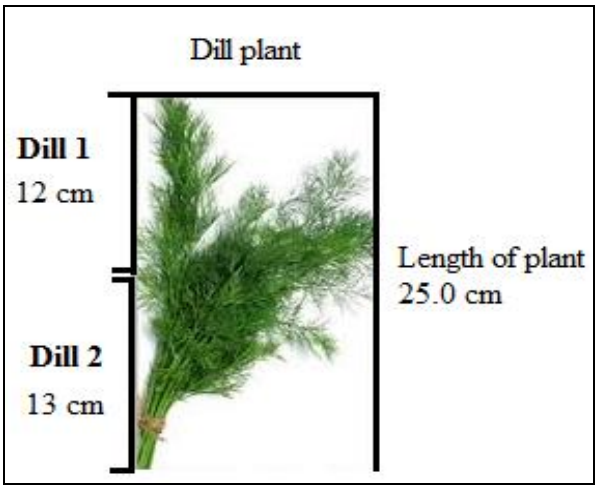


**Figure 3.73** The labelling of the dill plant into upper and lower parts for arsenic distribution determination.

**Table 3.25** The extraction of arsenic compounds from dill plant using trifluoroacetic acid and speciation using HPLC-HG-WC-ETAAS. The results are calculated using dry mass (N=2)

| | **Dill 1** | **Dill 2** |
|---|---|---|
| **Total As, µg/g** | 0.414 ± 0.004 | 0.429 ± 0.003 |
| **Total extracted As, µg/g** | 0.398 ± 0.002 | 0.399 ± 0.009 |
| **As(III), µg/g** | 0.201 ± 0.004 | 0.225 ± 0.007 |
| **As(V), µg/g** | 0.137 ± 0.002 | 0.147 ± 0.008 |
| **Total iAs, µg/g** | 0.338 ± 0.005 | 0.372 ± 0.011 |
| **Extraction efficiency** | 96.1 % | 93.0% |
| **% inorganic content** | [81.6 ± 1.3] % | [86.7 ± 2.7] % |

### 3.3.8.3- Vegetable and water samples from Balıkesir Bigadiç Turkey

Samples of water and vegetable were collected from the Boron element mine site Balikesir in the southern part of Turkey. The samples were collected from four gardens that were approximately 3 to 4 km from the mining site. From each garden, one type of vegetable sample plus the water used for irrigation were collected. From garden 1 (G1), Garden rocket was collect, in garden 2 (G2) Dill was collected, in garden 3 (G3) Lettuce was collected and in garden 4 (G4) Parsley was collected. The results of the analysis of water sample for total arsenic determination using the CF-HG-WC-ETAAS are given in Table 3.25.

Chromatographic speciation study for the inorganic arsenic species was also applied to the water samples using the HPLC-HG-WC-ETAAS. The results of this study is also given in Table 3.26

Total arsenic was determined when sample arrived in the laboratory in both the water and vegetable samples by using the same procedure as the vegetable collected from Beypazarı Ankara as given section 2.5.6.

For the total arsenic, CF-HG-WC-ETAAS method was used and after extracting with 1.0 % (v/v) trifluoroacetic acid the speciation of the inorganic arsenic species was carried out using the HPLC-HG-WC-ETAAS. The results of the studies are given in Table 3.27. The results were calculated using the calibration equation y= 0.1889c + 0.0129 and the total arsenic content from the vegetable samples were very much correlated with the water used to irrigate it.

**Table 3.26** The results for total arsenic in water samples collected from **Balıkesir** in four different gardens (N= 5). CF-HG-WC-ETAAS was used.

| | **Garden 1** | **Garden 2** | **Garden 3** | **Garden 4** |
|---|---|---|---|---|
| Total As, µg/mL | 0.045 ± 0.004 | 0.047 ± 0.008 | 0.083 ± 0.012 | 0.046 ± 0.007 |
| As(III), µg/mL | 0.012 ± 0.002 | 0.015 ± 0.002 | 0.026 ± 0.005 | 0.009 ± 0.001 |
| As(V), µg/mL | 0.033 ±0.004 | 0.032 ±0.003 | 0.057 ± 0.007 | 0.037 ± 0.003 |

**Table 3.27** The extraction of iAs using trifluoroacetic acid and speciation using HPLC-HG-WC-ETAAS for Balıkesir vegetable samples. The results are calculated using dry mass (N=3)

| | **Garden rocket (G1)** | **Dill (G2)** | **Lettuce (G3)** | **Parsley (G4)** |
|---|---|---|---|---|
| Total As, µg/g | 0.241 ± 0.018 | 0.158 ± 0.006 | 0.479± 0.028 | 0.114 ± 0.014 |
| Total extracted As (µg/g) | 0.231±0.0101 | 0.152±0.005 | 0.460 ±0.022 | 0.107±0.0027 |
| As(III) (µg/g) | 0.067± 0.004 | 0.045±0.0013 | 0.121 ± 0.01 | 0.012± 0.002 |
| As(V) (µg/g) | 0.139± 0.012 | 0.088± 0.013 | 0.297± 0.023 | 0.063± 0.008 |
| Total iAs (µg/g) | 0.206± 0.013 | 0.133± 0.013 | 0.418± 0.025 | 0.075± 0.008 |
| Extraction efficiency % | 95.9 | 96.2 | 96.3 | 93.9 |
| % iAs Content | 89.2 ± 9.8 | 87.5 ± 11.1 | 90.9 ± 8.3 | 65.8 ± 2.6 |
| Water content (%) | 92.8 | 86.9 | 91.1 | 86.39 |

# CONCLUSION

An analytical technique that involves chromatographic separation of inorganic arsenic species and hydride generation system with atom trapping system using an Ir-coated tungsten coil was developed and validated using certified reference materials. The methods provide relatively easy, low cost and fast on-line pre concentration of iAs determination using TGA. The chromatographic separation was achieved by using an anion exchange column with a phosphate buffer of pH 5.8. This developed technique is sensitive and can be used to determine inorganic arsenic species at ng/L range. Furthermore the methods developed can be applied in laboratories having a simple AAS instrument and a hydride generation system with a very low additional cost. The systems can be easily manufactured in any laboratory and use in routine analysis.

ICP-MS has a great power of detection but suffers from many interferences and the use of phosphate buffer is avoided due to deposits in cones. On the other hand, this buffer is very efficient and can easily be used with AAS or AFS systems. The developed method has analytical figures of merit comparable to or better than relatively expensive techniques such as GFAASS and ICP-MS. In addition, it is possible to realize chromatographic speciation with good detection power.

The use of TGA as an efficient pre-reduction reagent has made it possible to use online analysis of As(V), and simultaneously can determine the inorganic arsenic species with the organic one including MMA and DMA. However its unpleasant odor can be really inconvenience to work with, but it was running in the online system the smell is hardly felt.

The atom trapping using tungsten coil coated with iridium produce a sensitive analytical signals that are very sharp due to fast heating rate of W coil which allowed the use of peak height values; half widths were less than a second. The peak area

values are rather small which resulted in a decrease in the reproducibility and enhancement factors. The chemical modifier gives the tungsten coil a longer life-time with high efficiency of trapping and releasing of the atomic species.

The only challenging parameter that could be faced in the study is to have clear separation of the arsenic species in the anion exchange column. The good separation of the species is necessary because enough time is required to trap and release a species before the elution of a second species. However by using the ammonium phosphate with phosphoric acid buffer at pH 5.8, a clear separation of the inorganic arsenic species was achieved.

In order to extend the applicability of this method for other analytes there are three requirements: 1. the analyte must be volatilized; As and all the hydride forming elements fulfill this requirement. 2. The analyte must be collected on a suitable trapping system; including W-coil either chemically modified or in bare state. 3. Trapped analyte should be thermally atomized in an absorption cell. Thus it means that the method can be applied to all hydride forming elements

## REFERENCES


[1] D. A. Skoog, D. M. West, J. F. Holler, S. R. Crouch, *Fundamentals of Analytical Chemistry*. Philadelphia: Saunders College Pub. , ISBN 0-03-005938-0 (1996) 8th Ed. p. 1

[2] From Wikipedia, the free encyclopedia http://en.wikipedia.org/wiki/Analytical_chemistry, access in 26-02-2014

[3] B. Welz, Michael Sperling *Atomic Absorption Spectrometry* Third, Completely Revised Edition Wiley-VCH Verlag GmBH, Germany, 1999

[4] A. Walsh, *The application of atomic absorption spectra to chemical analysis*, Spectrochim. Acta 7 (1955) 108–117

[5] M. Slavin, *Atomic Absorption Spectroscopy*, 2nd Edition A Wiley-Interscience Publication, John Wiley & Sons (1978)

[6] L. H. J. Lajunen, Spectrochemical *Analysis by Atomic Absorption and Emission*, The Royal Society of Chemistry, London, 1992

[7] J. Dědina, *Atomization of volatile compounds for atomic absorption and atomic fluorescence spectrometry: On the way towards the ideal atomizer*, Spectrochim. Acta Part B 62 (2007) 846–872

[8] O. Y. Ataman, *Vapor generation and atom traps: Atomic absorption spectrometry at the ng/L level*, Spectrochim. Acta Part B 63 (2008) 825–834

[9] O. A. Güell, James A. Holcombe, *Monte Carlo optimization of graphite furnace geometry and sample distribution for copper*, Spectrochim. Acta Part B 43/4-5 (1988) 459-480

[10] O. A. Güell, James A. Holcombe, *A Monte Carlo study of GFAA signal dependence on furnace length*, Spectrochim. Acta Part B 44/2 (1989) 185-196

[11] O. A. Güell, James A. Holcombe, *Monte Carlo optimization of signal-to-noise ratio for electrothermal atomizers*, Spectrochim. Acta Part B 47/14 (1992) 1535-1544

[12] J. Dedina, Dimiter L. Tsalev, *Hydride Generation Atomic Absorption Spectrometry*, Chichester [England]; New York: Wiley & Sons, c1995, ISBN 0471953644

[13] J. Dědina, I. Rubeška, *Hydride atomization in a cool hydrogen–oxygen flame burning in a quartz tube atomizer*, Spectrochim. Acta Part B 35 (1980) 119–128

[14] J. Dědina and Bernhard Welz, *Quartz Tube Atomizers for Hydride Generation Atomic Absorption Spectrometry: Mechanism for Atomization of Arsine*- invited lecture, J. Anal. At. Spectrom. 7 (1992) 307–314

[15] J. Dědina, *Generation of Volatile Compounds for Analytical Atomic Spectroscopy*, *Encyclopedia of Analytical Chemistry* R.A. Meyers (Ed.) Copyright 2010 John Wiley & Sons Ltd

[16] F. Laborda, E. Bolea and J. R. Castillo, *Electrochemical hydride generation as a sample-introduction technique in atomic spectrometry: fundamentals, interferences, and applications*, Anal. Bioanal. Chem. 388 (2007) 743–751

[17] X. Guo, R. E. Sturgeon, M. Zoltan, G. J. Gardner, *UV Vapor Generation for Determination of Selenium by Heated Quartz Tube Atomic Absorption Spectrometry*, Anal. Chem. 75 (2003) 2092-2099

[18] S. Gil, I. Lavilla, C. Bendicho, *Ultrasound-Promoted Cold Vapor Generation in the Presence of Formic Acid for Determination of Mercury by Atomic Absorption Spectrometry*, Anal. Chem. 78 (2006) 6260-6264

[19] S. A. Medel, M.C. Valdes-Hevia, Temprano, N. B. Garcia, M.R. Ferninder de la Campa, *Generation of Cadmium Atoms at Room Temperature Using Vesicles and Its Application to Cadmium Determination by Cold Vapor Atomic Spectrometry*, Anal. Chem.67 (1995) 2216-2223

[20] Y. Lai Feng, R. E. Sturgeon, J. W. Lam, *Generation of Atomic and Molecular Cadmium Species from Aqueous Media*, Anal. Chem. 75 (2003) 635-640

[21] A. D'Ulivo, J. Dedina, M. Zoltan, R. E. Sturgeon, Q. Wang, B. Welz, *Mechanisms of chemical generation of volatile hydrides for trace element determination* (IUPAC Technical Report) Pure Appl. Chem., 83 (2011) 1283-1340

[22] W. Holak, *Gas-Sampling Technique for Arsenic Determination by Atomic Absorption Spectrophotometry*, Anal. Chem. 41 (1969) 1712-1713

[23] R. S. Braman, *Membrane Probe-Spectral Emission Type Detection System for Mercury in Wate*r Anal. Chem. 43 (1971) 1462-1467

[24] R. S. Braman, Lewis L. Justen, Craig C. Foreback, *Direct Volatilization-Spectral Emission Type Detection System for Nanogram Amounts of Arsenic and Antimony*, Anal. Chem. 44 (1972) 2195-2199

[25] K. C. Thompson D. R. Thomerson, *Atomic-absorption Studies on the Determination of Antimony, Arsenic, Bismuth, Germanium, Lead, Selenium, Tellurium and Tin by Utilising the Generation of Covalent Hydrides* Analyst 44 (1974) 595-601

[26] W. B. Bobbins, J. A. Caruso, *Development of Hydride Generation Methods for Atomic Spectroscopic Analysis*, Anal. Chem. 51 (1979) 889A

[27] J. Dědina, "Flow methods in gas–liquid separations", in *Flow Analysis with Atomic Spectrometric Detection*, A. Sanz-Medel (Ed.), pp. 237–273, Elsevier, Amsterdam (1999)

[28] F. Laborda, E. Bolea, M. T. Baranguan, J. R. Castillo, *Hydride generation in analytical chemistry and nascent hydrogen: when is it going to be over?* Spectrochim. Acta Part B 57 (2002) 797–802

[29] S. A. Pergantis, W. Winnik, E. M. Heithmar, W. R. Cullen, *Investigation of arsine-generating reactions using deuterium-labeled reagents and mass spectrometry*, Talanta 44 (1997) 1941-1947

[30] A. D'Ulivo, M. Zoltan, R. E. Sturgeon, *The mechanism of formation of volatile hydrides by tetrahydroborate(III) derivatization: A mass spectrometric study performed with deuterium labeled reagents*, Spectrochim. Acta Part B 60 (2005) 423–438

[31] A. D'Ulivo, M. Zoltan, J. Meija, R. E. Sturgeon, *Gas chromatography–mass spectrometry study of hydrogen–deuterium exchange reactions of volatile hydrides of As, Sb, Bi, Ge and Sn in aqueous media*, Spectrochim. Acta Part B 61 (2006) 778–787

[32] R. E. Sturgeon, S. N. Willie, S. S. Berman, *Hydride Generation-Atomic Absorption Determination of Antimony in Seawater with in Situ Concentration in a Graphite Furnace,* Anal. Chem. 57 (1985) 2311-2314

[33] R. Calixto de Campos, R. Araújo Gonçalves, G. Birman Tonietto, J. Marcus Godoy, G. Pedrini Brandão *High performance liquid chromatography hydride generation in situ trapping graphite furnace atomic absorption: a new way of performing speciation analysis spectrometry using GFAAS as detector*, Microchem. J. 84 (2006) 26–30

[34] P. K. Petrov, I. Serafimovski, T. Stafilov, D.L. Tsalev, *Flow injection hydride generation electrothermal. Atomic absorption spectrometric determination of toxicologically relevant arsenic in urine*, Talanta 69 (2006) 1112–1117

[35] M. Grotti, C. Lagomarsino, R. Frache, *Multivariate study in chemical vapor generation for simultaneous determination of arsenic, antimony, bismuth, germanium, tin, selenium, tellurium and mercury by inductively coupled plasma optical emission spectrometry*, J. Anal. At. Spectrom., 20 (2005), 1365–1373

[36] M. Antunes Vieiraa, A. Schwingel Ribeiroa, L. Felicidade Diasb, A. Jose Curtius, *Determination of Cd, Hg, Pb and Se in sediments slurries by isotopic dilution calibration ICP-MS after chemical vapor generation using an on-line system or retention in an electrothermal vaporizer treated with iridium*, Spectrochim. Acta Part B 60 (2005) 643 – 652

[37] G. Ertas, O. Y. Ataman, *Electrothermal Atomic Absorption Spectrometric Determination of Gold by Vapor Formation and in Situ Trapping in Graphite Tubes*, Appl. Spectrosc. 58 (2004) 1243–1250

[38] B. Dociekal, P. Mareka, M. Vobecky, *Radiotracer investigation of nickel tetracarbonyl generation and in situ nickel deposition within a graphite furnace*, J. Anal. At. Spectrom., 15 (2000) 131-135

[39] A. S. Luna, H. Borges Pereira, I. Takase, R. Araujo Goncalves¸ R. Edward Sturgeon, R. Calixto de Campos, *Chemical vapor generation—electrothermal atomic absorption spectrometry: new perspectives*, Spectrochim. Acta Part B 57 (2002) 2047–2056

[40] M. Antunes Vieira, B. Welz, A. Jose Curtius, *Determination of arsenic in sediments, coal and fly ash slurries after ultrasonic treatment by hydride generation atomic absorption spectrometry and trapping in an iridium-treated graphite tube*, Spectrochim. Acta Part B 57 (2002) 2057–2067

[41] D. Karadeniz Korkmaz , N. Ertas , O. Yavuz Ataman, *A novel silica trap for lead determination by hydride generation atomic absorption spectrometry*, Spectrochim. Acta Part B 57 (2002) 571–580

[42] D. Korkmaz, C. Demir, F. Aydin, O. Y. Ataman, *Cold vapour generation and on-line trapping of cadmium species on quartz surface prior to detection by atomic absorption spectrometry*, J. Anal. At. Spectrom., 20 (2005) 46–52

[43] R. J. Watling, *The use of a slotted Quartz tube for the determination of arsenic, antimony, selenium and mercury*, Anal. Chim. Acta 94 (1977) 181–186

[44] R. J. Watling, *The use of a slotted tube for the determination of lead, zinc, cadmium, bismuth, cobalt, manganese and silver by atomic absorption spectrometry*, Anal. Chim. Acta 97 (1978) 395–398

[45] N. Ertas, D. Karadeniz Korkmaz, S. Kumser, O. Y. Ataman, *Novel traps and atomization techniques for flame AAS*, J. Anal. At. Spectrom., 17 (2002) 1415–1420

[46] X. Hou, B. T. Jones, *Tungsten devices in analytical atomic spectrometry*, Spectrochim. Acta Part B 57 (2002) 659–688

[47] H. Berndt, G. Schaldach, *Simple Low-cost Tungsten-coil Atomiser for Electrothermal Atomic Absorption Spectrometry*, J. Anal. At. Spectrom. 3 (1988) 709–712

[48] B. Docekal, P. Marek, *Investigation of in situ trapping of selenium and arsenic hydrides within a tungsten tube atomizer*, J. Anal. At. Spectrom. 16 (2001) 831–837

[49] O. Cankur, N. Ertaş, O. Y. Ataman, *Determination of bismuth using on-line preconcentration by trapping on resistively heated W coil and hydride generation atomic absorption spectrometry*, J. Anal. At. Spectrom. 17 (2002) 603–609

[50] F. Barbosa Jr, S. Simiao de Souza, F. J. Krug, *In situ trapping of selenium hydride in rhodium-coated tungsten coil electrothermal atomic absorption spectrometry* J. Anal. At. Spectrom. 17 (2002) 382-388

[51] O. Cankur, O. Y. Ataman, *Chemical vapor generation of Cd and on-line preconcentration on a resistively heated W-coil prior to determination by atomic absorption spectrometry using unheated quartz absorption cell*, J. Anal. At. Spectrom. 22 (2007) 791–799

[52] I. Kula, Y. Arslan, S. Bakırdere, O.Y. Ataman, *A novel analytical system involving hydride generation and gold-coated W-coil trapping atomic absorption spectrometry for selenium determination at ng/L level*, Spectrochim. Acta Part B, 63 (2008) 856–860

[53] S. Titretir, E. Kendüzler, Y. Arslan, İ. Kula, S. Bakırdere, O. Y. Ataman, *Determination of antimony by using tungsten trap atomic absorption spectrometry*, Spectrochim. Acta Part B 63 (2008) 875–879

[54] O. Alp, N. Ertas, *In situ trapping of antimony hydride on iridium-coated tungsten coil and interference studies*, J. Anal. At. Spectrom. 23 (2008) 976–980

[55] R. Liu, P. Wu, M. Xi, K. Xu, Y. Lv, *Inorganic arsenic speciation analysis of water samples by trapping arsine on tungsten coil for atomic fluorescence spectrometric determination*, Talanta 78 (2009) 885–890

[56] X. Hou, Z. Yang, B. T. Jones, *Determination of selenium by tungsten coil atomic absorption spectrometry using iridium as a permanent chemical modifier*, Spectrochim. Acta Part B 56 (2001) 203-214

[57] From Wikipedia, the free encyclopedia, http://en.wikipedia.org/wiki/Arsenic. Retrieved in 26 May 2014

[58]*"Arsenic: As(III) sulfide compound data*". WebElements.com. Retrieved in 26 May 2014

[59] K. A. Francesconi, D. Kuehnelt, *Determination of arsenic species: A critical review of methods and applications, 2000–2003*, Analyst, 129 (2004) 373–395

[60] B. Kumar Mandal, K. T. Suzuki, *Arsenic round the world: a review*, Talanta 58 (2002) 201–235

[61] J.E. Fergusson, *The Heavy Elements: Chemistry, Environmental Impact and Health Effects*, Pergamon Press, Great Britain, 1990, p. 614

[62] World Health Organization, *Arsenic in Drinking Water*, 2001, Geneva, Fact sheet 210

[63] S. Ahuja, *Arsenic contamination of groundwater, mechanism, analysis and remediation*, A John Wiley & Sons, INC., Publication page 53

[64] C. I. Davidson, G. Bruce. Wiersma, K. W. Brown, W. D. Goold, T. P. Mathison, M. T. Reilly, *Airborne trace elements in Great Smoky Mountains, Olympic, and Glacier National Parks*, Environ. Sci. Technol. 19 (1985) 27-35

[65] *Guidelines for Drinking Water Quality, Recommendations*, 2nd ed., vol. 2, World Health Organisation, Geneva, 1996

[66] S. M. Nagvi, C. Vaishnavi, H. Singh, *Toxicity and metabolism of arsenic in vertebrates*, in: J.O. Nriagu (Ed.), *Arsenic in the Environment. Part II: Human Health and Ecosystem Effects*, John Wiley and Sons, Inc, New York, 1994, pp. 55–91

[67] R. M. Raie, *Regional Variation in As, Cu, Hg, and Se and Interaction between them*, Ecotoxicol. Environ. Safety 35 (1996) 248-252

[68] E. Marafante, F. Bertolero, J. Edel, R. Pietra, E. Sabbioni, *Intracellular interaction and biotransformation of arsenite in rats and rabbits*, Sci. Total Environ. 24 (1982) 27-39

[69] M. Vahter, E. Marafante, L. Dencker, *Tissue Distribution and Retention of $^{74}$As-Dimethylarsinic Acid in Mice and Rats*, Arch. Environ. Contam. Toxicol. 13 (1984) 259-264

[70] J. P. Buchet, R. Lauwerys, H. Roels, *Comparison of the Urinary Excretion of Arsenic Metabolites After a Single Oral Dose of Sodium Arsenite, Monomethylarsonate, or Dimethylarsinate in Man*, Int. Arch. Occup. Environ. Health 48 (1981) 71-79

[71] B. Kumar Mandal, Y. Ogra, K. T. Suzuki, *Identification of Dimethylarsinous and Monomethylarsonous Acids in Human Urine of the Arsenic-Affected Areas in West Bengal, India*, Chem. Res. Toxicol. 14 (2001) 371-378

[72] X. Chris Le, Xiufen Lu, Mingsheng Ma, William R. Cullen, H. Vasken Aposhian, Baoshan Zheng, *Speciation of Key Arsenic Metabolic Intermediates in Human Urine*, Anal. Chem. 72 (2000) 5172-5177

[73] G. K. H. Tam, S. M. Charbonneau, F. Bryce, C. Pomroy, E. Sandi, *Metabolism of inorganic arsenic ($^{74}As$) in humans following oral ingestion*, Toxicol. Appl. Pharmacol. 50 (1979) 319-322

[74] J. P. Buchet, R. Lauwerys, H. Roels, *Urinary Excretion of Inorganic Arsenic and Its Metabolites After Repeated Ingestion of Sodium Metaarsenite by Volunteers*, Int. Arch. Occup. Environ. Health 48 (1981) 111-118

[75] F. Zheng, B. Hu, *Dual-column capillary microextraction (CME) combined with electrothermal vaporization inductively coupled plasma mass spectrometry (ETV-ICP-MS) for the speciation of arsenic in human hair extracts*, J. Mass. Spectrom. 45 (2010) 205–214

[76] M. J. Ellenhorn, *Arsenic, in: Ellenhorn's Medical Toxicology: Diagnosis and Treatment of Human Poisoning*, 2nd ed., Williams and Wilkins, Baltimore, 1997, p. 1538.

[77] W. R. Cullen, K. J. Reimer, *Arsenic Speciation in the Environment*, Chem. Rev. 89 (1989) 713-764

[78] Section of Environmental Epidemiology & Toxicology Office of Public Health, Louisiana Department of Health & Hospitals (888) 293-7020; www.seet.dhh.la.gov.*NFORMATION FOR HEALTH CARE PROFESSIONALS ARSENIC EXPOSURE & TOXICITY,* Revised: January 2009

[79] S. Maeda, *Biotransformation of arsenic in the freshwater environment*, in: J. O. Nriagu (Ed.), *Arsenic in the Environment Part I, Cycling and Characterization*, Wiley, New York, 1994, pp. 155–187

[80] D. G. Kinniburgh, and P. L. Smedley, (Editors), BGS and DPHE. 2001 Arsenic contamination of groundwater in Bangladesh, *British Geological Survey Technical Report WC/00/19*

[81] J. S. Petrick, F. Ayala-Fierro, W. R. Cullen, Dean E. Carter, H. Vasken Aposhian, Highlight: *Monomethylarsonous Acid (MMAIII) Is More Toxic Than Arsenite in Chang Human Hepatocytes*, Toxicology and Applied Pharmacology 163 (2000) 203–207

[82] S. Lin, W. R. Cullen, D. J. Thomas, *Methylarsenicals and Arsinothiols Are Potent Inhibitors of Mouse Liver Thioredoxin Reductase*, Chem. Res. Toxicol. 12 (1999) 924-930

[83] M. Styblo, S. V. Serves, W. R. Cullen, D. J. Thomas, *Comparative Inhibition of Yeast Glutathione Reductase by Arsenicals and Arsenothiols*, Chem. Res. Toxicol. 10 (1997) 27-33

[84] M. Styblo, L. M. Del Razo, L. Vega, D.R. Germolec, E. L. LeCluyse, G. A. Hamilton, W. Reed, C. Wang, W. R. Cullen, D. J. Thomas, *Comparative toxicity of trivalent and pentavalent inorganic and methylated arsenicals in rat and human cells*, Arch. Toxicol. 74 (2000) 289-299

[85] J. C. Belton, N. C. Benson, M. Leslie Hanna, R. T. Taylor, *Growth inhibitory and cytotoxic effects of three arsenic compounds on cultured Chinese hamster ovary cells*, J. Environ. Sci. Health 20 A (1985) 37-72

[86] H. Wolochow, E. M. Putman, M. Doudoroff, W. Z. Hassid, H. A. Barker, *Preparation of sucrose labeled with $C^{14}$ in the glucose or fructose component*, J. Biol. Chem. 180 (1949) 1237-1242

[87] H. B. F. Dixon, *the Biochemical Action of Arsonic Acids Especially As Phosphate Analogues*, Adv. Inorg. Chem. 44 (1997) 191-227

[88] WHO *Arsenic Compounds, Environmental Health* Criteria 224, 2nd ed., World Health Organization, Geneva, 2001

[89] Environmental Protection Agency, Ambient *Water Quality Criteria for Arsenic*, U.S. Environ. Prot. Agency Rep., 440/5-80-021, 1980, p. 1

[90] J. Tyson, *the Determination of Arsenic Compounds: A Critical Review*, Hindawi Publishing Corporation ISRN Analytical Chemistry Volume 2013, 1-24

[91] D. M. Templeton, F. Ariese, R. Cornelis, L.-G. Danielsson, H. Muntau, H. P. van Leeuwen, R. Lobinski, *Guidelines for terms related to chemical speciation and fractionation of elements. Definitions, structural aspects, and methodological approaches (IUPAC Recommendations 2000)*, Pure Appl. Chem., 72 (2000) 1453-1470

[92] A. Gonzalvez, M. L. Cervera, S. Armenta, M. de la Guardia, "*A review of non-chromatographic methods for speciation analysis*," Anal. Chim. Acta, 636 (2009) 129–157

[93] C. K. Jain., I. Ali, *Arsenic: occurrence, toxicity and speciation techniques*, Wat. Res., 34 (2000) 4304-4312

[94] M. A., Quevauviller P., M. E. A., Griepink B., *Quality Assurance for Environmental Analysis*, Elsevier, Amsterdam, The Netherlands, (1995) pp. 95-100

[95] I. Komorowicz, D. Barałkiewicz, *Arsenic speciation in water by high-performance liquid chromatography/inductively coupled plasma mass spectrometry–method validation and uncertainty estimation*, Rapid Commun. Mass Spectrom. 28 (2014) 159–168

[96] T. Narukawa, T. Suzuki, K. Inagaki, A. Hioki, *Extraction techniques for arsenic species in rice flour and their speciation by HPLC–ICP-MS*, Talanta 130 (2014) 213–220

[97] N. M. Smith, R. Lee, D. T. Heitkemper, K. DeNicola Cafferky, A. Haque, Alden K. Henderson, *Inorganic arsenic in cooked rice and vegetables from Bangladeshi households*, Sci. Total Environ. 2006, 370, 294–301

[98] D. C., Sanz J. E. Sanz, R. Munoz-Olivas, C. Camara, *Current perspectives in analyte extraction Strategies for tin and arsenic speciation* J. Chromatogr. A., 1153 (2007) 114-129

[99] H. Abdolmohammad-Zadeh, A. Jouyban, R. Amini, *Ultratrace determination of arsenic in water samples by electrothermal atomic absorption spectrometry after pre-concentration with Mg–Al–Fe ternary layered double hydroxide nano-sorbent*, Talanta 116 (2013) 604–610

[100] M. Ines, S. Melecchi, V. Flores Peres, C. Dariva, C. Alcaraz Zini, F. Contieri Abad, M. Miranda Martinez, E. Bastos Caramao, *Optimization of the sonication extraction method of Hibiscus tiliaceus L. flowers*, Ultrasonics Sonochemistry 13 (2013) 242–250

[101] G. Raber, S. Khoomrung, M. S. Taleshi, J. S. Edmonds, K. A. Francesconi, *Identification of arsenolipids with GC/MS*, Talanta 2009, 78, 1215–1218

[102] R. A. Diaz-Bone, M. Hollmann, O. Wuerfel, D. Pieper, *Analysis of volatile arsenic compounds formed by intestinal microorganisms: rapid identification of new metabolic products by use of simultaneous EI-MS and ICP-MS detection after gas chromatographic separation*, J. Anal. At. Spectrom., 24 (2009) 808–814

[103] N. Campillo, R. Penalver, P. Vinas, I. López-García, M. Hernández-Córdoba, *Speciation of arsenic using capillary gas chromatography with atomic emission detection*, Talanta 77 (2008) 793–799

[104] A. A. Ammann, Arsenic Speciation Analysis by Ion Chromatography - *A Critical Review of Principles and Applications,* Am. J. Anal. Chem., 2 (2011) 27-45

[105] R. Łobinski, D. Schaumloffel, J. Szpunar, *mass spectrometer in bioinorganic analytical chemistry*, Mass Spectrom. Rev., 2006, 25, 255– 289

[106] A. G. Howard, C. Salou, *Arsenic speciation by cryogenic trap hydride generation atomic absorption spectroscopy: performance enhancement by pre-derivatization*, J. Anal. At. Spectrom. 13 (1998) 683–686

[107] J. Carlos Gonzalez, I. Lavilla, C. Bendicho, *Evaluation of non-chromatographic approaches for speciation of extractable As(III) and As(V) in environmental solid samples by FI-HGAAS*, Talanta 59 (2003) 525-534

[108] M. E. Sigrist, H. R. Beldomenico, *Determination of inorganic arsenic species by flow injection hydride generation atomic absorption spectrometry with variable sodium tetrahydroborate concentration*s, Spectrochim. Acta Part B 59 (2004) 1041-1045

[109] J. Frank, M. Krachler, W. Shotyk, *Direct determination of arsenic in acid digests of plant and peat samples using HG-AAS and ICP-SF-MS*, Anal. Chim. Acta, 530 (2005) 307–316

[110] S. Musila, T. Matoušeka, *On-line pre-reduction of pentavalent arsenicals by thioglycolic acid for speciation analysis by selective hydride generation cryotrapping-atomic absorption spectrometry*, Spectrochim. Acta Part B 63 (2008) 685–691

[111] E. Pitzalis, D. Ajala, M. Onor, R. Zamboni, A. D'Ulivo, *Chemical Vapor Generation of Arsane in the Presence of L-Cysteine. Mechanistic Studies and Their Analytical Feedback*, Anal. Chem. 79 (2007) 6324-6333

[112] T. Matoušek, A. Hernández-Zavala, M. Svoboda, L. Langrová, B. M. Adair, Z. Drobná, D. J. Thomas, M. Stýblo , J. Dědina, *Oxidation state specific generation of arsines from methylated arsenicals based on L-cysteine treatment in buffered media for speciation analysis by hydride generation-automated cryotrapping-gas chromatography-atomic absorption spectrometry with the multiatomizer*, Spectrochim. Acta Part B 63 (2008) 396–406

[113] D. L. Tsalev, M. Sperling, B. Welz, *Flow-injection hydride generation atomic absorption spectrometric study of the automated on-line pre-reduction of arsenate, methylarsonate and dimethylarsinate and high-performance liquid chromatographic separation of their L-cysteine complexes*, Talanta 51 (2000) 1059–1068

[114] T. Matouseka, M. Johansson, J. Dedina, W. Frech, *Spatially resolved absorption measurements of antimony atom formation and dissipation in quartz tube atomizers following hydride generation*, Spectrochim. Acta Part B 54 (1999) 631-643

[115] A. Shraim, B. Chiswell, H. Olszowy, *Speciation of arsenic by hydride generation–atomic absorption spectrometry (HG–AAS) in hydrochloric acid reaction medium*, Talanta 50 (1999) 1109–1127

[116] S. Simiao de Souza, D. Santos Jr., F. J. Krug, F. Barbosa Jr., *Exploiting in situ hydride trapping in tungsten coil atomizer for Se and As determination in biological and water samples*, Talanta 73 (2007) 451-457

[117] R. Liu, P. Wu, K. Xu, Y. Lv, X. Hou, *Highly sensitive and interference-free determination of bismuth in environmental samples by electrothermal vaporization atomic fluorescence spectrometry after hydride trapping on iridium-coated tungsten coil*, Spectrochim. Acta Part B 63 (2008) 704-709

[118] C. G. Bruhn, V. N. Huerta, J. Y. Neira, *Chemical modifiers in arsenic determination in biological materials by tungsten coil electrothermal atomic absorption spectrometry* Anal. Bioanal. Chem. 378 (2004) 447-455

[119] E. Krakovska, *Tungsten atomizer-the theory of atomization reaction*s, Spectrochim. Acta Part B 52 (1997) 1327-1332

[120] T. Matousek, J. M. Currier, N. Trojankova, R. Jesse Saunders, M. C. Ishida, C. Gonzalez-Horta, S. Musil, M. Zoltan, M. Styblo, J. Dedina, *Selective hydride generation-cryotrapping-ICP-MS for arsenic speciation analysis at picogram levels: analysis of river and sea water reference materials and human bladder epithelial cells* J. Anal. At. Spectrom. 28 (2013) 1456-1465

[121] K. H. Al-Assaf, J. F. Tyson, P. C. Uden, *Determination of four arsenic species in soil by sequential extraction and high performance liquid chromatography with post-column hydride generation and inductively coupled plasma optical emission spectrometry detection*, J. Anal. At. Spectrom. 24 (2009) 376–384

[122] https://www.google.com.tr/search?q=ph+diagram+of+arsenic&tbm
Last retrieved in 16/08/2014

**Curriculum Vitae**

**2014**

**Personal Information**

**Name:** Mr. Njaw Njie

**Sex:** Male

**Current Resident Address:** Middle East Technical University, Department of Chemistry C/49, 06800 Ankara, Turkey

Tel: (0090) 312 261 1470 or 0554 971 8392

Email: njawn@yahoo.com

**Work Experience**

Knowledge in the use of ICP-MS, ICP-OES and AAS for the determination of essential and non-essential elements and for molecular characterization, I have learned the use of FTIR, Raman UV-VIS and NIR  Middle East Technical University.

Analysis of activated carbon for phenazone absorption property

Graduate assistant in Department of Chemistry, Middle East Technical University. Supervising students in their lab experiments in General Chemistry Laboratory between 2010 and 2013.

Worked as a teaching assistant in the University of the Gambia between 2005-2006 and 2008- 2009.

I was serving as Secretary General in The Science Club in University of the Gambia. We initiate projects such as community cleaning, using cow dungs for

natural gas production, and teaching science subject to high school students between 2002 and 2003.

Interested in the areas of chemistry especially analytical chemistry, and method development in scientific research.

**Education**

**1. Middle East Technical University**

**a. PhD in Analytical chemistry**, between 2009 and 2014

C. GPA: 3.5

GRE Score 146/170

**PhD Thesis**

Atom Traps and Vapor Generation Atomic Absorption Spectrometry for Inorganic Arsenic Speciation Analysis

**b- Master of Science in Chemistry,** between 2006 and 2008

**MSc Thesis**

Use of Multi-Walled Carbon Nanotubes in Matrix Solid Phase Dispersion Extraction Combined with Gas Chromatography (GC-FID)

**2. University of the Gambia**

**Barchelor's Degree in Science,** between 2000 and 2004

Bachelor of Science in Chemistry; with a Major in Chemistry and Minor in Biology

**Conferences and Seminars Attended**

1. XI. Ulusal Spektroskopi Kongresi (11th National Spectroscopy Congress), 23-26 June 2009, Gazi University Turkey.

2. Agilent seminar on the use and application of ICP-MS/MS, FTIR and Raman hosted by SEM in Ankara, Turkey 2014.

3. Thermo Scientific Instruments presentation (Ankara Swiss hotel April 2014)

**Conference Presentations**

1. M. A. Ibraheim, N. Njie, E. Yıldırım, M. H. Abdelalah, O. Y. Ataman, "Interference Studies for Antimony by Hydride Generation Atomic Trapping Slotted Quartz Tube Flame Atomic Absorption Spectrometry", Poster P1-07, Book of Abstracts, p. 49, 8th Aegean Analytical Chemistry Days, 16-20 September 2012, İzmir Institute of Technology, İzmir, Turkey.

2. M. A. Ibraheim, N. Njie, E. Yıldırım, F. Şenol, M. H. Abdelalah, O. Y. Ataman, "Speciation of Antimony(III) and Antimony(V) by Hydride Generation Atomic Trapping Slotted Quartz Tube Flame Atomic Absorption Spectrometry", Poster P1-08, Book of Abstracts, p. 50, 8th Aegean Analytical Chemistry Days, 16-20 September 2012, İzmir Institute of Technology, İzmir, Turkey.

3. G. Karaman, A. Atakol, S. Bora, N. Njie, E. Yıldırım, S. Bakırdere, O. Y. Ataman, "Boron determination by ICP-MS in food samples", Book of abstracts, PI-44, s. 77, XI. National Spectroscopy Congress (USK 2009), 23-26 June 2009, Gazi Üniversitesi, Ankara.

4. Njaw Njie, O. Yavuz Ataman, "Atom traps meet chromatography and speciation in Chios", 9th Aegean Analytical Chemistry Days, 29 September-3 October 2014, Chios, Greece.

**Computer Education**

Computer Operation and Windows 98 and Microsoft Word, and now acquainted with internet usage

**Awards and Scholarships**

1. Award of the Gambia Government Scholarship for BSc: from 06/2001 to 09/2004.
2. Islamic Development Bank M.Sc Scholarship: from 09/2006 to 06/2008.
3. TUBITAK Scholarship for Ph.D. Fellowships for foreign country citizens from 2009 to 2010 and between 2011 and 2012.

**Languages**

Fluent in English

Intermediate Turkish

Basic French

Basic German (But currently studying)